

Allosteric regulation and targeting of Abl SH2-kinase interface and other cytoplasmic tyrosine kinases

THÈSE N° 6987 (2016)

PRÉSENTÉE LE 29 AVRIL 2016

À LA FACULTÉ DES SCIENCES DE LA VIE

CHAIRE FONDATION ISREC EN ONCOLOGIE TRANSLATIONNELLE
PROGRAMME DOCTORAL EN BIOTECHNOLOGIE ET GÉNIE BIOLOGIQUE

ÉCOLE POLYTECHNIQUE FÉDÉRALE DE LAUSANNE

POUR L'OBTENTION DU GRADE DE DOCTEUR ÈS SCIENCES

PAR

Allan Joaquim LAMONTANARA

acceptée sur proposition du jury:

Prof. M. Dal Peraro, président du jury
Prof. O. Hantschel, directeur de thèse
Prof. S. Knapp, rapporteur
Prof. S. Grzesiek, rapporteur
Prof. P. Goczy, rapporteur



ÉCOLE POLYTECHNIQUE
FÉDÉRALE DE LAUSANNE

Suisse
2016

*"Most people say that it is the intellect which makes a great scientist.
They are wrong: it is character"*
—Albert Einstein

To my friends and family who were always here for me throughout this adventure.
To my friend Orest who was a great source of inspiration and continues to be so ...

Acknowledgements

This thesis marks the end of my journey in obtaining my PhD. I have not traveled alone and I have been kept on track thanks to the support of numerous people. I am delighted to dedicate these few words to all those who contributed in many ways to my PhD. These 4 years have been a period of intense learning, not only scientifically, but mostly on a personal level.

I would like to express my appreciation and thanks my advisor Prof. Oliver Hantschel. He supported me greatly and was constantly available to guide me during my PhD. I thank you for your willingness to share your knowledge and time with me. I would also like to thank my mentor Prof. Michel Aguet and my thesis committee: Prof Matteo Dal Peraro, Prof. Stefan Knapp, Prof. Stephan Grzesiek and Prof. Pierre Gönczy for their help in improving this manuscript and the time they dedicated to read and discuss my work. I also thanks the ISREC, Swiss Cancer League and NCCR for financially supporting my projects.

This work would have not been possible with the technical help from the EPFL staff. I would like to thank all members of the proteomics core facility, Marc Chambon and Gerardo Turcatti from the Biomolecular Screening Facility and finally David Hacker and Shen Xiao from the Protein Expression Core facility. I am also grateful to the EMBL SAXS facility in Hamburg and especially Giancarlo Tria, Alejandro Panjkovich and Prof. Dmitri Svergun for their tremendous help in analyzing the SAXS data. Thanks also to Bruno Fauvet from the Hilal Lashuel laboratory for his help in analyzing light scattering data. I am also thankful to our collaborator Prof. Shohei Koide.

In my daily work I had the chance to spend my time with great colleagues. I had very supportive labmates both technically and personally. I would like to take the time to thank them. Sandrine, this work would have not been possible without your constant patience and technical assistance during my PhD. You helped me to become an independent scientist in our lab and I would never thank you enough for that. Basak, my dear office mate, I still remember this night singing Rocky Balboa songs. You were always here for me and I thank you for the great time and laughters we shared. Sina, our first post-doc, you were always available whenever I had a question and always answered them with a smile. You are great scientist, very rational and I wish you the best with your family. I am also grateful to my more recent colleagues. Nadine, I have never seen such a smiley person, thanks for all, please always stay such a

Acknowledgements

cheerfull person. Tim, thanks for bearing with my constant questions and complains. You are a great scientist, you are passionate and that is all I need. Barbara, thanks for all your help and contribution to this study and for the time we spent together. I wish you all the best for your future life.

I would like to give a special thanks to my late friend Orest Kuzyk. Orest, no matter what, you were always cheerfull and there for me. You are one of the most inspiring scientist and person I have ever met. Even if you cannot read those words, I will always be grateful I had met you. You inspired me and many other people, thank you so much. I would also like to thanks your lovely wife -Andrea- I will be there for you whenever needed.

My life in Lausanne will not have been the same without the loving friends I have. I would like to deeply thanks my flatmates and friends Jawahar and Nicolas. Jawahar, thanks for all your support and all the moments we shared together. Nicolas, 'Patrick', you know how much our friendship is important to me. Thanks for everything you have done, it kept me sane during though times. Thanks also for teaching me LaTeX, it was worth the investment for this thesis. I would also like to thanks Bogdan and Mirco from the LTCM team for all the nights out and dinners as well as Jonathan. I am also so happy I met Mirko and Sonja, you guys are the most amazing couple I have known. Thanks for all your support and I wish you a joyfull life with little Dimi. Hvala !

Thanks to all the friends I met in BSNL, they are many of them: Jonathan, Roman, Anne-Laure, Galyna...thanks for the great moments we had organizing these events and for the dinners together. Special thanks to Fatima and Prem, always here to cheer me up when needed.

Merci à tous mes amis Lyonnais et à la clique: PMU, Nicolas, Mélanie, Aurélie et Michel. Vous êtes géniaux, même si je resterai imbattable au tarot ! Merci pour tout, notre groupe représente beaucoup pour moi.

Finalement, je remercie ma famille: mes parents, mon frère, mes cousins et mes grands-parents pour tout leur amour et patience. Sans vous je ne serais jamais arrivé si loin. Merci.

Lausanne, 05th February 2016

A.J. L.

Publications and conferences

Publications

A.J. Lamontanara*, E.B. Gencer*, O. Kuzyk* and O. Hantschel. *Mechanisms of resistance to BCR-ABL and other kinase inhibitors*, in *Biochimica Et Biophysica Acta-Proteins And Proteomics*, vol. 1834, num. 7, 2013 [review article, *contributed equally].

A.L. Mahul-Mellier, B. Fauvet, A. Gysbers, I. Dikiy, A. Oueslati, S. Georgeon, **A.J. Lamontanara**, A. Bisquertt, D. Eliezer, E. Masliah, G. Halliday, O. Hantschel, H.A. Lashuel. *c-Abl phosphorylates α -synuclein and regulates its degradation: implication for α -synuclein clearance and contribution to the pathogenesis of Parkinson's disease*, in *Human Molecular Genetics*, vol. 23, num. 11, 2014

A.J. Lamontanara, S. Georgeon, G. Tria, D.I. Svergun and O. Hantschel. *The SH2 domain of Abl kinases regulates kinase autophosphorylation by controlling activation loop accessibility*, in *Nature Communications*, vol. 5, num. 5470, 2014.

J. Wojcik, **A.J. Lamontanara**, G. Grabe, A. Koide, L. Akin, B. Gerig, O. Hantschel, and S. Koide. *Allosteric Inhibition of Bcr-Abl Kinase by High-Affinity Monobody Inhibitors Directed to the SH2-Kinase Interface*, in *Journal of Biological Chemistry*, in revision, 2016.

Conferences and courses

EMBO - Protein expression, purification and characterization course (one week). Hamburg, Germany (3-11 September 2012). Poster presentation: "Targeting a critical SH2-kinase interface in Bcr-Abl oncoprotein."

EMBO - Conference on Allosteric interactions in cell signaling and regulation. Paris, France (14-17 May 2013).

EMBO - Conference on Cellular signalling and cancer therapy. Cavtat, Croatia (23-27 May 2014). Poster presentation: "The SH2 domain of Bcr-Abl regulates kinase autophosphorylation by controlling activation loop accessibility. "

Publications and conferences

3rd Faculty and Staff retreat of the Swiss Cancer Center Lausanne. Lausanne, Switzerland (11-12 November 2014). Short oral presentation: "Regulation of Bcr-Abl kinase activity by the allosteric SH2-kinase interface."

NCCR - Chemical Biology retreat. Villars-sur-Ollon, Switzerland (11-13 June 2014). Poster presentation: "The SH2 domain of Bcr-Abl regulates kinase autophosphorylation by controlling activation loop accessibility."

Abstract

Due to their central role in normal cellular physiology, the activity of protein kinases is tightly regulated and their aberrant activation can lead to cancer. Chronic myelogenous leukemia (CML) is a blood cancer characterized by unregulated growth of myeloid cells caused by a fusion protein, Bcr-Abl, a constitutively active form of the Abelson tyrosine kinase (Abl). While treatment with drugs targeting the ATP binding pocket of Abl leads to durable therapeutic responses, the development of drug resistance remains a major clinical problem. Targeting additional sites on kinases outside the conserved ATP pocket is thought to be a promising strategy to overcome drug resistance.

We hypothesized that protein-interacting domains such as SH2 act as allosteric regulator of kinase activity and conformation. This project aimed at understanding the molecular mechanisms underlying regulation of Abl kinases via the SH2-kinase allosteric interface as well as developing a screening strategy for small-molecules disrupters of this interface. I used recombinant Abl tyrosine kinases and conformation-specific kinase inhibitors to analyse changes in conformation and phosphorylation that occur after Abl activation. I could show that the Abl SH2-kinase interface enabled trans-phosphorylation of the activation loop and disruption of the SH2-kinase interaction abolished its phosphorylation. To determine the sufficiency of targeting the SH2-kinase interface for Bcr-Abl inhibition, high-affinity monoclonal antibodies targeting the kinase-binding surface of the Abl SH2 were developed in collaboration with the laboratory of Shohei Koide and their effects tested. The new monoclonal antibodies inhibited Bcr-Abl kinase activity *in vitro* and in cells, and induced cell death in a CML cell line. We further used one of the monoclonal antibodies to develop a screening assay based on the Homogeneous Time Resolved Fluorescence (HTRF) principle. We successfully showed that some specific donor/acceptor combinations could serve as a basis for high-throughput screening.

Finally, we have studied allosteric regulation of several other cytoplasmic tyrosine kinases with an emphasis on the Btk kinase. We showed that the Btk kinase was strongly dependent on its SH2 domain for activation loop autophosphorylation, a feature that was also observed in transfected mammalian cells. The long-term goal is to identify new allosteric regulations in oncogenic cytoplasmic tyrosine kinases that will help developing new types of therapeutics for hematological malignancies or solid tumors.

Keywords: Allosteric regulation, cytoplasmic tyrosine kinases, Abl kinase, autophosphorylation, monoclonal antibodies, cancer, chronic myeloid leukemia.

Résumé

En raison de leur rôle central dans la physiologie cellulaire, l'activité des protéines kinases est étroitement régulée et leur activation aberrante est souvent impliquée dans la formation de cancers. La Leucémie Myéloïde Chronique (CML) est un cancer du sang caractérisé par une croissance non régulée des cellules myéloïdes. Cette croissance est due à une protéine de fusion, Bcr-Abl, une forme constitutivement active de la tyrosine kinase Abelson (Abl). Bien que le traitement avec des médicaments ciblant le site de liaison à l'ATP de la kinase Abl conduit à des réponses thérapeutiques durables, le développement de résistances aux médicaments reste un problème clinique majeur. Le ciblage de nouveaux sites, en dehors de la poche de liaison à l'ATP, peut être une stratégie prometteuse pour surmonter la résistance aux médicaments.

Nous avons émis l'hypothèse que les domaines de liaisons tels que les domaines SH2 ou SH3 peuvent agir comme régulateur allostérique de l'activité kinase. Ce projet consiste à comprendre les mécanismes moléculaires sous-jacents qui régulent la kinase Abl via l'interface formée entre les domaines SH2 et kinase ainsi qu'en l'élaboration d'une stratégie de screening permettant de découvrir des molécules perturbatrices de cette interface. J'ai purifié des mutants de la protéine Abl et ai utilisé des inhibiteurs spécifiques permettant d'analyser la phosphorylation se produisant après l'activation d'Abl. J'ai pu montrer que l'interface SH2-kinase d'Abl favorise la trans-phosphorylation de la boucle d'activation, un élément clé pour l'activation d'Abl. La perturbation de cette interface empêche l'activation de la kinase Abl. Pour déterminer si empêcher la formation de l'interface SH2-kinase peut inhiber la protéine Bcr-Abl, des monobodies de haute affinité ciblant l'interface ont été développés en collaboration avec le laboratoire de Shohei Koide. Ces nouveaux monobodies ont inhibé l'activité de la kinase Bcr-Abl *in vitro* et dans des cellules, et ont induit la mort cellulaire dans une lignée dérivée de patients atteints de CML. Nous avons également utilisé un des monobodies pour développer un screening basé sur le principe de 'Homogeneous Time Resolved Fluorescence' (HTRF). Nous avons montré avec succès que certaines combinaisons spécifiques de donneur/accepteur peuvent servir de base pour un screening à haut débit.

Enfin, nous avons étudié la régulation allostérique de plusieurs autres tyrosines kinases cytoplasmiques et plus spécialement la kinase Btk. Nous avons montré que la kinase Btk était fortement dépendante de son domaine SH2 pour phosphoryler sa boucle d'activation, une observation confirmée dans des cellules de mammifères. L'objectif à long terme est d'identifier

Résumé

de nouvelles façons de cibler les protéines kinases impliquées dans des hémopathies malignes ou des tumeurs solides.

Mot-clés : Régulation allostérique, tyrosines kinases cytoplasmiques, kinase Abl, autophosphorylation, monobodies, cancer, leucémie myéloïde chronique.

Contents

Acknowledgements	i
Publications and conferences	iii
Abstract	v
Résumé	vii
List of figures	xiii
List of tables	xv
1 Introduction	1
1.1 Protein tyrosine kinases	1
1.1.1 Non-catalytic domains	1
1.1.2 Kinase domain	2
1.1.3 Implication of cytoplasmic tyrosine kinases in cancer	3
1.2 c-Abl: a prototypic cytoplasmic tyrosine kinase	4
1.2.1 The Abl kinase family	4
1.2.2 c-Abl regulation via autoinhibition and phosphorylation	4
1.3 Chronic myeloid leukemia and Bcr-Abl fusion protein	6
1.3.1 Chronic myeloid leukemia	6
1.3.2 Bcr-Abl: driver of chronic myeloid leukemia	6
1.4 Targeted therapy and development of resistances	7
1.4.1 First-generation tyrosine kinase inhibitor: imatinib as the magic bullet?	7
1.4.2 Structural mechanisms of imatinib binding	8
1.4.3 Development of resistances to imatinib	9
1.4.4 Second- and third-generation Abl inhibitors	10
1.5 Current challenges in targeting kinases	12
1.6 Targeting allosteric regulatory sites in Abl	13
1.6.1 Targeting the myristate pocket	13
1.6.2 Targeting the SH2-kinase interface	15
1.7 Aims of the work	16
	ix

Contents

2	Results	19
2.1	Characterization of bacterially expressed Abl SH2-kinase domain unit proteins	19
2.1.1	Expression and purification of recombinant Abl SH2-kinase	19
2.1.2	Recombinant Abl SH2-KD unit recapitulates kinase regulation by the SH2 domain	20
2.1.3	SAXS reconstruction of the Abl SH2-KD unit	22
2.2	Abl SH2-KD autophosphorylation ability	24
2.2.1	Mapping of autophosphorylation sites	24
2.2.2	The Abl SH2 is indispensable for activation loop autophosphorylation	24
2.3	Efficient trans-autophosphorylation requires the SH2 domain	26
2.4	The Abl SH2 domain maintains an open conformation of the activation loop	30
2.5	Targeting the Abl SH2-kinase interface with monobodies	30
2.5.1	Characterization of AS25 and AS27 monobodies	30
2.5.2	AS25 and AS27 inhibit the Abl SH2-KD activity <i>in vitro</i>	33
2.5.3	AS25 and AS27 expression decreased Abl PP and Bcr-Abl phosphorylation in cells	33
2.5.4	AS25 and AS27 induced cell death by apoptosis in K562 cells	35
2.6	Development of screening assays for Abl SH2-KD interface disrupters	38
2.6.1	Acrylodan-based fluorescent assay	38
2.6.2	HTRF-based screening assay	42
2.7	Roles of non-catalytic domains in cytoplasmic tyrosine kinases: focus on the Btk kinase	48
2.7.1	Targeted cytoplasmic tyrosine kinases and expression levels	48
2.7.2	Expression trials in S2 insect cells	49
2.7.3	Role of non-catalytic domains in activation loop phosphorylation	49
2.7.4	Btk kinase autophosphorylation <i>in vitro</i>	51
3	Discussion	53
3.1	Role of the Abl SH2 domain in the kinase autophosphorylation	53
3.2	Disruption of the Abl SH2-KD interface using monobodies	55
3.3	Screening assay development for Abl SH2-kinase interface disrupters	57
3.4	Allosteric regulation in cytoplasmic tyrosine kinases	58
3.4.1	Recombinant protein expression strategy	58
3.4.2	Activation loop autophosphorylation: a focus on the Btk kinase	58
3.4.3	General strategies for studying positive allosteric mechanisms	60
3.4.4	Targeting allosteric sites in kinases: combination therapies	61
3.5	Concluding remarks and future perspectives	62
4	Material and Methods	63
4.1	Abl protein expression, purification and biophysical analysis	63
4.1.1	Cloning of Abl constructs	63
4.1.2	Abl co-expression with YopH phosphatase and purification	63
4.1.3	Multi-angle light scattering analysis of purified Abl constructs	64

4.1.4	Circular dichroism spectroscopy	64
4.1.5	Small-Angle X-ray scattering	64
4.2	Abl kinase assays and autophosphorylation	65
4.2.1	<i>In vitro</i> kinase assays	65
4.2.2	Mapping of Abl autophosphorylation sites	65
4.2.3	Abl autophosphorylation assays	66
4.2.4	Abl transphosphorylation assays	66
4.3	HEK293 cell transfections	67
4.4	Western blotting, immunoprecipitation and antibodies	67
4.4.1	Western blotting analysis and antibodies	67
4.4.2	Abl immunoprecipitation	68
4.5	Expression and purification of recombinant monobodies	68
4.6	Retroviral transduction and FACS analysis of K562 cells expressing monobodies	68
4.7	Cytoplasmic tyrosine kinase characterization	69
4.7.1	Recombinant purification from <i>E. coli</i>	69
4.7.2	Expression and purification trial from S2 insect cells	69
4.7.3	HEK293 cells transfections	69
4.7.4	Fluorescence polarization assay with Btk SH2 domain	70
4.7.5	Btk autophosphorylation assay	70
4.8	Screening assays	70
4.8.1	Acrylodan labeling and measurements	70
4.8.2	HTRF measurements of AS25-SH2 complexes	71
Bibliography		73
Curriculum Vitae		85

List of Figures

1.1	Structural organisation overview of cytoplasmic tyrosine kinases	2
1.2	Typical structural organization of an active and inactive kinase domain	3
1.3	Autoinhibited structure of c-Abl	5
1.4	Structural organization of c-Abl and Bcr-Abl.	7
1.5	Structural features of imatinib binding to the Abl kinase	9
1.6	Structural comparison of the Abl kinase in complex with imatinib, nilotinib and dasatinib	12
1.7	Number of kinase inhibitors approved over the last 15 years	13
1.8	GNF-2 induced bending of α I-helix in Abl kinase	14
1.9	Abl SH2-kinase unit in active conformation	16
1.10	Structural overview of Abl, Fes, Csk and Src SH2/3-kinase units	17
2.1	Purification and validation of the Abl SH2-KD purity and homogeneity	20
2.2	Central Abl SH2-KD and KD mutants used in this study	21
2.3	Recombinant Abl SH2-KD recapitulates regulation via the SH2 domain	22
2.4	Structural analysis of the the Abl SH2-KD using SAXS	23
2.5	Mapping of autophosphorylated tyrosines in recombinant Abl SH2-KD	25
2.6	Disruption of the SH2-kinase interface impairs Abl autophosphorylation	27
2.7	Autophosphorylation kinetics of tyrosines 245 and 412	28
2.8	Autophosphorylation of Abl SH2-KD WT at different protein concentrations	28
2.9	The activation loop is a poor substrate for trans-phosphorylation in the absence of the SH2-KD interface	29
2.10	The SH2 domain induces a fully active conformation of the activation loop	31
2.11	AS25 binding mode and purification	32
2.12	Inhibition of the Abl SH2-KD with monoclonal antibodies <i>in vitro</i>	33
2.13	Inhibition of Abl PP phosphorylation in HEK293 cells by AS25 and AS27 monoclonal antibodies	34
2.14	Inhibition of Bcr-Abl phosphorylation in HEK293 cells by AS25 and AS27 monoclonal antibodies	36
2.15	Effects of AS25 and AS27 monoclonal antibodies on transduced K562 cells	37
2.16	Acrylodan-based screening principle	39
2.17	Kinase activity of Abl SH2-KD cysteine mutants	39
2.18	Fluorescence spectrum of Abl SH2-KD cysteine mutants	40

List of Figures

2.19	Fluorescence spectrum of Abl SH2-KD cysteine mutants comparing intact SH2-KD interface and disrupted interface via I164E mutation	41
2.20	Effect of AS25 on fluorescence spectrum of the Abl SH2-KD* E187C	42
2.21	Screening principle using indirect HTRF	43
2.22	Signal-to-noise ratio of 28 HTRF pair combinations	45
2.23	Repeats of combinations 3, 8 and 27 at different protein concentrations	46
2.24	Time-course signal-to-noise ratio of combinations 3,8 and 27	47
2.25	Effect of cleaved AS25 on HTRF signal	47
2.26	Purification of Zap70 KD from transfected S2 cells	49
2.27	Activation loop phosphorylation of several Btk, Brk and Hck kinases constructs in HEK293 cells	50
2.28	Effect of several Btk mutations on activation loop phosphorylation	51
2.29	Autophosphorylation ability of the Btk kinase in solution	52
3.1	Role of the Abl SH2-KD interface in activation loop opening summarized in a graphical model	55
3.2	Comparison of AS25 and 7c12 binding to Abl SH2	56
3.3	Model of positive allosteric regulation via protein-interacting domains	61

List of Tables

2.1	Enzymatic kinetic parameters for Abl SH2-KD and KD mutants	22
2.2	Identified <i>in vitro</i> autophosphorylation sites in the Abl SH2-KD	24
2.3	Tested HTRF pair combinations	44
2.4	Selected cytoplasmic tyrosine kinases and expression in BL21 and HEK293 cells	48

1 Introduction

1.1 Protein tyrosine kinases

Protein phosphorylation is a key biochemical hallmark of metazoans mediated by essential enzymes called protein kinases. By transferring a γ -phosphate of ATP and covalently attaching it to serine, threonine or tyrosine residues, kinases allow for quick and specific propagation of cellular signals.

The human genome encodes 518 kinases (Manning et al., 2002), of which 90 are tyrosine kinases. The protein tyrosine kinase family is divided into two types of proteins: trans-membrane receptor tyrosine kinases (RTKs) and cytoplasmic tyrosine kinases (CTKs), which are then further grouped into subfamilies based on protein sequence homology.

The CTK family consists of 34 known members, all containing a central core kinase domain and several non-catalytic domains (Robinson et al., 2002) (figure 1.1).

1.1.1 Non-catalytic domains

Non-catalytic domains are very diverse and can have important roles in cellular localization or binding of downstream targets (Neet and Hunter, 1996). For example domains such as SH2 which bind phospho-tyrosines allow tight spatial regulation and specific binding of CTKs to tyrosine-phosphorylated protein targets. The 121 SH2 domains (Machida et al., 2007) are well conserved among proteins and their role have been extensively studied. In several CTKs, it has been shown that they promote the so-called processive phosphorylation in which the kinase binds pre-phosphorylated substrate ("primed" substrate) via its SH2 and catalyzes other phosphorylation events before dissociating (Patwardhan and Miller, 2007). This phenomenon is usually required for efficient phosphorylation of protein substrates in kinases such as Abl (Mayer et al., 1995) or Src (Scott and Miller, 2000). SH3 domains bind proline-rich motifs and are as well important for recognizing cellular substrates, protein regulation and can even enhance SH2-dependent processive phosphorylation (Pellicena and Miller, 2001).

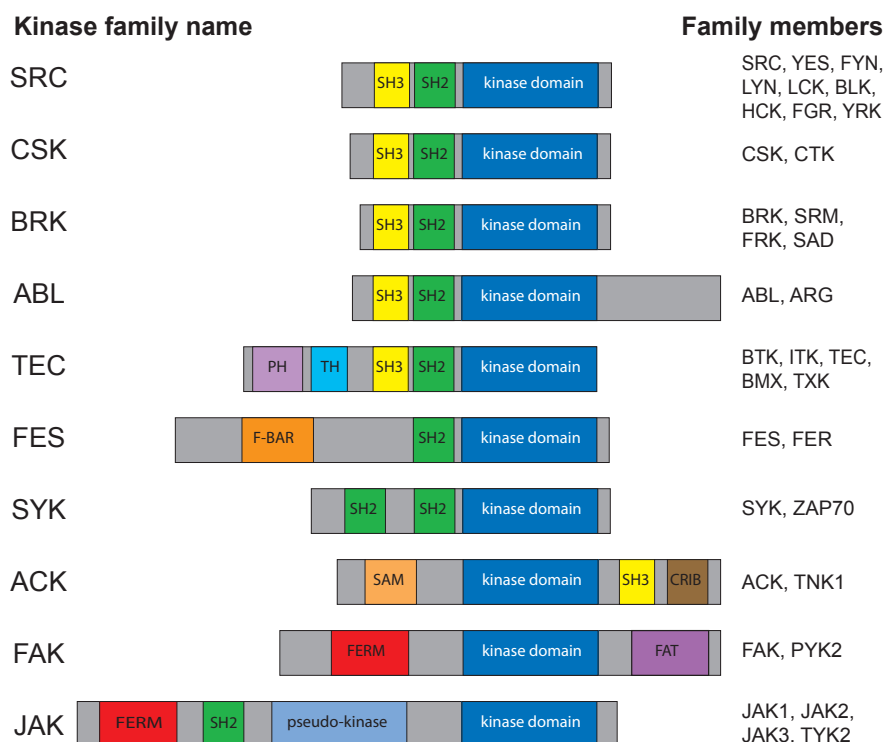


Figure 1.1 – Structural organisation overview of cytoplasmic tyrosine kinases.

Non-catalytic domain names are the following. SH2/SH3: Src-homology 2/3; PH: Pleckstrin-homology; TH: Tec-homology; F-BAR: Bin-Amphiphysin-Rvs; SAM: Sterile- α -motif; CRIB: Cdc42/Rac-interactive-binding-motif; FERM: 4.1 protein-ezrin-radixin-moesin; FAT: focal-adhesion-targeting.

Other domains such as PH and FERM allow proteins to be localized to the membrane through binding to phospho-lipids. They are usually essential for protein kinase activity and pathway activation. For example plasma membrane localization of Btk protein is an essential step for its role in B-cell activation and mutations in its PH domain can lead to X-linked agammaglobulinemia (XLA) (Mauno et al., 1995).

Finally some of these domains are implicated in protein-protein interaction complexes (SAM, CRIB). The CRIB domain in Ack kinase is indispensable for its interaction with the activated form of Cdc42 GTPase to promote cell survival and multiplication (Kato-Stankiewicz et al., 2001).

1.1.2 Kinase domain

The kinase domain is a highly conserved domain of about 300 amino-acids that transfers phosphates to the hydroxyl-group of protein substrates. The structure of a kinase domain can be sub-divided into two domains, or lobes (figure 1.2). The smaller N-terminal lobe, or N-lobe, is composed of five stranded β -sheets and a prominent α helix called helix α C. The C-lobe is

larger and mostly α -helical. ATP binds in a deep cleft located between these two lobes just beneath a conserved glycine-rich loop (Cox et al., 1994). This loop coordinates ATP binding via backbone interactions. Optimal phosphate transfer requires a precise sequence of spatial arrangements of several residues located in the glycine-rich (gly-rich) loop, the α C helix and the catalytic loop (HRD motif) (Huse and Kuriyan, 2002).

The C-lobe contains a very flexible loop called activation loop. The activation loop has the capacity to undergo large conformational changes and is switching between a closed ("inactive") conformation to an open ("active") conformation usually stabilized by phosphorylation of a particular tyrosine residue in the loop (figure 1.2). In the open conformation the loop serves as a platform for further substrate binding (Huse and Kuriyan, 2002).

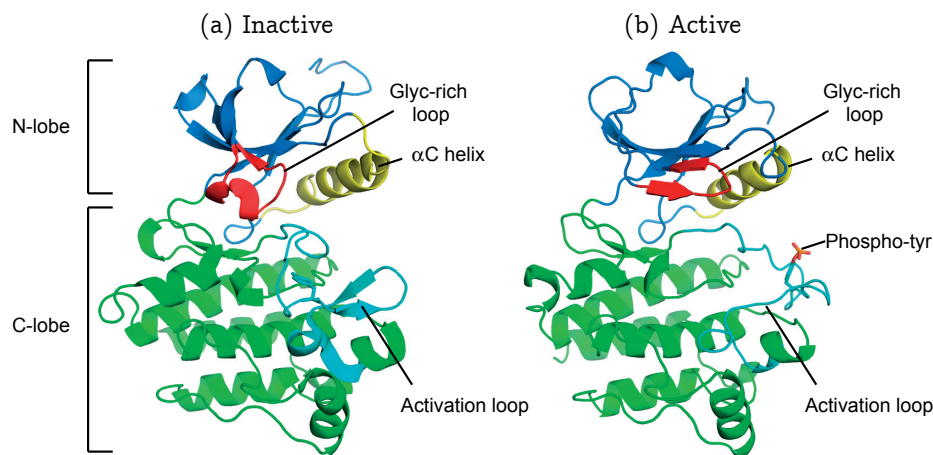


Figure 1.2 – Typical structural organization of an active and inactive kinase domain.

(a) Cartoon representation of the inactive Abl kinase domain (PDB: 1IEP). (b) Cartoon presentation of active Lck kinase (PDB: 3LCK). N- and C- lobes are shown in blue and green respectively. α C helix is shown in yellow. The activation loop (in light blue) switches between a closed conformation (a) to an open conformation (b) where in most tyrosine kinases a tyrosine residue is phosphorylated (phospho-tyr).

1.1.3 Implication of cytoplasmic tyrosine kinases in cancer

Due to their important roles in most aspects of cellular signaling, deregulation of CTKs activity by point mutations, translocations, deletions or duplications, can result in over-activation leading to cancer and other malignancies (Hubbard and Till (2000), Blume-Jensen and Hunter (2001)).

The discovery of the Src protein in 1978 (Levinson et al., 1978) led not only to the uncovering of tyrosine phosphorylation but also to the fact that protein kinases can have high transforming ability. Src kinase is now an established oncogene that can aberrantly activate pathways downstream of several RTKs. Src-family kinases (SFKs) have now well documented roles in tumor progression and invasion. SFKs can have various roles in malignancies such as breast, colorectal, prostate or lung cancer (Zhang and Yu, 2012).

Many CTKs can be oncogenic drivers and passengers in various tumor types. Btk kinase, essential for the development of B-cells, is an important drug target in chronic lymphocytic leukemia and multiple myeloma. Similarly the B-cell Syk kinase is a therapeutic target in non-Hodgkin's lymphoma, or B-cell lymphomas. Brk kinase is amplified in subtypes of breast cancer and mutations in Ack1 were identified in lung adenocarcinoma and ovarian carcinoma.

One of the paradigmatic representative of tyrosine kinases in cancer is c-Abl, which has an essential implication in chronic myeloid leukemia.

1.2 c-Abl: a prototypic cytoplasmic tyrosine kinase

1.2.1 The Abl kinase family

c-Abl is a member of the CTK family and the prototype of a sub-family which includes two members: c-Abl (ABL1) and its only paralogue Arg (ABL2, Abl related gene). Members of this family are highly conserved throughout the metazoans and ubiquitously expressed. c-Abl is localised at various sites in the cell including cytoplasm, nucleus but also mitochondria and endoplasmic reticulum (Wetzler et al., 1993).

The human ABL1 gene can give rise to two alternative splicing transcripts: ABL1a and ABL1b (Renshaw et al., 1988). The 1b splicing variant is myristoylated at the N-terminus (glycine 2) whereas the 1a variant is 19 amino acids shorter and not myristoylated (figure 1.4).

The two variants of c-Abl show a modular organization similar to that of members of Src family. They are characterized by a core tyrosine kinase domain that is preceded by SH2 and SH3 domains. Unique to c-Abl is the downstream region also called the 'last exon region'. This region is a long carboxy-terminal extension containing nuclear localization signals (NLS) that allows the protein to shuttle between nucleus and cytoplasm (Taagepera et al., 1998). This region is also implied in the interaction with F-actin (Hantschel et al., 2005) and has proline-rich motifs that function as binding sites for SH3 domains of adaptor proteins.

Cellular processes in which c-Abl is implicated range from regulation of cell growth and survival, oxidative stress and DNA damage response to actin dynamics and cell migration (Van Etten, 1999).

1.2.2 c-Abl regulation via autoinhibition and phosphorylation

Because of its involvement in many cellular processes essential for cell viability, the tyrosine kinase activity of c-Abl is very tightly controlled and c-Abl is mostly inactive in cells (Van Etten (1999), Smith et al. (1999)). Structural and biochemical studies have revealed multiple autoinhibitory mechanisms. The autoinhibition relies on a complex set of intramolecular interactions that keep the kinase in a closed and inactive conformation. The myristoyl group in the cap region has a major role in the autoinhibition of c-Abl 1b (Hantschel et al., 2003).

1.2. c-Abl: a prototypic cytoplasmic tyrosine kinase

The myristate can nestle into a deep hydrophobic pocket in the kinase C-lobe thus forcing the SH2 and SH3 domains to dock against the kinase lobes and keeping the kinase inactive (Pluk et al. (2002), Nagar et al. (2003)) (figure 1.3). In this so-called "clamped" conformation, the SH2 domain forms a tight protein-protein interface with the C-lobe of the kinase domain via a network of hydrogen bonds. The SH3 domain participates in this autoinhibited conformation by interacting with the SH2-kinase linker region that can adopt a poly-proline type II conformation. Conversion of inactive c-Abl to its active form requires the disruption of these intramolecular interactions (Hantschel et al., 2003). SH2 and SH3 binders can provoke a disassembling of the clamp conformation and dislodge the myristate. Following the breakdown of inhibitory contacts, the full activation of Abl kinase is achieved by the phosphorylation of several tyrosine residues. The non-myristoylated form c-Abl 1a seems to be regulated by intramolecular interactions as well, however, the elements that replace the function of the myristate remain to be determined.

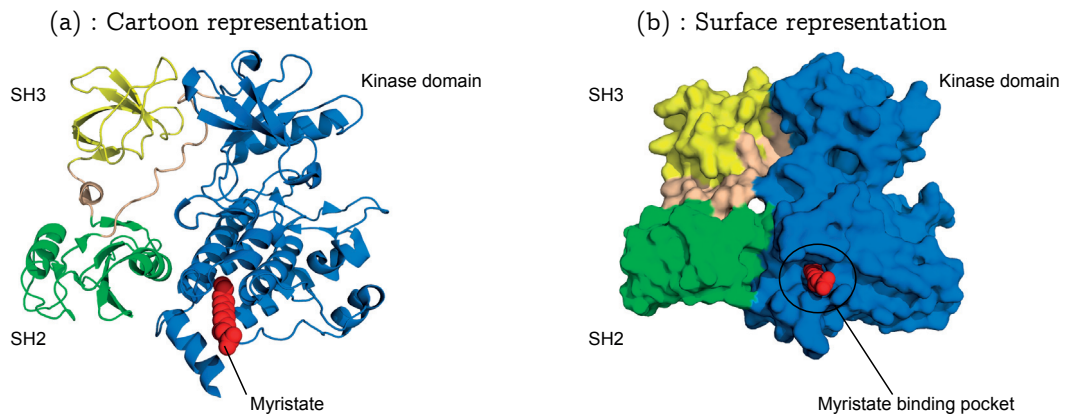


Figure 1.3 – Autoinhibited structure of Abl kinase. Autoinhibited conformation of ABL kinase (PDB: 1OPK). Cartoon (a) and surface (b) representations are shown. Kinase domain, SH2 and SH3 are shown in blue, green and yellow respectively. The myristate is shown with red spheres. The SH2-kinase linker is shown in light pink. In this autoinhibited form, the SH2 and SH3 clamp against the kinase domain, locking the kinase in an inactive state.

As for many other tyrosine kinases, c-Abl activity in cells is heavily dependent on phosphorylation sites located throughout the protein. It has been shown that the mutation of tyrosine 245 (Y245) and tyrosine 412 (Y412) to phenylalanine prevents c-Abl from activation revealing the important roles of these sites (Dorey et al., 2001). Phosphorylation of the Y245 in the SH2-kinase domain linker could inhibit the docking of the SH3 domain, stabilizing the kinase in the active conformation. This phosphorylation is coupled by a concomitant phosphorylation of Y412 in the activation loop which stabilizes the loop in a conformation that is compatible with substrate binding (Brasher and Van Etten, 2000). Due to its ability to act as a dominant oncogene once deregulated, c-Abl is a medically important and long studied protein. Its role has been extensively studied in a specific type of blood cancer called chronic myeloid leukemia.

1.3 Chronic myeloid leukemia and Bcr-Abl fusion protein

1.3.1 Chronic myeloid leukemia

In 1845, the pathologist John Hughes Bennett reported a case of spleen and liver hypertrophy in which death took place from "blood suppuration" in the *Edinburgh Medical Journal* (Bennett, 1845). Only a few weeks later, Rudolf Virchow in Berlin published a very similar case. Although one cannot know for sure, these cases probably represented the first descriptions of the disease later known as chronic myeloid leukemia (CML).

CML is a form of leukemia characterized by the unregulated growth of predominantly myeloid cells in the bone marrow and the accumulation of these cells in the blood and peripheral organs. CML occurs in all age groups but most commonly after 50 years of age and accounts for 15 % of adult leukemias (Jemal et al., 2010). CML displays three major clinical phases (Jabbour and Kantarjian, 2014). In most patients, the disease manifests as a long chronic phase that shows an increased count of peripheral blood myeloid progenitors but often remains undiscovered for years. Upon progression patients enter the accelerated phase characterized by splenomegaly and an increasing number of blast cells (immature cells). If left untreated the disease progresses to a fatal blast crisis where hematopoietic differentiation is blocked and blast cells accumulate in the bones and in the blood.

A real breakthrough in the field was the discovery of an abnormally small chromosome in cells from CML sick patients by cytogeneticists Peter Nowell and David Hungerford (Nowell and Hungerford, 1960). Later named the Philadelphia chromosome, this discovery made CML the first cancer to be clearly linked to a genetic abnormality. Thirteen years later, Janet Rowley showed that the Philadelphia chromosome was the result of a reciprocal translocation between chromosomes 9 and 22. The Philadelphia translocation juxtaposes the ABL1 gene on chromosome 9 with the breakpoint cluster region gene (BCR) on chromosome 22 leading to the expression of the fusion protein called Bcr-Abl (Rowley, 1973). The resulting fusion protein is a constitutively activated form of the Abl kinase contributing to cellular transformation.

1.3.2 Bcr-Abl: driver of chronic myeloid leukemia

In CML, the most common Bcr-Abl fusion is a protein of 210 kDa also known as Bcr-Abl p210. Bcr-Abl p210 contains the whole c-Abl sequence except the N-terminal region, replaced by Bcr. Absence of the N-terminal "cap" region prevents myristoylation of the protein and releases c-Abl from autoinhibition (McWhirter and Wang, 1991)(figure 1.4).

It has also been shown that the Bcr contains a coiled-coiled domain that is essential for leukemogenesis (McWhirter et al., 1993). This domain induces Bcr-Abl oligomerization which also disrupts c-Abl inhibition by inducing strong autophosphorylation of Abl critical tyrosine residues. Not only the fusion with Bcr affects autoinhibitory mechanisms but it also allows Bcr-Abl to activate many type of mitogenic signals.

1.4. Targeted therapy and development of resistances

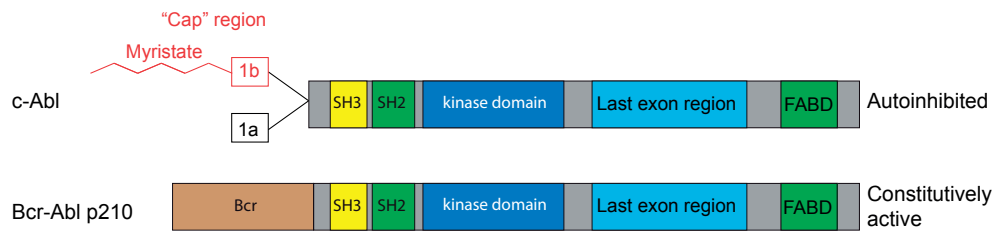


Figure 1.4 – Structural organization of c-Abl and Bcr-Abl. Upon translocation with Bcr, c-Abl loses its cap region and thus cannot be myristoylated anymore and becomes constitutively active. FABD: F-actin binding domain.

Via a plethora of interactors, Bcr-Abl activates proliferative and anti-apoptotic pathways such as MAPK (Sanchez-Arevalo-Lobo et al., 2005) or PI3K-Akt (Skorski et al., 1997). Bcr-Abl has even been shown to directly induce strong phosphorylation of STAT5, thereby activating it, and completely by-passing the canonical JAK/STAT pathway (Hantschel et al., 2012). STAT5 activation is required for leukemogenesis (Ye et al., 2006) and one of the most critical pathways for CML maintenance. STAT5 is now considered as a signalling hallmark of CML (Shuai et al., 1996).

All these alterations result in a constitutive activation of multiple survival signals by the p210 oncoprotein that contributes to transformation and resistance to apoptosis. Importantly, expression of Bcr-Abl alone is sufficient for the transformation of hematopoietic stem cells, leading to CML in humans and in a CML-like disorder in mice (Daley et al., 1990). The central role of the Abl kinase in the pathophysiology of CML was a chance for the development of molecular targeted therapies using highly specific Bcr-Abl tyrosine kinase inhibitors.

In the first half of the 20th century, CML patients were predominantly treated with chemotherapy (Silver et al., 1999) until the introduction of recombinant interferon α (rIFN α) (Talpa et al., 1986) and allogeneic stem cell transplantation (SCT) that both became standard-of-care for CML patients (Beatty, 1997). The success of rIFN α was limited because less than 50% of patients had significant responses with most of the patients suffering from side-effects (Homewood et al., 1997). Despite being a possible curative therapy, SCT suffered from high mortality and morbidity rates (Doney et al. (1978), McGlave et al. (1981)).

The true revolution in CML treatment, and more generally in cancer research, was the introduction in 2001 of the first specific tyrosine kinase inhibitor called imatinib.

1.4 Targeted therapy and development of resistances

1.4.1 First-generation tyrosine kinase inhibitor: imatinib as the magic bullet?

Due to the highly conserved structure of the protein kinase domain of the 518 human kinases, there were doubts that kinases could be targeted specifically.

Chapter 1. Introduction

But early compounds, termed tyrphostins (short name for tyrosine phosphorylation inhibitors, Yaish et al. (1988), Gazit et al. (1989)), could discriminate between serine/threonine and tyrosine kinases.

In the late 1990s, a lead compound from a protein kinase C inhibitors screening was modified and showed inhibition of a limited number of kinases *in vitro*: the Abl kinase and the receptor tyrosine kinases KIT and PDGFR (Buchdunger et al. (1996), Druker et al. (1996)). Due to the central role of Bcr-Abl kinase in CML, targeting of the Abl kinase domain has been further followed-up. Medicinal chemistry optimization led to the development of imatinib (Capdeville et al., 2002). The good tolerability and efficacy in the phase I and II clinical trials led to the approval of imatinib in 2001 by the US Food and Drug Administration (FDA) and shortly after by the European Medicines Agency (EMA) under the name Gleevec (Druker et al., 2001).

Imatinib was then the first kinase inhibitor and targeted therapy in cancer patients and was thought to be the "magic bullet" against cancer. It has converted CML from a deadly cancer to a chronic condition, in which most patients have a good quality-of-life. Today, imatinib is used as the first line therapy to treat CML patients in all disease phases as well as for gastrointestinal stromal tumors (Heinrich et al., 2003) and a few other diseases. The elucidation of the molecular mechanisms-of-action of imatinib has provided a solid basis for the understanding of kinase inhibitor binding and has helped to identify key mechanisms by which cancer cells may become resistant.

1.4.2 Structural mechanisms of imatinib binding

Imatinib lays at the interface between the N- and C-terminal lobes of the Abl kinase domain, in the so-called hinge-region (Nagar et al. (2002), Schindler et al. (2000), figure 1.5). Its binding site overlaps with the ATP binding and imatinib is therefore an ATP-competitive inhibitor. Imatinib forms a number of interactions, especially hydrogen bonds, with both the N- and C-lobes of the kinase domain. Drug binding induces a down folding of the Gly-rich loop maintained by a water-mediated hydrogen bond between residues Y272 and N341 (figure 1.5). The flexibility of the Gly-rich loop is important for the binding of imatinib as the conformational changes of the loop increases surface complementarity with the drug.

Another important aspect is that imatinib mostly binds to the closed conformation of the Abl activation loop. This binding mode is referred as type 2 kinase inhibition, which is characterized by an inactive conformation of the activation loop that folds into the active site occluding substrate binding (figure 1.5). More importantly, residue D381 in the conserved Asp-Phe-Gly (DFG) motif, located at the beginning of the activation loop and being essential for the coordination of ATP, is found displaced from its inward facing orientation in active kinases toward the "out" conformation. This not only prevents kinase activity but the concomitant inward rotation of residue F401 of the DFG motif exposes a hydrophobic region directly adjacent to the ATP site that is recognized by type 2 inhibitors (hydrophobic site 1, figure 1.5). Another hydrophobic region that is not contacted by ATP is exploited by the imatinib molecule and

1.4. Targeted therapy and development of resistances

contributes to its high binding specificity (hydrophobic site 2, figure 1.5). Access to this site is controlled by the so-called gatekeeper residue, which is a threonine (residue T334) in Bcr-Abl and which forms a hydrogen bond with imatinib.

Despite the great clinical efficacy, the success story of imatinib has been hampered by the emergence of drug resistances (Lamontanara et al., 2012).

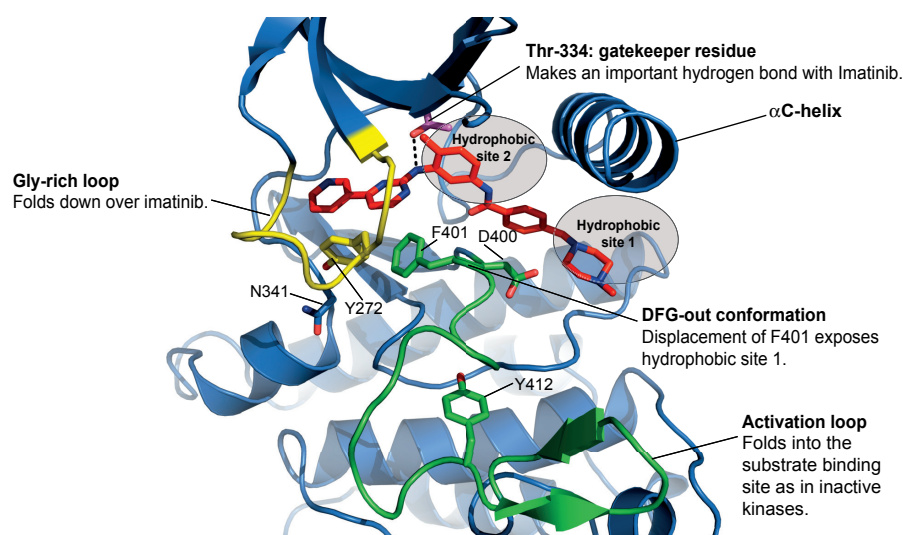


Figure 1.5 – Structural features of imatinib binding to the Abl kinase. A cartoon representation of the crystal structure of the Abl kinase domain bound to imatinib (red sticks) is shown (PDB: 1IEP). Imatinib binds an inactive conformation of the Abl kinase with the activation loop (green) occluding the substrate binding site and the DFG motif displaced in the out conformation, exposing hydrophobic site 1. The binding of imatinib induces a down folding of the Gly-rich loop (yellow). The gatekeeper residue (T334, purple) makes an important hydrogen bond with imatinib and controls access to the hydrophobic site 2. Figure modified from Lamontanara et al. (2012).

1.4.3 Development of resistances to imatinib

Just before the introduction of imatinib to the market, scientists began to observe a number of leukemic derived cells lines resistant to the drug (Mahon et al., 2000). This was rapidly followed by clinical resistance in patients (Gorre et al., 2001) and led the efforts to understand the underlying mechanisms. Patients that failed to achieve responses at predefined time points were described as primarily resistant to therapy, and those who lost previously obtained regression were considered as secondarily resistant and developed so-called acquired resistances.

Many types of resistance mechanisms to imatinib have been studied. While some Bcr-Abl independent resistances were observed such as upregulation of drug efflux (Illmer et al., 2004), most patients relapse because of Bcr-Abl dependent mechanisms such as Bcr-Abl overexpression (Gadzicki et al., 2005) or most commonly, mutations in the Abl kinase domain.

Chapter 1. Introduction

The major mutational hotspot is the gatekeeper residue of Bcr-Abl and the T334I mutation was the first identified in relapsed CML patients (Gorre et al., 2001). The absence of the hydroxyl group normally provided by the side chain of residue T334 (figure 1.5) prevents formation of a hydrogen bond with imatinib. In addition, isoleucine is a bulkier residue and therefore sterically hinders imatinib binding. This strongly increases the IC₅₀ of imatinib to concentrations exceeding the plasma concentrations that can be reached in patients.

The Gly-rich loop is a second hotspot for mutations in Bcr-Abl. Mutations such as Y272H/F and E274K/V are most commonly observed (Soverini et al., 2012). The Y272H/F mutation results in the loss of the hydrogen bond that normally keeps the Gly-rich loop locking imatinib in its binding site (Roumiantsev et al., 2002) (figure 1.5). In comparison to the T334I mutation, the degree of resistance of Gly-rich loop mutations is relatively mild. Typically less than a 10-fold increase in IC₅₀ relative to unmutated Bcr-Abl is observed. But this change is sufficient to restore Bcr-Abl kinase activity in imatinib-treated patients carrying these mutations.

A third mutation hot-spot is the activation loop, with residue H415 being the most frequently mutated. The crystal structure of the Abl kinase domain carrying the H415P mutation displays the active conformation of the activation loop to which imatinib binds less readily (Young et al., 2006). In line with this observation, the H415P mutation was shown to strongly activate Abl kinase activity providing a possible explanation for the observed imatinib resistance (Sherbenou et al., 2010). Thus, activation loop mutations, although not contacting imatinib directly, shift the equilibrium towards the active conformation of the kinase domain, which weakens imatinib binding.

Drug resistance is one of the main driver in continuing research and development of new inhibitors. This has led to the approval of several second- and third-generation inhibitors.

1.4.4 Second- and third-generation Abl inhibitors

Because most resistant point mutations only mildly decrease imatinib efficiency (not more than 10-fold, O'Hare et al. (2005)), increasing the plasma drug concentration seemed a possible way to deal with resistance. Higher doses of imatinib in the initial phase of therapy were shown to increase the depth and kinetic of responses, which is associated with improved survival (Hehlmann et al., 2011). The downside of this approach is the increased toxicity observed at higher imatinib doses and only mutants conferring rather mild (2-3-fold increased IC₅₀) resistance are likely targetable using this approach. Therefore, efforts have concentrated on the development of new drugs that target Bcr-Abl carrying point mutations in the kinase domain directly.

Three second-generation inhibitors have been approved for the treatment of imatinib-resistant or -intolerant patients: nilotinib, dasatinib and bosutinib. Nilotinib and dasatinib have also been approved for front-line therapies.

Nilotinib was developed based on the structure of the Abl-imatinib complex and inhibits

1.4. Targeted therapy and development of resistances

most of the common mutations, although some Gly-rich loop mutations are only partially inhibited. The drug retains the main scaffold of imatinib and binds very similarly to the inactive conformation of the Abl tyrosine kinase (type 2 inhibitor, figure 1.6). Nilotinib showed a better fit to the kinase (figure 1.6) with a less stringent binding allowing for higher flexibility and explaining its efficiency for resistant mutants (Weisberg et al., 2007). Nilotinib is very specific and mainly targets the same kinases as imatinib; Abl1/2, KIT, PDGFRA/B and DDR1/2 (Rix et al. (2007), Hantschel et al. (2008)).

For dasatinib, the mechanism of inhibition differs drastically from imatinib and nilotinib. The crystal structure of the dasatinib-Abl complex showed that the drug binds the active form of the Abl kinase domain (activation loop opened, type 1 inhibitor)(figure 1.6, Tokarski et al. (2006)). Dasatinib occupies a different part of the cleft between the N- and C-lobe. While the central core overlaps with imatinib, the rest of the molecule extends in the opposite direction, pointing toward the solvent. The drug does not occupy the hydrophobic site 2 (figures 1.5 and 1.6) and therefore does not need a DFG-out conformation to bind. In contrast to imatinib, no conformational changes of the Gly-rich loop were observed. This allows dasatinib to bind with less stringent conformational requirements, which contributes to its high efficacy. Dasatinib has a much broader target spectrum than imatinib and nilotinib. It potently inhibits all Src kinases, most Tec kinases, almost the entire EphA/B family but also serine-threonine kinases in addition to the kinases inhibited by imatinib and nilotinib.

Bosutinib has very similar properties to dasatinib in terms of inhibition type (type 1), potency (low nanomolar IC_{50}) and spectrum of kinase domain mutations being inhibited (Golas et al. (2003), Puttini et al. (2006)). Bosutinib has an even broader target spectrum than dasatinib (Bantscheff et al. (2007), Rensing Rix et al. (2009)).

All second-generation inhibitors remained inefficient at inhibiting the common point mutation T334I (gatekeeper mutation). This prompted the development of third-generation inhibitors specifically targeting the gatekeeper mutation. So far, one such inhibitor has been approved: ponatinib.

Ponatinib is a type 2 inhibitor that efficiently targets the T334I mutation (O'Hare et al., 2009). It binds in a very similar manner as imatinib and nilotinib, but an ethynyl linkage (C-C triple bond) allows ponatinib to avoid sterical clashes with the T334I mutant. Ponatinib has medium specificity targeting Src kinases but also receptor tyrosine kinases, such as KIT, PDGFR, VEGF, and the FGFR family members. Its good efficacy in patients carrying the T334I mutation (Cortes et al., 2013) has led to the FDA-approval of ponatinib in December 2012.

One year following approval, the FDA requested to suspend drug marketing as more than 25% patients suffered from severe arterial or venous thrombosis (Valent et al., 2014). In January 2014, ponatinib was reintroduced in the market but for a limited number of patients: the ones harbouring the T334I mutation, or patients for whom no other inhibitors are indicated or tolerated. These safety issues greatly hampered the use of the only current inhibitor on the market that can target the T334I mutation.

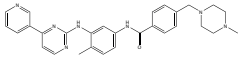
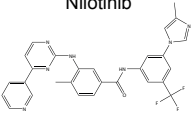
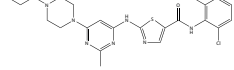
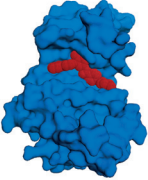
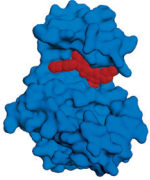
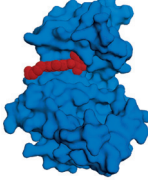
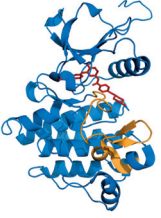
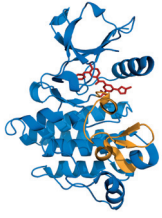
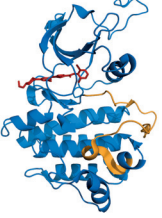
Name and structure	<p>Imatinib</p> 	<p>Nilotinib</p> 	<p>Dasatinib</p> 
Generation	First	Second	Second
Surface representation			
Binding mode	 <p>Type 2</p>	 <p>Type 2</p>	 <p>Type 1</p>

Figure 1.6 – Structural comparison of the Abl kinase in complex with imatinib, nilotinib and dasatinib. For each inhibitor its name, structure and generation is shown. The complexes with Abl kinase are displayed using surface representation of the kinase (blue) and respective inhibitors (red). Finally binding type (1 or 2) is shown with cartoon representation of the kinase (blue) with activation loop in brown and inhibitors with a stick representation (red).

1.5 Current challenges in targeting kinases

After the milestone approval of imatinib in 2001, an exploding amount of therapeutic kinase inhibitors have been developed and approved over the last decade (figure 1.7). As of April 2015, 28 kinase inhibitors have been approved (Wu et al., 2015) with an average number of 1 per year between 2000 and 2009 increasing to more than 3 per year between 2010 and 2015 (figure 1.7). Most of the approved inhibitors target tyrosine kinases (figure 1.7) and 26 out of the 28 approved drugs have been developed for cancer therapy showing the important implication of the tyrosine kinase group in targeted cancer therapy. Despite the drastic progress in kinase-based drug discovery over the past 15 years, the field of classical kinase inhibitor is facing several challenges.

First, only a small-subset of kinases are targeted. This clear bias is illustrated by the fact that three groups of tyrosine kinases - namely Bcr-Abl, ErbBs and VEGFRs - account for 18 out of the 28 approved drugs.

Second, for most of the current treatments using ATP-competitors, patients develop resistances through points mutations, usually in the kinase domain, decreasing drastically drug efficiency. As for Abl, it is common to observe mutations of the gatekeeper residue and for

1.6. Targeting allosteric regulatory sites in Abl

example lung adenocarcinomas patients that were treated with gefitinib or erlotinib acquired resistance due to the T790M mutation in EGFR (Pao et al., 2005), which corresponds to the T334 gatekeeper residue position in Bcr-Abl.

Finally, developing highly specific ATP-competitors has been discouraging and an inherent problem with kinase inhibitors. This fact is explained by the high sequence similarity and folding among kinase domains. In fact, almost all current inhibitors have dozens of off-target kinases (Davis et al. (2011), Anastassiadis et al. (2011)) leading to compromised tolerability and sometimes life-threatening side-effects (as observed with ponatinib).

A more effective approach would be to simultaneously or alternatingly target sites outside the ATP-pocket, commonly named allosteric sites (Fang et al., 2012). These sites need to be critical for the regulation of kinase activity or the recruitment of substrates to be viable drug targets. Hence, a deep understanding of allosteric kinase regulatory mechanisms is necessary to exploit exclusive structural and biochemical features of particular oncogenic kinases

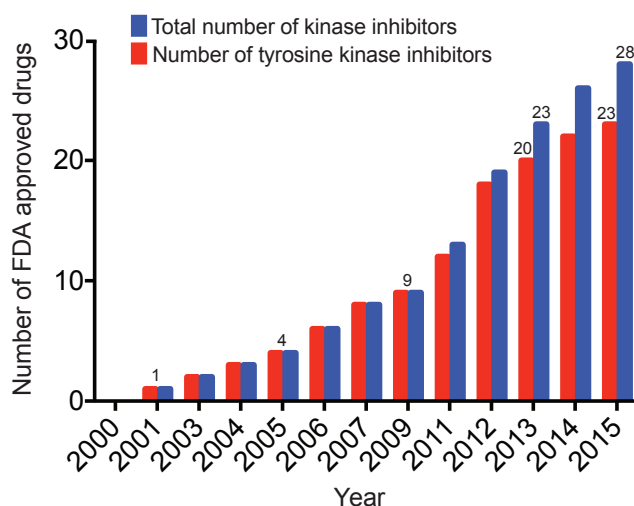


Figure 1.7 – Number of kinase inhibitors approved over the last 15 years. Red bars represent tyrosine kinase inhibitors and blue bars all types of kinase inhibitors. Based on Wu et al. (2015).

1.6 Targeting allosteric regulatory sites in Abl

1.6.1 Targeting the myristate pocket

As described in Section 1.2.2, the Abl 1b kinase isoform harbours a N-terminal myristoylation that is accommodated in a deep allosteric binding pocket in the tyrosine kinase domain. Because the N-terminal myristoylation region is missing in Bcr-Abl fusion protein, it was suggested that the myristate binding pocket could be targeted using compound mimicking myristate effects and push the protein to its autoinhibited form (Hantschel et al., 2003).

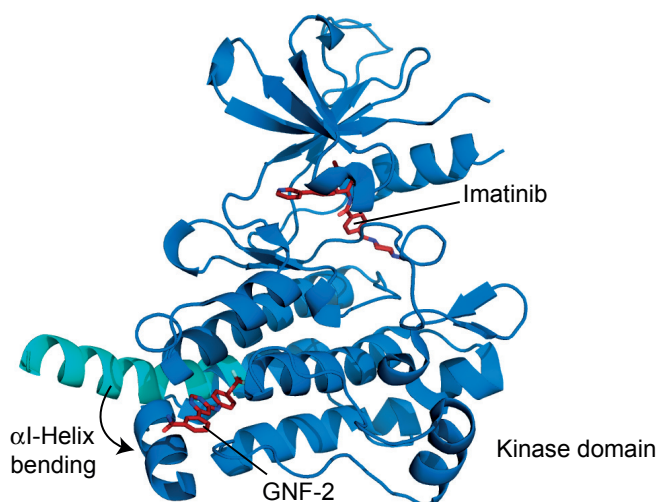


Figure 1.8 – GNF-2 induced bending of α I-helix in Abl kinase. Binding of GNF-2 to the myristate pocket in Abl kinase C-lobe (blue, PDB: 3K5V) induces a sharp bend of helix α I as compared to activated Abl (cyan, PDB: 2QOH). This bending mimicks the binding of the myristate in the same pocket

This pocket has indeed been successfully targeted by compounds such as GNF-2 in Bcr-Abl dependent cell lines and *in vitro*. Binding experiments using recombinant Abl kinase confirmed that GNF-2 was acting as a non-ATP-competitive kinase inhibitor (Adrián et al., 2006). As supported by mutagenesis studies and kinase assays, functional inhibition by GNF-2 requires the involvement of the SH3 and SH2 domain to induce the autoinhibited clamped conformation (Adrián et al., 2006).

Despite its very good potency against certain imatinib resistant mutations, this compound failed to inhibit the T334I mutation (Adrián et al., 2006). Interestingly, it has shown efficacy against this mutation when combined with classical ATP competitive inhibitors (Khateb et al., 2012). The crystal structure of the Abl kinase domain bound to both GNF-2 and imatinib has been recently obtained (Zhang et al., 2010). Once bound to the myristate pocket, mostly through hydrophobic interactions, GNF-2 induces a sharp bending of the C-terminal helix α I (figure 1.8) also observed when a myristate was bound and facilitating the stabilization of an inhibited conformation. Oddly, the binding of imatinib to the kinase domain in complex GNF-2 seemed very similar to the kinase bound to imatinib only and this could not explain the synergistic effects observed in cells.

To shed light on why such combination of a myristate pocket binder with classical ATP competitors could efficiently inhibit the gatekeeper mutant, hydrogen-exchange mass-spectrometry has been carried out using a compound with improved pharmacokinetic properties termed GNF-5 (Zhang et al., 2010). In addition to changes in the myristate pocket, changes in peptides near the ATP-binding site were also seen, implying that binding of GNF-5 affected the ATP-site. This showed that allosteric targeting of Abl kinase can cause dynamic perturbations to residues in the ATP-binding site and provided a mechanism by which synergistic interactions

between these two sites could occur. Recent studies have shown that binding of imatinib to Abl kinase leads to an unexpected open conformation of the multidomain SH3-SH2-kinase c-Abl core. The combination of imatinib with the allosteric inhibitor GNF-5 restored the closed, inactivated state (Skora et al., 2013).

1.6.2 Targeting the SH2-kinase interface

Although the canonical function of the SH2 domain is the binding of phosphotyrosine residues, additional regulatory roles of the SH2 domain in CTKs have been recently discovered. Upon Abl kinase activation, the SH2 domain has been shown to bind to the tip of the kinase N-lobe in diverse structural studies, forming a tight SH2-kinase interface (figure 1.9) (Grebien et al., 2011). The interaction, mostly hydrophobic, is maintained through the critical I164 residue located in the SH2. Importantly, none of the SH2 residues implied in this interaction are involved in phosphotyrosine binding.

The first evidence that the SH2-kinase interface observed in active Abl influences leukemogenesis was recently provided in a study of the Bcr-Abl SH2-kinase interface. In this study, a mutation disrupting the SH2-kinase interface, the isoleucine 164 to glutamate mutation (I164E), reduced catalytic activity and autophosphorylation sites (Grebien et al., 2011). On the contrary, the T231R mutation stabilizing the interaction between the SH2 and the kinase via formation of an additional ionic interaction with glutamate 294 (figure 1.9) drastically increased Bcr-Abl autophosphorylation ability. Of note, the T231R mutation was observed in a patient resistant to imatinib (Sherbenou et al., 2010), highlighting the possible importance of this new mechanism of action for Bcr-Abl activity and inhibition. Interestingly, the I164E mutation also sensitized Bcr-Abl kinase resistant mutants (e.g, the T334I mutation) to imatinib and other Abl kinase inhibitors. More importantly disruption of the SH2-kinase domain interface using the I164E mutation completely abolished leukemia formation in a mouse bone marrow transplantation model (Grebien et al., 2011).

The authors then generated single-domain binding proteins based on the fibronectin type III domain (FN3), termed monobodies, able to bind the Abl SH2 domain. Monobodies are small proteins of 10 kDa that can bind with high affinity and specificity to their targets making them robust alternatives to antibodies (Koide et al., 1998). Monobodies are stables and easily expressed in *E. coli* and do not harbour any disulfide bonds, making them functional even in reducing environments such as cytoplasm. They can readily be used as genetically encoded intracellular inhibitors, and can be useful tools for *in vitro* studies using mammalian cells or in solution. Monobodies are usually highly specific and achieve affinity in the low nanomolar range and have been proven to be excellent tools for dissecting signalling networks and finding new possible therapeutic targets (Sha et al., 2013). The binding of a monobody to the Abl SH2 domain, could indeed interfere with the formation of the interface, indicating that this interface could be a pharmacologically tractable target. The monobody also inhibited Bcr-Abl kinase activity (Grebien et al., 2011).

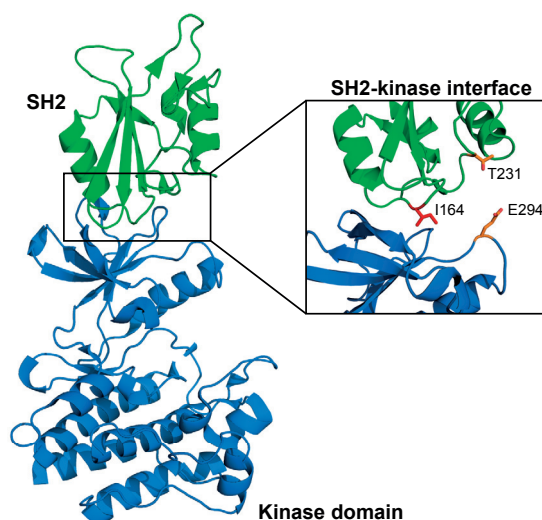


Figure 1.9 – Abl SH2-kinase unit in active conformation. Upon activation, the SH2 (green) binds at the tip of the kinase N-lobe (blue) forming a tight SH2-kinase interface (PDB: 1OPL). The isoleucine 164 (I164) in the SH2 is a crucial residue and its mutation disrupts the interaction between the two domains. Mutation of threonine 231 (T231) to arginine makes an ionic interaction with glutamate 294 (E294) and increases the interaction.

Interestingly the SH2 orientation toward the kinase domain was similar between Abl, Fes and Csk, and always sitting on the top of the kinase N-lobe albeit with different orientations (figure 1.10). The physiological relevance of this interface was more extensively studied in the case of the Fes kinase (Filippakopoulos et al., 2008). A similar construct was obtained for Src but showed little to no interactions between the SH2 and kinase domain (Cowan-Jacob et al., 2005).

1.7 Aims of the work

Despite its importance in the development of leukemogenesis, the molecular mechanisms underlying the Abl SH2-kinase interface are poorly characterized. With the development of resistances against tyrosine kinase inhibitors and side-effects observed with some of them, it is becoming evident that new type of regulatory sites should be found. My project aims at understanding the regulation of Abl kinase via the SH2-kinase interface. Through this work we would like to analyze the Abl SH2-kinase allosteric regulation using an *in vitro* recombinant system and to further confirm its therapeutic usage.

With the exception of a few kinases, little is known about the domain arrangements and conformations in active CTKs. Regulation of CTKs has not been studied in a defined standardized way through comparative analysis of enzymatic and structural characterization. Allosteric regulation in kinases might imply complex molecular re-wiring with long-range communications that need to be further investigated. Understanding these mechanisms will pave the way to the exploitation of regulatory secondary sites in kinases.

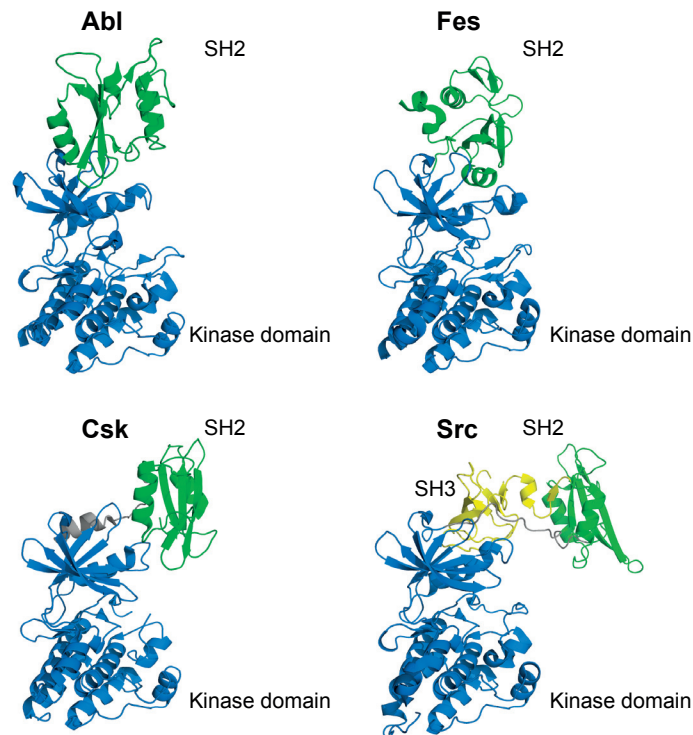


Figure 1.10 – Structural overview of Abl, Fes, Csk and Src SH2/3-kinase units. Abl (PDB: 1OPL), Fes (PDB: 3BKB) and Csk (1K9A) display similar features where their SH2 domains (green) sit on top of their kinase domains (blue) with different orientations. In Src (PDB: 1Y57), little to no interaction is observed between the SH3/2 domain and the kinase.

The three major questions of my thesis are:

- Can we obtain highly pure and active recombinant Abl kinase constructs and recapitulate SH2-kinase regulation *in vitro*? In that context several constructs harbouring point mutations will be analyzed in order to better understand the molecular mechanisms implied. This will also permit to shed light on the role and influence of phosphorylation on the positive kinase regulation by the Abl SH2 domain.
- Can the Abl SH2-kinase be a possible therapeutic target? I would like to confirm the importance of the Abl SH2-kinase interface as a possible therapeutic and targetable interface with the help of monoclonal antibodies and develop screening assays for small-molecules that could interfere with the formation of this interface.
- Is allosteric kinase activation via SH2, or other non-catalytic domains, a possible feature of several other CTKs? I would like to define a standardized way of studying multi-domain constructs of CTKs in solution and in cells and to further establish the role of possible allosteric mechanisms in concerned CTKs.

2 Results

2.1 Characterization of bacterially expressed Abl SH2-kinase domain unit proteins

2.1.1 Expression and purification of recombinant Abl SH2-kinase

The detailed understanding of allosteric mechanisms in Abl kinase and the potential roles of new allosteric protein-drug interactions demands a method for the production of proteins in the milligram scale.

We have set-up an *E.coli* expression system that gave good yield, purity and kinase activity. The protocol is based on the co-expression of different Abl kinase mutants with a tyrosine-phosphatase named Yersinia Outer Phosphatase (YopH) (Seeliger et al., 2005). YopH is a phosphatase essential for Yersinia virulence that has a very high non-specific tyrosine phosphatase activity (Bliska et al., 1991).

To confirm that the protocol in place could give highly pure and stable recombinant Abl kinase, the wild-type (WT) SH2-kinase domain (SH2-KD) unit was first purified by nickel affinity and ion exchange chromatography. The Abl SH2-KD protein eluted with a gradient of imidazole in a single peak (data not shown) and the pooled fractions were analyzed by SDS-PAGE (figure 2.1a). The major part of the protein contaminants was eliminated in the flowthrough and wash fractions (figure 2.1a). At this step, the main impurity was the YopH protein, which tends to unspecifically bind Nickel affinity resin despite the lack of His-tag.

Based on the strongly different pI, subsequent anion exchange chromatography on a MonoQ column was used to remove the YopH contaminant. The YopH impurity was correctly eliminated in the anion exchange flowthrough (figure 2.1a). Abl SH2-KD was eluted with a linear gradient of NaCl (0-350 mM). Only one major peak was observed (figure 2.1b) and the fractions were pooled. The fraction contained pure SH2-kinase protein and almost no detectable phosphatase activity, as determined using an *in vitro* phosphatase assay (data not shown). Protein identity was confirmed by mass spectrometry and was in close agreement with the expected

Chapter 2. Results

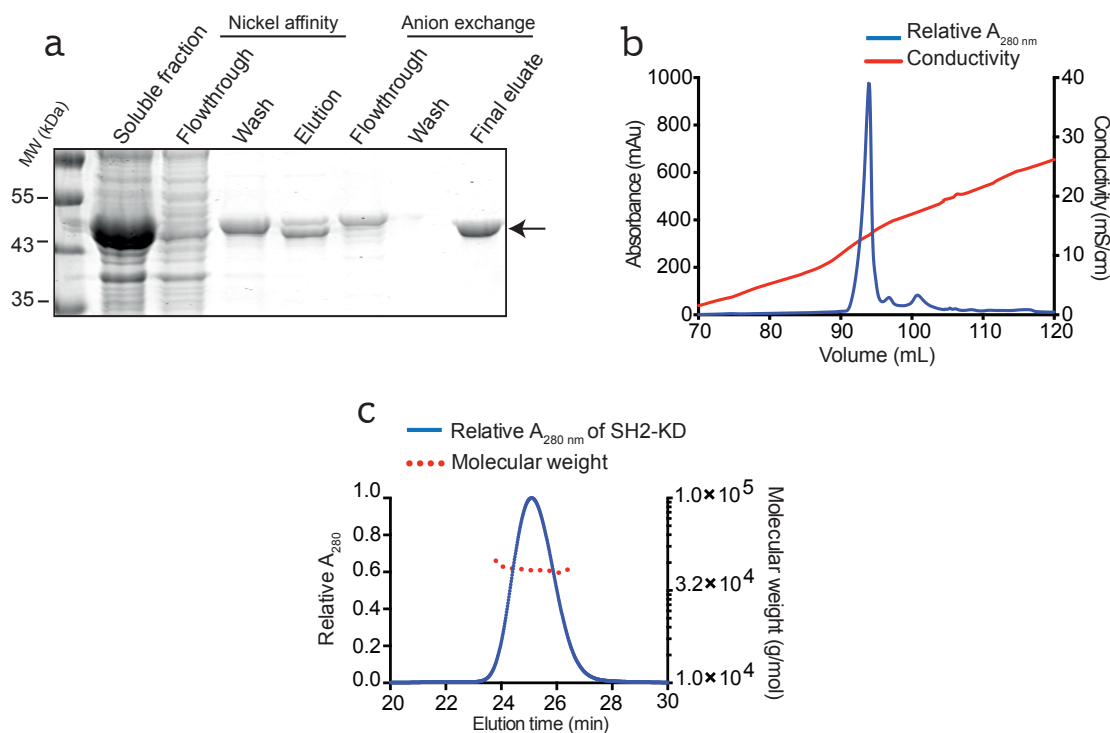


Figure 2.1 – Purification and validation of the Abl SH2-KD purity and homogeneity.

(a) Coomassie staining of fraction collected at different steps of purification. (b) Chromatogram of anion exchange showing a main peak for the Abl SH2-KD after NaCl elution. (c) Gel filtration coupled with a multi-angle light-scattering analysis of the Abl SH2-KD.

molecular mass (46681 Da for an expected weight of 46666 Da). No tyrosine phosphorylation was detectable with mass spectrometry showing that the purification workflow gives pure and unphosphorylated Abl SH2-KD.

To confirm monodispersity, we analyzed purified Abl SH2-KD using a gel filtration coupled to a Multi-Angle Light Scattering system (MALS). The Abl SH2-KD WT eluted as a single monodisperse peak with a calculated mass of about 43 kDa (± 5 kDa) (figure 2.1c). Despite MALS being a very sensitive technique to detect protein aggregation, none was found in the recombinant protein preparation. Encouraged by the quality of the purified Abl SH2-KD WT, I purified several Abl kinase mutants for biochemical and biophysical characterization.

2.1.2 Recombinant Abl SH2-KD unit recapitulates kinase regulation by the SH2 domain

Following the same protocol as for the Abl SH2-KD WT, I purified several Abl SH2-KD mutants as well as Abl kinase domain only (KD).

2.1. Characterization of bacterially expressed Abl SH2-kinase domain unit proteins

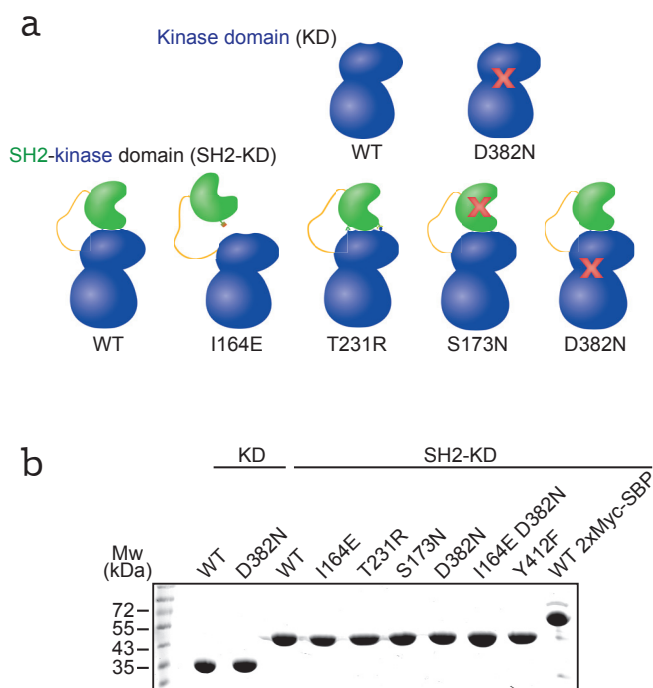


Figure 2.2 – Central Abl SH2-KD and KD mutants used in this study. (a) Schematic representation of the central mutants used in this study. (b) Coomassie staining of 20 μg of the purified mutants. Figure modified from Lamontanara et al. (2014).

The main mutants used in this study are the following (figure 2.2a):

- The I164E mutation in the SH2 domain predicted to decrease interaction with the KD N-lobe and the T231R predicted to increase it (Grebien et al., 2011)
- The S173N mutant in the SH2 domain impaired in phospho-tyrosine binding
- Kinase-activity defective Abl KD and SH2-KD mutants via the D382N mutation

All of the mutants were obtained with very good purity (figure 2.2b) and were monomeric and monodisperse (data not shown).

To confirm that the recombinant proteins could recapitulate the role of the SH2 domain observed in cells (Grebien et al., 2011), *in vitro* enzyme kinetic experiments using an optimal Abl substrate peptide (Abltide) was performed. We observed an increase of the Abl SH2-KD V_{max} when compared with KD (figure 2.3a and table 2.1). As expected the I164E nullified the increase whereas the T231R slightly increased the V_{max} compared to Abl SH2-KD WT. The phosphotyrosine binding deficient S173N mutant had similar enzymatic properties to WT. The far-ultraviolet circular dichroism spectra of SH2-KD WT and I164E were virtually identical, indicating that the decrease in kinase activity was not due to protein unfolding or loss of stability when the SH2-KD interface is disrupted (figure 2.3b).

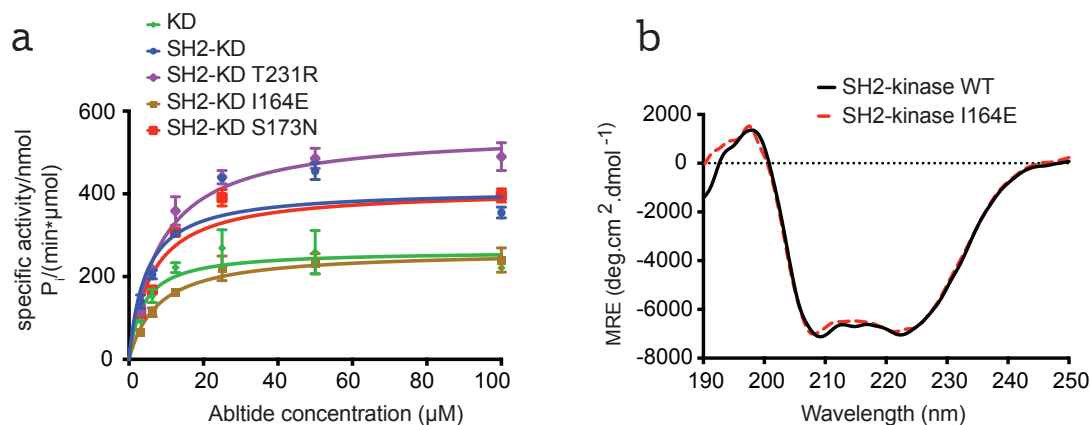


Figure 2.3 – Recombinant Abl SH2-KD recapitulates regulation via the SH2 domain. (a) Purified Abl mutants were assayed for kinase activity against an optimal Abl peptide and the kinetics fitted using the Michaelis-Menten equation ($n = 2$). (b) Far-UV circular dichroism analysis of Abl SH2-KD WT and I164E showed no difference in folding upon interface disruption. MRE: Mean Residue Ellipticity. Figure modified from Lamontanara et al. (2014).

Table 2.1 – Enzymatic kinetic parameters for Abl SH2-KD and KD mutants. V_{max} and K_M values computed from figure 2.3a using Michaelis and Menten equation.

Constructs	V_{max} [nmole P_i min^{-1} μM^{-1}]	K_m [μM]
KD	≈ 260	≈ 4
SH2-KD	≈ 410	≈ 5
SH2-KD I164E	≈ 260	≈ 8
SH2-KD T231R	≈ 550	≈ 8
SH2-KD S173N	≈ 400	≈ 6

Despite the lack of tyrosine phosphorylation, the bacterially expressed Abl proteins exhibited robust *in vitro* kinase activity, in line with the results of Abl KD purified from insect cells (Schindler et al., 2000). This showed that previous observations on the allosteric role of the SH2 domain in cells could be recapitulated *in vitro* with bacterially expressed Abl proteins.

2.1.3 SAXS reconstruction of the Abl SH2-KD unit

To confirm that the structure of the Abl SH2-KD unit in solution was indeed the top-hat conformation where the SH2 domain would sit on top of the kinase, we conducted Small-Angle-X-ray Scattering (SAXS) reconstruction experiments in collaboration with Dmitri Svergun at EMBL Hamburg. The SAXS revealed increasingly extended conformation in KD ($D_{max} = 70 \text{ \AA}$) to SH2-KD ($D_{max} = 95 \text{ \AA}$) to SH2-KD I164E ($D_{max} = 110 \text{ \AA}$) (figure 2.4a). The Abl SH2-KD and KD *Ab initio* reconstructions revealed rigid structures that fit very well the available crystal structures (figure 2.4b,c). These results indicated that the SH2 is indeed interacting with the N-lobe of the KD in solution.

2.1. Characterization of bacterially expressed Abl SH2-kinase domain unit proteins

For the SH2-KD I164E mutant, the data suggested significant domain rearrangements, as rigid body modelling using the available domain structures did not provide a satisfactory fit. Indeed, the Kratky plot (figure 2.4a) showed an increase in the flexibility of the I164E mutant because a shift from the expected peak was observed. Thus, the potential flexibility of the mutant and the scattering data was analysed in terms of co-existing conformer ensembles. The selected ensembles that elucidated the conformational space of possible SH2 domain positions with respect to the KD are displayed in figure 2.4c. The SH2 significantly shifted from its top-hat position confirming the central role of the I164 residue in maintaining a tight interaction with the tip of the KD.

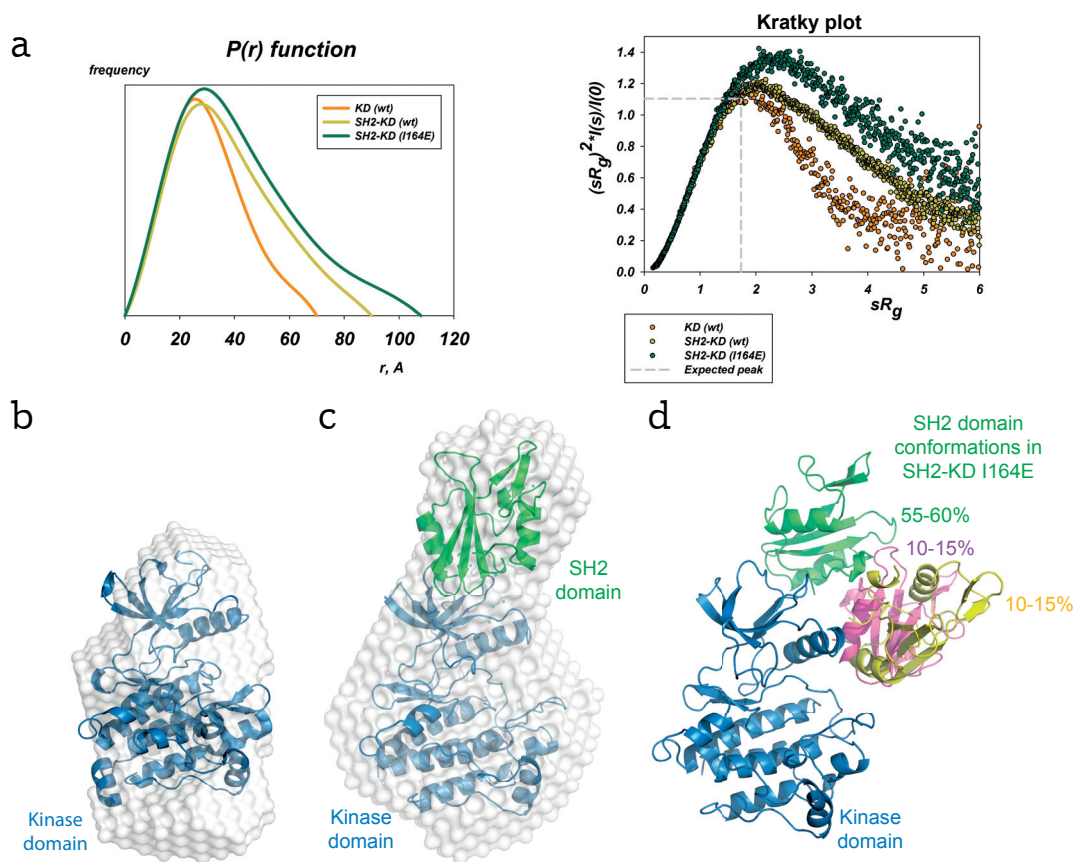


Figure 2.4 – Structural analysis of the Abl SH2-KD using SAXS. (a) $P(r)$ distance distribution functions (left panel) and normalized Kratky plots (right panel) are shown. The expected peak (grey dashed line) represents the theoretical peak assuming an ideal guinier region of a globular particle. (b,c) *Ab initio* reconstruction of Abl KD and SH2-KD super-imposed to their crystal structures (PDB: 1OPL for KD and 1OPL molecule B for SH2-KD). (d) Flexible characterization of the SH2-KD I164E mutant of three possible positions based on ensemble optimization method. Figure modified from Lamontanara et al. (2014).

2.2 Abl SH2-KD autophosphorylation ability

2.2.1 Mapping of autophosphorylation sites

Active Abl is phosphorylated on several sites in cells and we sought to map these sites *in vitro* to check for autophosphorylation sites. After incubation with excess ATP, we identified phosphorylated sites using mass spectrometry. Among the 24 tyrosines present in the SH2-KD protein, we found that 9 became phosphorylated (table 2.2 and figure 2.5). All identified sites were found highly annotated in the phosphosite repository (www.phosphosite.org) and previously identified in multiple phospho-proteomics data sets from Bcr-Abl expressing cancer cell lines. These results showed that the Abl SH2-KD retained specificity *in vitro* because all the sites found were also reported in cells. Two important regulatory sites were found to be autophosphorylated: the tyrosines 412 and 245.

Table 2.2 – Identified *in vitro* autophosphorylation sites in the Abl SH2-KD.

The peptide counts, sequences of the identified phosphorylation peptides, locations and Phosphosite.org record counts of mapped SH2-KD autophosphorylation sites are shown. The phosphorylation site is denoted in bold on the peptide sequence.

Site	Peptide count	Sequence	Location	Phosphosite record number
Y147	9	KHSWYHGPVSRN	SH2	211
Y158	2	RNAAEYLLSSGINGSFLVRE	SH2	57
Y204	3	KLYVSSSRF	SH2	550
Y245	71	KRNKPTVYGVSPNYDKW	SH2-kinase linker	314
Y272	14	KLGGGQYGEVYEGVWKK	N-lobe, Gly-rich loop	287
Y276	8	KLGGGQYGEVYEGVWKK	N-lobe, Gly-rich loop	338
Y283	4	KKYSLTVAVKT	N-lobe	56
Y412	7	RLMGDTYTAHAGAKF	C-lobe, activation loop	1714
Y432	3	KWTAPESLAYNKF	C-lobe	160

2.2.2 The Abl SH2 is indispensable for activation loop autophosphorylation

Giving the importance of Abl phosphorylation for its activation, we analyzed the mechanisms of autophosphorylation using unphosphorylated kinases. We incubated several Abl SH2-KD mutants with excess ATP and monitored increase in total phosphotyrosine levels over-time using a dot-blot assay system. Strikingly, the Abl KD was deficient in autophosphorylation (figure 2.6a), despite its robust activity toward an exogenous substrate (figures 2.3a). In contrast, Abl SH2-KD showed rapid and robust increase in autophosphorylation that was further potentiated via the T231R mutation. However, the I164E mutant showed a strong decrease in autophosphorylation ability. The S173N mutant was not affected compared to the WT protein, indicating that total Abl kinase autophosphorylation does not require phospho-tyrosine binding of the SH2 (figure 2.6a-c).

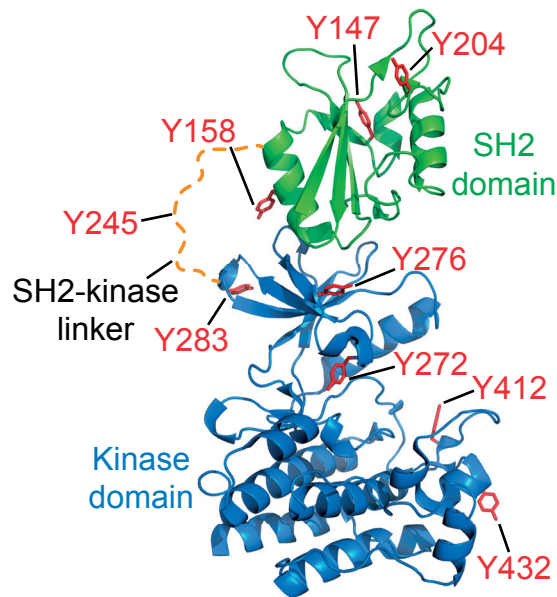


Figure 2.5 – Mapping of autophosphorylated tyrosines in recombinant Abl SH2-KD. The positions of phosphorylation sites mapped by mass-spectrometry after Abl SH2-KD autophosphorylation are shown as red sticks on the structure of the Abl SH2-KD (PDB: 1OPL molecule B).

Next, we analyzed autophosphorylation ability at two important regulatory sites which are tyrosine 245 (in the SH2-KD linker) and tyrosine 412 (in the activation loop). As reliable phosphorylation site-specific antibodies are available for both sites we also used the dot-blot system. Autophosphorylation of Y412 was strongly decreased in the I164E mutant (figure 2.6d-f); however the T231R mutant protein showed a strong increase in phosphorylation kinetics at Y412 (figure 2.6d-f). In contrast disrupting (I164E) or enhancing (T231R) the SH2-KD interface did not significantly affect autophosphorylation ability at Y245 (figure 2.6g-i). Notably autophosphorylation at Y245 seemed to precede Y412 because it began earlier and showed a steeper incline (figure 2.7).

Thus, we tested possible interdependence of these two phosphorylation events using purified Y245F and Y412F mutants. The two mutants excluded cross-reactivities of the phospho-specific antibodies. The Y245F mutant showed decreased autophosphorylation kinetics at Y412 (figure 2.6d-f), however the ability of the Y412F to autophosphorylate at Y245 was unchanged (figure 2.6g-i). Prior Y245 phosphorylation could enhance Y412 phosphorylation by the binding of phospho-Y245 to the Abl SH2 domain, therefore we also tested the S173N mutant, that render the SH2 incapable of phospho-tyrosine binding. As expected, the S173N mutant was autophosphorylated at Y245 with the same kinetic as WT (figure 2.6g-i). In contrast, the Y412 phosphorylation was strongly impaired by the S173N mutation (figure 2.6d-f).

These experiments showed that the Abl SH2-KD interface is one of the major determinants that enables Abl autophosphorylation (Lamontanara et al., 2014).

In the absence of the SH2-KD interaction, the Abl KD is defective in the autophosphorylation of the activation loop (Y412). Of note, the observed effects are more pronounced than the differences in V_{\max} for phosphorylation of a peptide substrate (figure 2.3). In addition the autophosphorylation experiments were done in Abl concentration well below K_M for substrate peptides, meaning that the differences in activation loop phosphorylation are unlikely to be due to differences in *in vitro* kinase activity.

2.3 Efficient trans-autophosphorylation requires the SH2 domain

Autophosphorylation can occur intramolecularly (in cis) or intermolecularly (in trans). Initial velocities of autophosphorylation of the Abl SH2-KD WT protein increased non-linearly with enzyme concentration, showing possible intermolecular interactions (figure 2.8a-b). The Van't Hoff analysis (log of initial velocity vs log of protein concentrations) gave a linear regression with a slope of 2 clearly confirming a second-order reaction due to intermolecular phosphorylation (figure 2.8b). This observation is in line with a trans-autophosphorylation ability.

We speculated that one or more tyrosine residues in the KD might be sterically less accessible for phosphorylation, because the KD protein did not show a strong impairment of *in vitro* kinase activity despite its inability to autophosphorylate. To test this hypothesis, we co-incubated pairs of active (WT) and catalytically deficient (D382N) KD and SH2-KD. Trans-phosphorylation was then monitored in the D382N by the WT protein on Y412. Co-incubation of active KD with inactive SH2-KD D382N showed robust trans-phosphorylation of the SH2-KD D382N activation loop (figure 2.9a-b). On the contrary, the Abl SH2-KD WT despite being a very active construct, was unable to trans-phosphorylate the Abl KD D382N in its activation loop (figure 2.9).

Using a similar experiment set-up, we showed that the robust phosphorylation of SH2-KD D382N by the KD was abolished by the disruption of the SH2-KD interface via the I164E mutation (figure 2.9c-f).

These experiments showed that the SH2-KD interface seems to have a major impact on Y412 accessibility for being trans-phosphorylated because absence of the SH2 or disruption of the interface renders the Y412 a poor substrate for phosphorylation (Lamontanara et al., 2014).

2.3. Efficient trans-autophosphorylation requires the SH2 domain

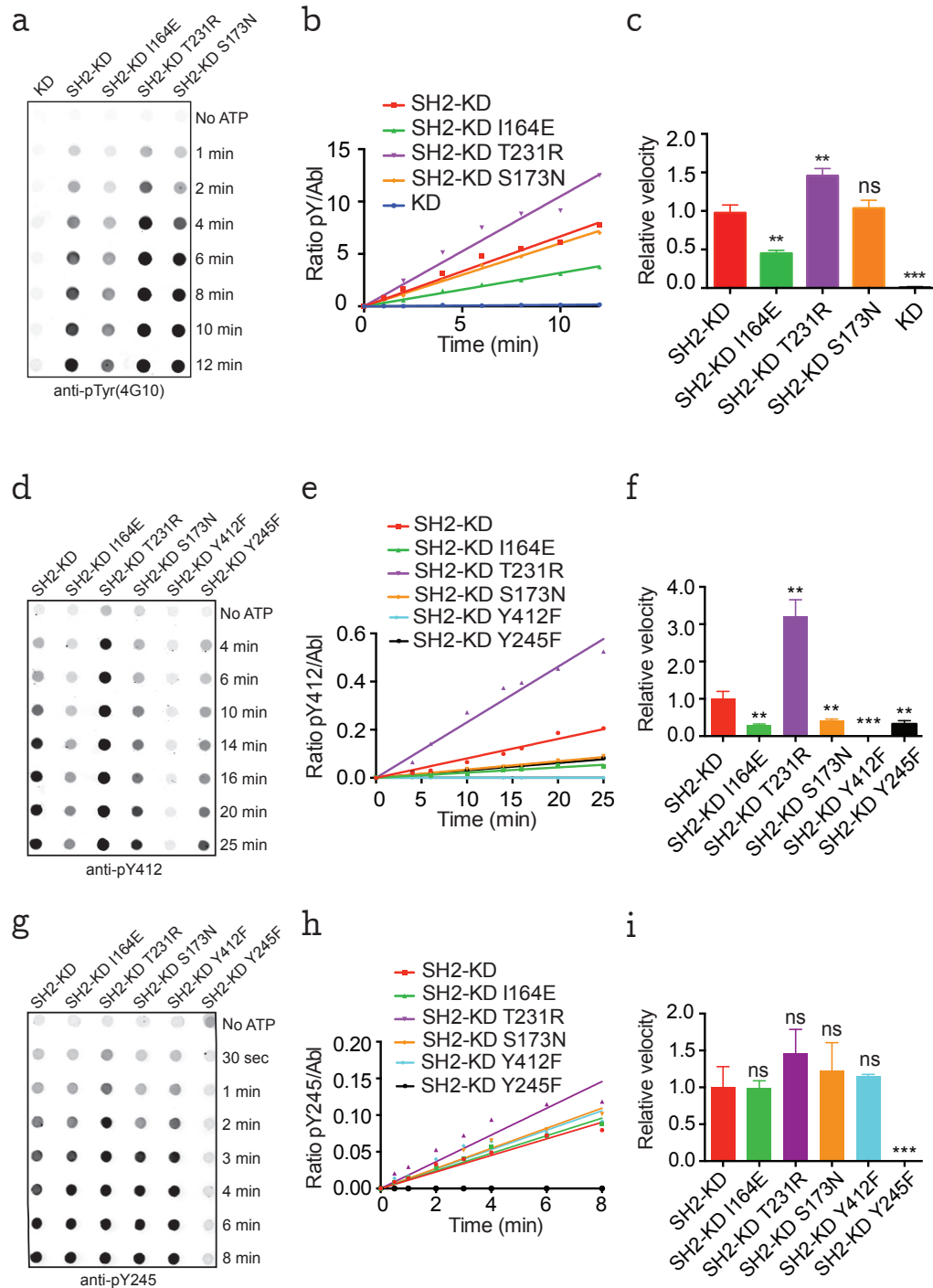


Figure 2.6 – Disruption of the SH2-kinase interface impairs Abl autophosphorylation.

(a,d,g) Indicated Abl mutants were incubated for the indicated times with ATP, dot blotted and incubated with total anti-pY (a), anti-pY412 (d) and anti-pY245 (g) antibodies. (b,e,h) Normalized total pY, pY412 and pY245 were plotted over incubation time. (c,f,i) Relative velocities of autophosphorylation for three biological repeats are shown. Average \pm sd are plotted. For each data set, the SH2-KD WT was set to 1 (NS, not significant; ** $P < 0.01$, *** $P < 0.001$, unpaired t -test). Figure modified from Lamontanara et al. (2014).

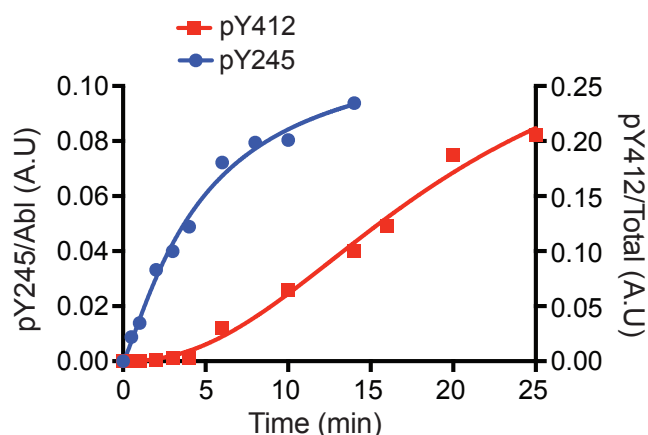


Figure 2.7 – Autophosphorylation kinetics of tyrosines 245 and 412. Kinetics of autophosphorylation at the Y245 (blue) and Y412 (red) showed a faster incline for the Y245 and a delayed Y412 autophosphorylation. Ratio of phosphorylation intensities to Abl amount as detected by Li-Cor are shown (arbitrarities units).

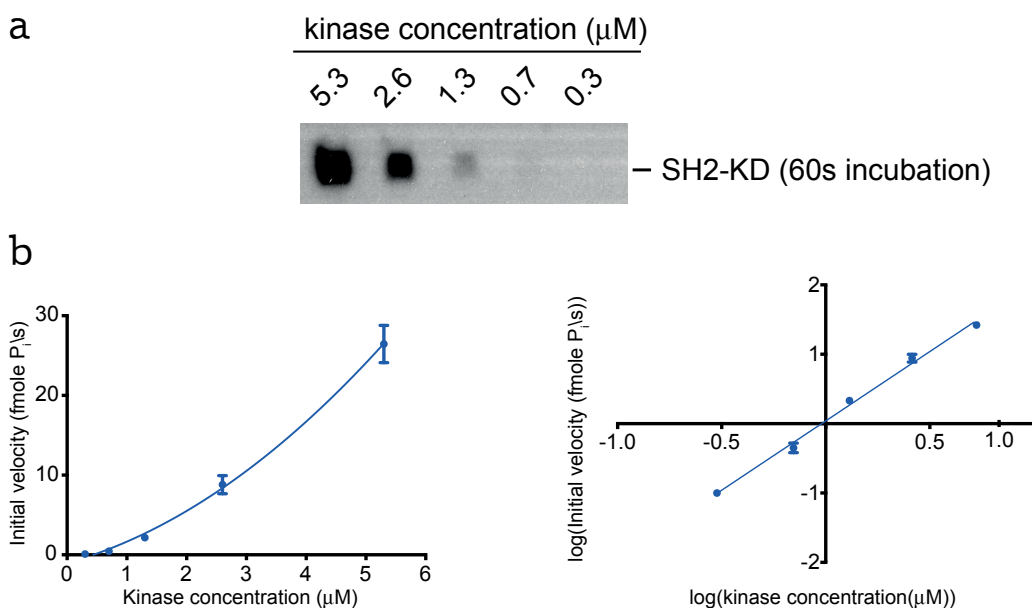


Figure 2.8 – Autophosphorylation of Abl SH2-KD WT at different protein concentrations. (a) Recombinant kinases were incubated at different concentrations with ^{32}P - γ -ATP, subjected to SDS-PAGE and autoradiography. (b) Quantification was done after gel drying using a scintillation counter. The initial velocity *vs* kinase concentration (left) is shown as well as the Van't Hoff plot (right) clearly showing a second-order reaction and confirming intermolecular phosphorylation.

2.3. Efficient trans-autophosphorylation requires the SH2 domain

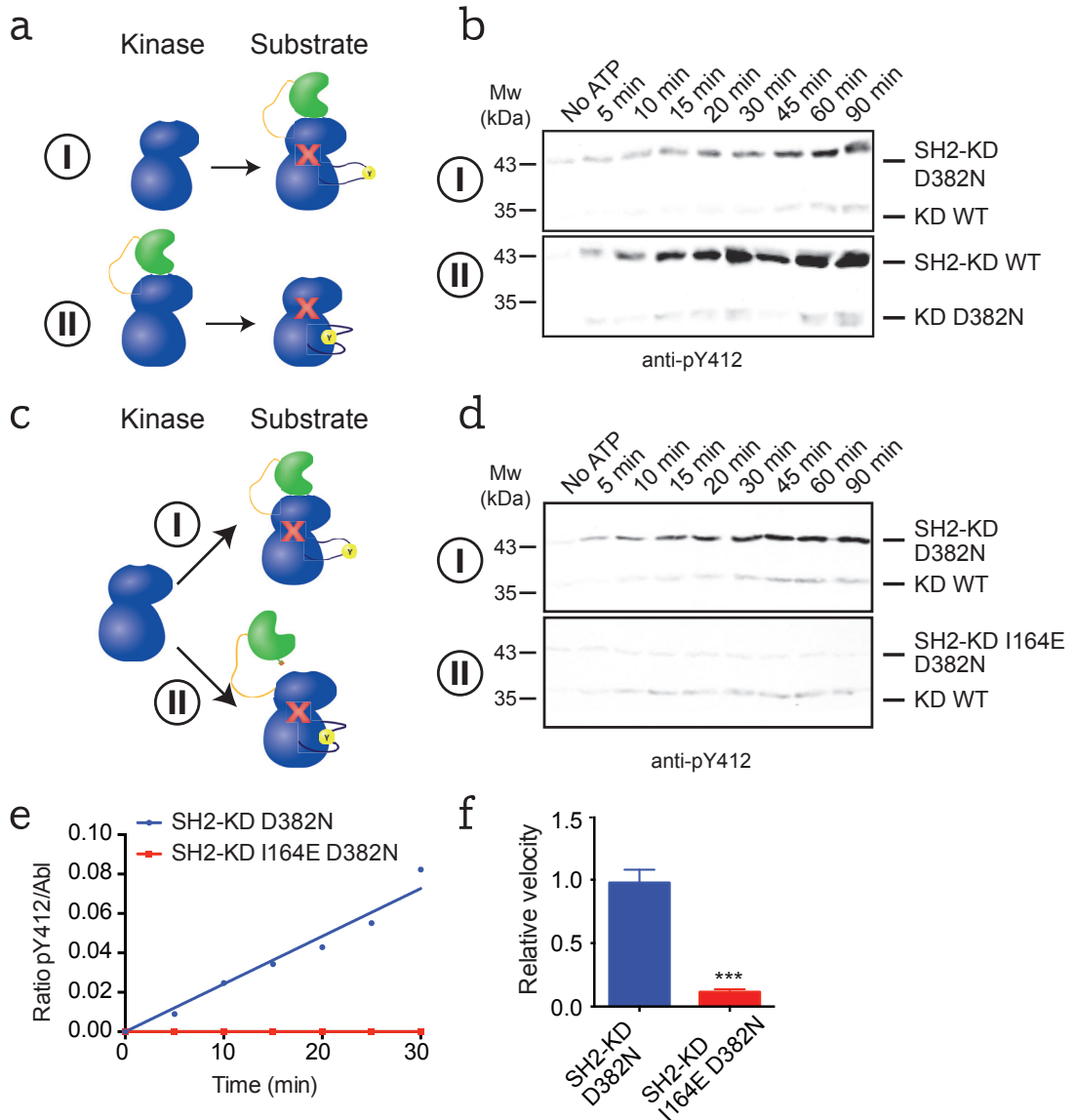


Figure 2.9 – The activation loop is a poor substrate for trans-phosphorylation in the absence of the SH2-KD interface. (a,c) Models illustrating the two combinations tested in b,d are shown. (b,d) Abl KD and SH2-KD were co-incubated for the indicated times and analyzed by Western Blot using anti-pY412 antibody. (e) Normalized pY412 signals plotted over incubation time for experiment shown in d. (f) Relative velocities for the autophosphorylation reaction shown in d. The average of three independent experiments \pm s.d. are plotted. SH2-KD WT was set to 1. Significance levels compared to SH2-KD are indicated (***P<0.001, unpaired t-test). Figure modified from Lamontanara et al. (2014).

2.4 The Abl SH2 domain maintains an open conformation of the activation loop

To assess the opening or closing of the Abl activation loop we used complexes with kinase-inhibitors. Analysis of the Abl KD with imatinib showed a type 2 binding with a close activation loop where the Y412 was not accessible for phosphorylation (Schindler et al., 2000). However a crystal structure of Abl kinase-dasatinib complex showed a type 1 binding with an open activation loop (Tokarski et al., 2006). Based on these observations, complexes of imatinib or dasatinib with KD and SH2-KD were prepared and were confirmed to be inactive and not able to autophosphorylate (data not shown). We then used these kinase-drug complexes as substrates for trans-autophosphorylation along with the SH2-KD and KD D382N and monitored Y412 phosphorylation over-time.

Similar to KD-imatinib complexes, the KD D382N was defective in Y412 trans-phosphorylation (figure 2.10a-c). This could be rescued (partially) in the KD-dasatinib complex where the Y412 phosphorylation readily increased in a linear manner. These results indicated that in the Abl KD, the activation loop is in a closed conformation similar to the Abl-imatinib complex and can be forced into opening when incubated with dasatinib.

We then included a 2xMyc-SBP tag to an active SH2-KD construct that allowed us to distinguish two SH2-KD units once co-incubated using their different molecular weights. In contrast to the results obtained with KD D382N, the SH2-KD D382N showed phosphorylation at Y412 to a similar degree to the SH2-KD-dasatinib complex (figure 2.10d-f). Strikingly, the SH2-KD-imatinib complex was strongly impaired in trans-phosphorylation at Y412 indicating that imatinib induced the closed-activation loop conformation. These results showed that the activation loop in the SH2-KD is similar to the dasatinib complex and is mostly populating open conformations that are more readily accessible for trans-phosphorylation.

2.5 Targeting the Abl SH2-kinase interface with monoclonal antibodies

To determine the sufficiency of targeting the Abl SH2-KD for Bcr-Abl inhibition, new monoclonal antibodies targeting the Abl SH2 have been developed. In collaboration with the Koide laboratory, we characterized two new monoclonal antibodies binding with a very high affinity to the Abl SH2 and inhibiting the formation of the SH2-KD interface.

2.5.1 Characterization of AS25 and AS27 monoclonal antibodies

Two monoclonal antibody clones termed AS25 and AS27 harbouring a N-terminal 10xHis tag were characterized by the Koide laboratory. They both bind the Abl SH2 in a very similar manner with nM affinity (10-20 nM, data obtained from Prof. Koide). The crystal structure of the AS25-Abl SH2 complex has been obtained (data from S. Koide, figure 2.11a). AS25 forms a cradled binding surface of more than 800 Å² with the Abl SH2. Notably, the I164 is a central

2.5. Targeting the Abl SH2-kinase interface with monobodies

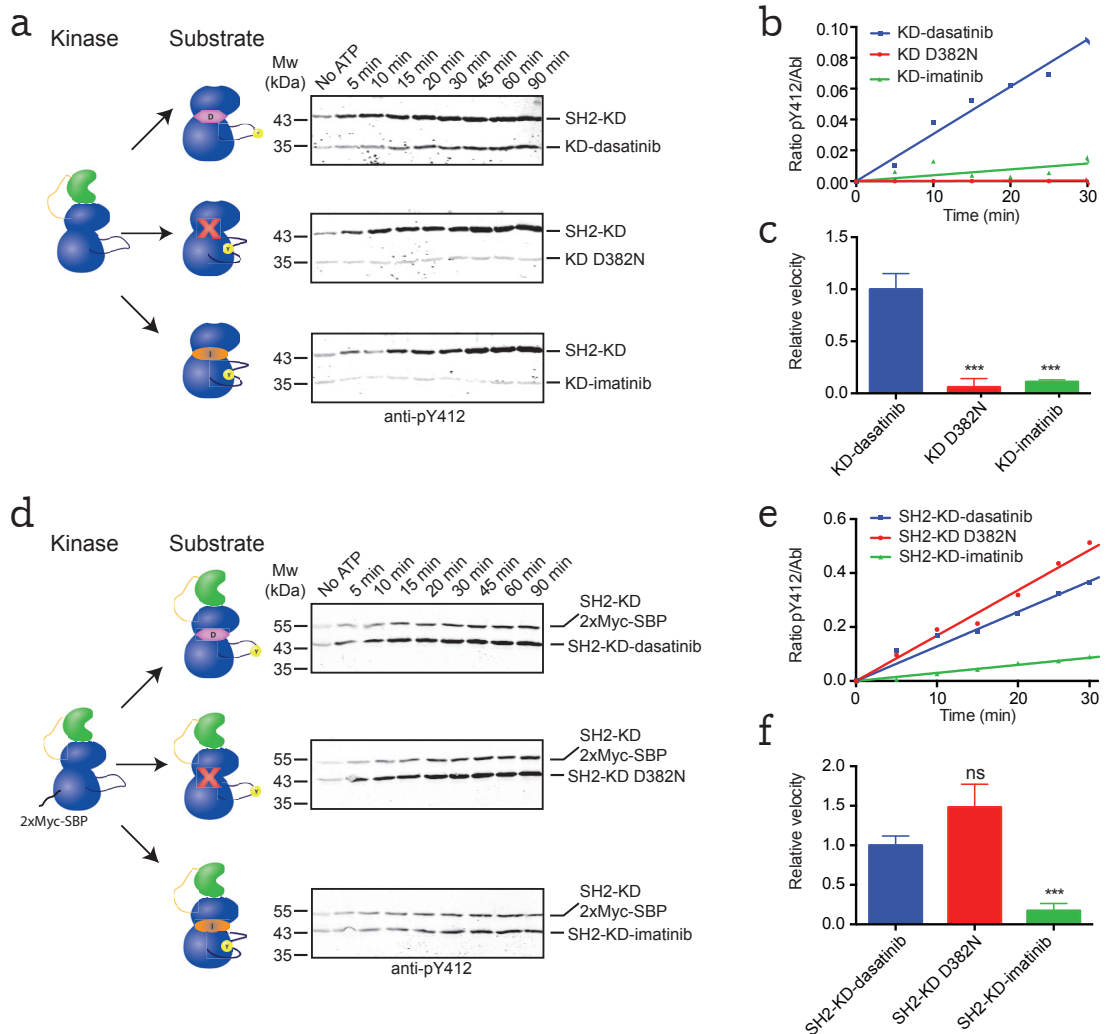


Figure 2.10 – The SH2 domain induces a fully active conformation of the activation loop. (a,d) Active SH2-KD was co-incubated with dasatinib, catalytically inactive or imatinib-bound KD (a) and SH2-KD (d) proteins for the indicated times and then analyzed by immunoblotting with an anti-pY412 antibody. (b,e) Normalized pY412 signals of immunoblots in a,d were plotted over time for the phosphorylated substrate (lower bands) of the reactions. (c,f) Relative velocities of the trans-phosphorylation reactions from three independent experiments are shown. Averages \pm s.d. are plotted. For each data set, the dasatinib complex was set to 1.0. Significance levels in comparison with dasatinib-bound KD (c) or SH2-KD (f) are indicated (NS, not significant; *** P <0.001, unpaired t-test). Figure modified from Lamontanara et al. (2014).

Chapter 2. Results

residue that if mutated is expected to prevent the binding of AS25. AS25/27 binding is expected to compete with and prevent the formation of the Abl SH2-KD interface.

AS25 and AS27 were purified with very high yields (>10 mg/L) using nickel affinity beads followed by a gel filtration (figure 2.11b,c). The monoclonal antibodies eluted in a main homogenous peak (peak 2, figure 2.11c) at a calculated molecular weight of 10 kDa very close to the expected one (12 kDa). Size-exclusion chromatography experiments showed efficient formation of AS25 complexes with Abl SH2-KD that was abolished with the I164E mutation confirming the central role of this residue for AS25/27 binding (data not shown).

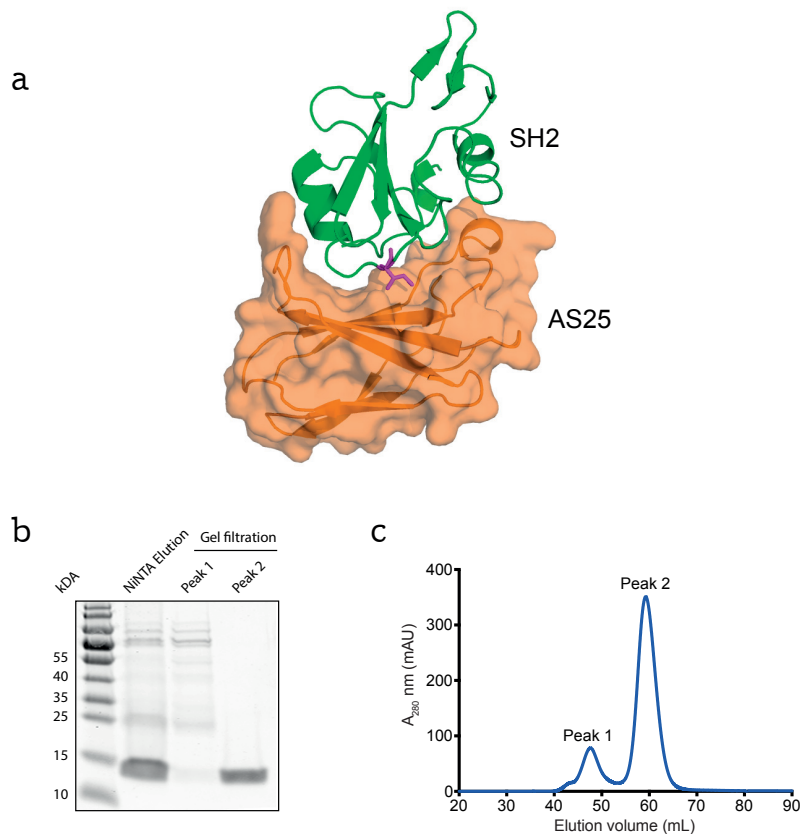


Figure 2.11 – AS25 binding mode and purification. (a) Crystal structure of the AS25 monoclonal antibody (orange, surface representation) binding to the Abl SH2 domain (green). The I164 is a central residue (purple). (b) Coomassie staining of purified AS25 after NiNTA and gel filtration. Peak 1 and 2 are corresponding to the peaks in c. (c) The NiNTA elution was loaded on a gel filtration. AS25 eluted in a sharp peak (peak 2) at the expected molecular weight. Peak 1 corresponded to contaminants.

2.5. Targeting the Abl SH2-kinase interface with monobodies

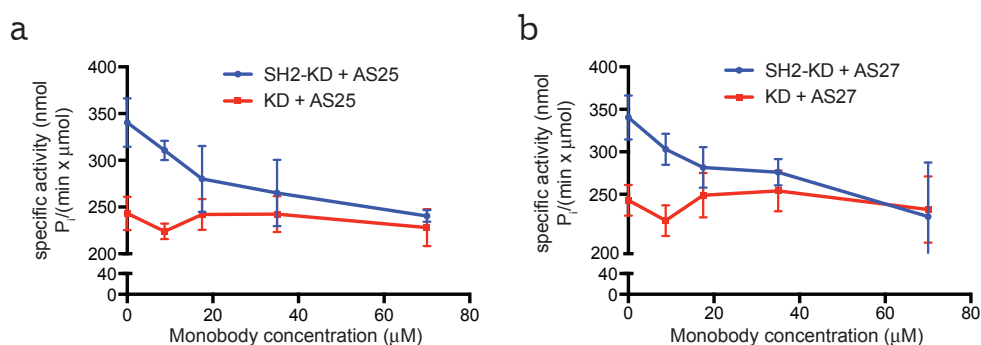


Figure 2.12 – Inhibition of the Abl SH2-KD with monobodies *in vitro*. (a) The activity of Abl KD (red) and SH2-KD (blue) were assayed against an optimal Abl peptide in the presence of indicated concentrations of AS25 monobody. (b) Similar as in a but with the AS27 monobody.

2.5.2 AS25 and AS27 inhibit the Abl SH2-KD activity *in vitro*

Giving the very high overlap between the binding of the AS25/27 monobodies and the kinase to the SH2 domain, we speculated that incubation of the monobodies with a purified Abl SH2-KD might affect kinase activity. *In vitro* kinase assays were performed using Abl SH2-KD or KD co-incubated with either the AS25 or AS27.

Substantial decrease of kinase activity of the SH2-KD was observed in a dose-dependent manner when co-incubated with the monobodies (figure 2.12). Importantly, no inhibition was detectable when KD was incubated with the monobodies arguing that the effect is SH2 dependent and specific. At the highest monobodies concentrations tested, the level of Abl SH2-KD activity was similar to Abl KD (figure 2.12).

The data suggested that we could target the Abl SH2-KD *in trans* to reproduce the effects of the I164E mutation. Therefore inhibition of Abl and Bcr-Abl by the monobodies was also tested in a cellular context.

2.5.3 AS25 and AS27 expression decreased Abl PP and Bcr-Abl phosphorylation in cells

To determine if AS25/27 could have an impact in a cellular context, HEK293 cells were co-transfected with constitutively activated full-length Abl (Abl "PP") or Bcr-Abl together with monobodies. We compared the effects of the two monobodies with a non-binding monobody named HA4 Y87A, that is unable to bind the Abl SH2 (Wojcik et al., 2010).

Both AS25 and AS27 expression strongly decreased total phosphotyrosine level of HEK293 transfected with Abl PP by $\approx 50\%$ (figure 2.13). Importantly, it almost abrogated Abl phosphorylation in the activation loop (Y412), a marker of activated Abl.

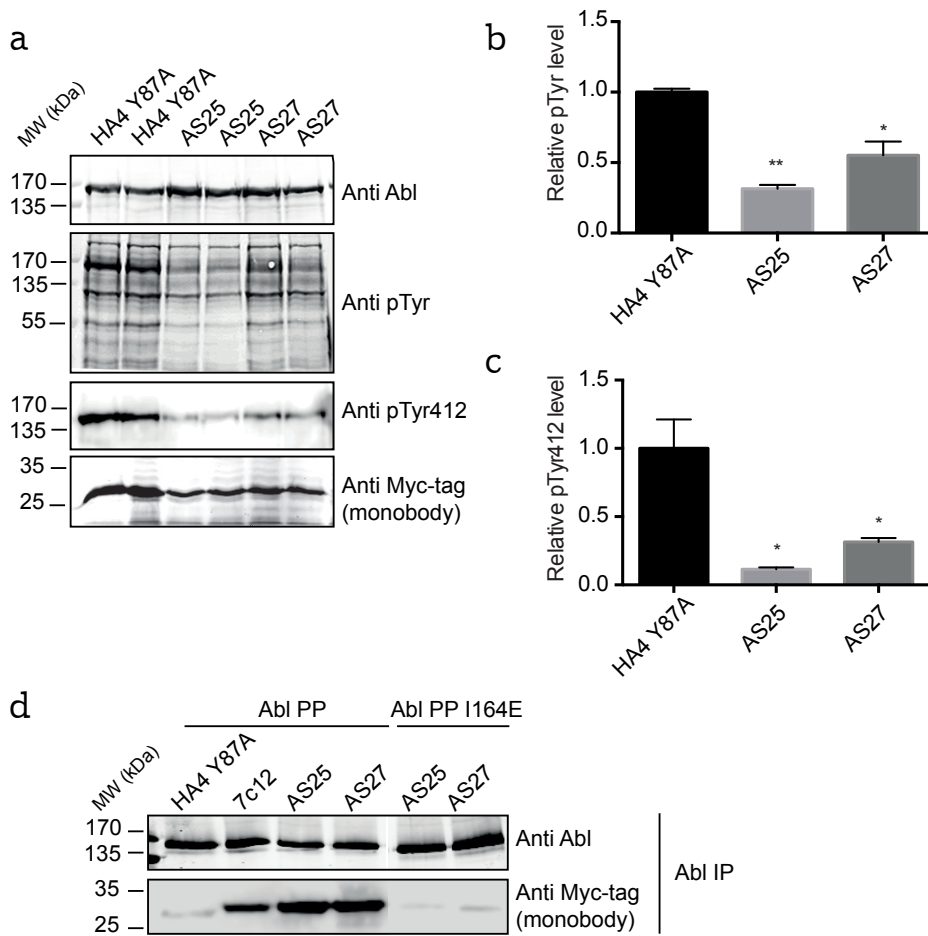


Figure 2.13 – Inhibition of Abl phosphorylation in HEK293 cells by AS25 and AS27 monobodies (a) HEK293 cells were co-transfected with a constitutively activated version of Abl (Abl "PP") and different set of monobodies harbouring a Myc-tag. Besides AS25 and AS27, HA4 Y87A was used as a negative non-binder control. Total tyrosine phosphorylation and activation loop tyrosine 412 phosphorylation levels were normalized to total amount of Abl PP expressed. Two repeats are shown for each monobody. (b) Relative total phosphotyrosine levels of experiments shown in a. HA4 Y87A level was set at 1. (c) Relative pY412 levels of AS25 and AS27 experiments shown in a. HA4 Y87A level was set at 1. (d) AS25, AS27, the first generation directed to the SH2-KD, 7c12, and HA4 Y87A were co-expressed as Myc-tagged proteins with Abl PP and Abl PP I164E. Immunoprecipitation with an anti-Abl antibody revealed equal levels of Abl PP in the immunoprecipitates (upper panel). Monobodies binding was detected using anti-Myc antibody (lower panel). Significance levels in comparison to HA4 Y87A are shown (** $P < 0.01$, * $P < 0.05$, unpaired t-test).

2.5. Targeting the Abl SH2-kinase interface with monobodies

These results are in line with our previous observations that targeting the Abl SH2-KD interface mostly has a negative influence on activation loop phosphorylation (figure 2.6). To confirm binding of the monobodies to the Abl SH2 domain in cells, Abl PP was immunoprecipitated and the samples blotted with an anti-Myc antibody as the monobodies expressed were harbouring the tag (figure 2.13d). We used as a positive control the monobody 7c12 which was already engineered to bind to Abl SH2-KD interface despite no strong physiological effects (Grebien et al., 2011). As expected 7c12 was found bound to Abl PP while the HA4 Y87A engineered to prevent monobody binding was not detectable after Abl pull-down. These results confirmed the specificity of the co-immunoprecipitation. AS25 and AS27 monobodies were easily detected after Abl PP immunoprecipitation confirming that they also bind Abl in cells. Finally, the Abl PP I164E mutation prevented the binding of AS25/27 monobodies, confirming the importance of this residue for their binding to the SH2.

To further validate AS25 and AS27 monobodies, we also co-expressed them with the Bcr-Abl kinase in HEK293 (figure 2.14). Expression of AS25/27 or 7c12 had no major effects on total phosphotyrosine levels while expression of the I164E mutant decreased the level by more than 50 %. Interestingly, the levels of activation loop phosphorylation (pY412) were significantly decreased in cells expressing the monobodies AS25 (>50%, *P<0.05) and AS27 (>60%, *P<0.05), although not as strongly as in the case of the I164E mutation (>80 %, **P<0.01).

2.5.4 AS25 and AS27 induced cell death by apoptosis in K562 cells

Despite several attempts to constitutively express AS25/27 in the CML cell line K562, we were unable to detect monobodies expression by western blot or flow cytometry for a co-expressed GFP six days after retroviral transduction. This difficulty prompted us to hypothesize that AS25/27 expression could be incompatible with K562 cells proliferation or survival. To test this possibility, we monitored the relative population of GFP positive, i.e. monobody-expressing cells, starting 24h after retroviral infection of K562 cells. The cells expressing AS25 and AS27 were rapidly depleted in culture as shown by decreased GFP positivity over time (figure 2.15a). This was not the case for cells expressing the non-binding mutant HA4 Y87A as well as the HA4 monobody shown before to bind the Abl SH2 but which did not prevent the Abl SH2-KD interface formation. In the case of AS25/27, the GFP positive population showed higher level of early and late apoptosis as detected by Annexin V and 7-AAD staining (figure 2.15b-c). These results indicated that AS25/27 induced apoptosis in K562 cells and that the observed effects were not due to the transduction itself or simple monobody expression as the HA4 and HA4 Y87A monobodies had no effects (results obtained by B. Gerig).

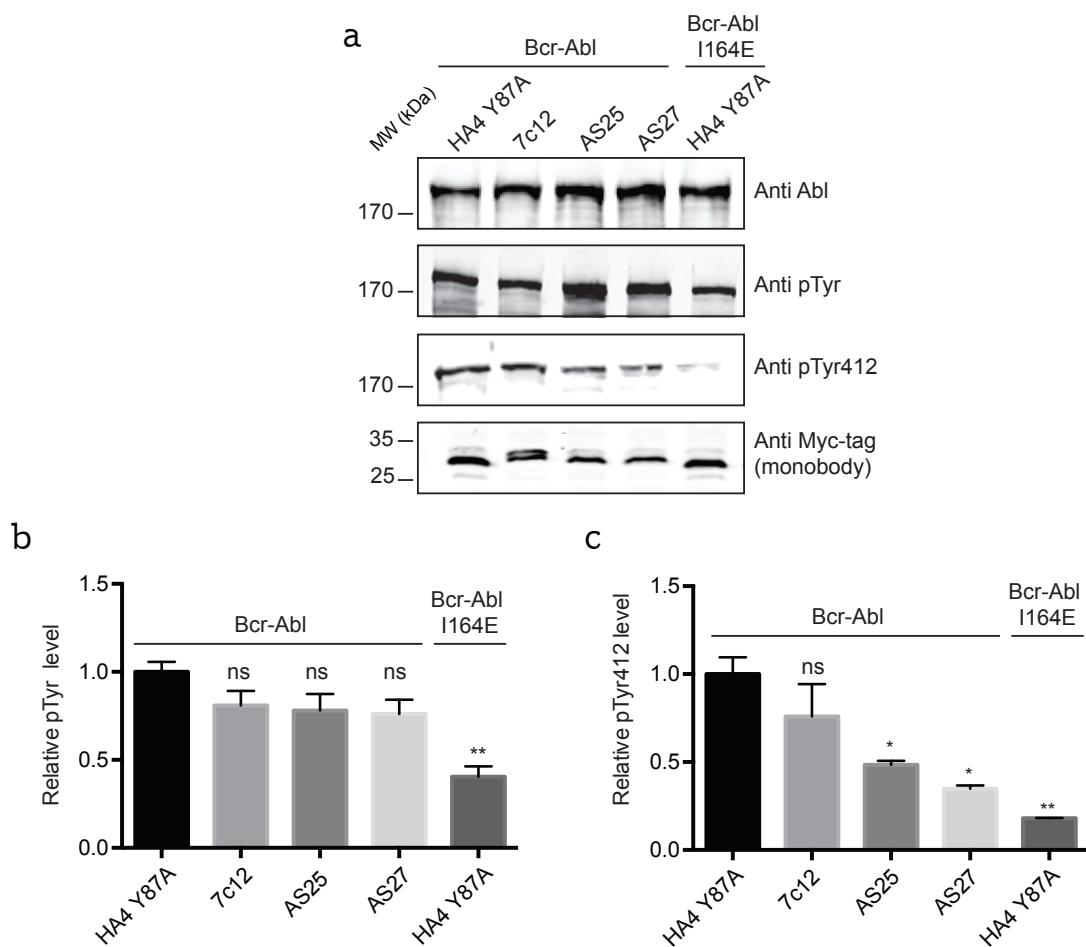


Figure 2.14 – Inhibition of Bcr-Abl phosphorylation in HEK293 cells by AS25 and AS27 monobodies. (a) HEK293 cells were co-transfected with Bcr-Abl expressing plasmid and different set of monobodies harbouring a Myc-tag. Besides AS25 and AS27, HA4 Y87A was used as a negative non-binder control. Total tyrosine phosphorylation and activation loop tyrosine 412 phosphorylation levels were normalized to total amount of Bcr-Abl expressed. (b) Relative total phosphotyrosine levels of experiments shown in a. HA4 Y87A level was set at 1. (c) Relative pY412 levels of experiments shown in a. HA4 Y87A level was set at 1. Significance levels in comparison to HA4 Y87A are shown (** $P < 0.01$, * $P < 0.05$, unpaired t-test).

2.5. Targeting the Abl SH2-kinase interface with monobodies

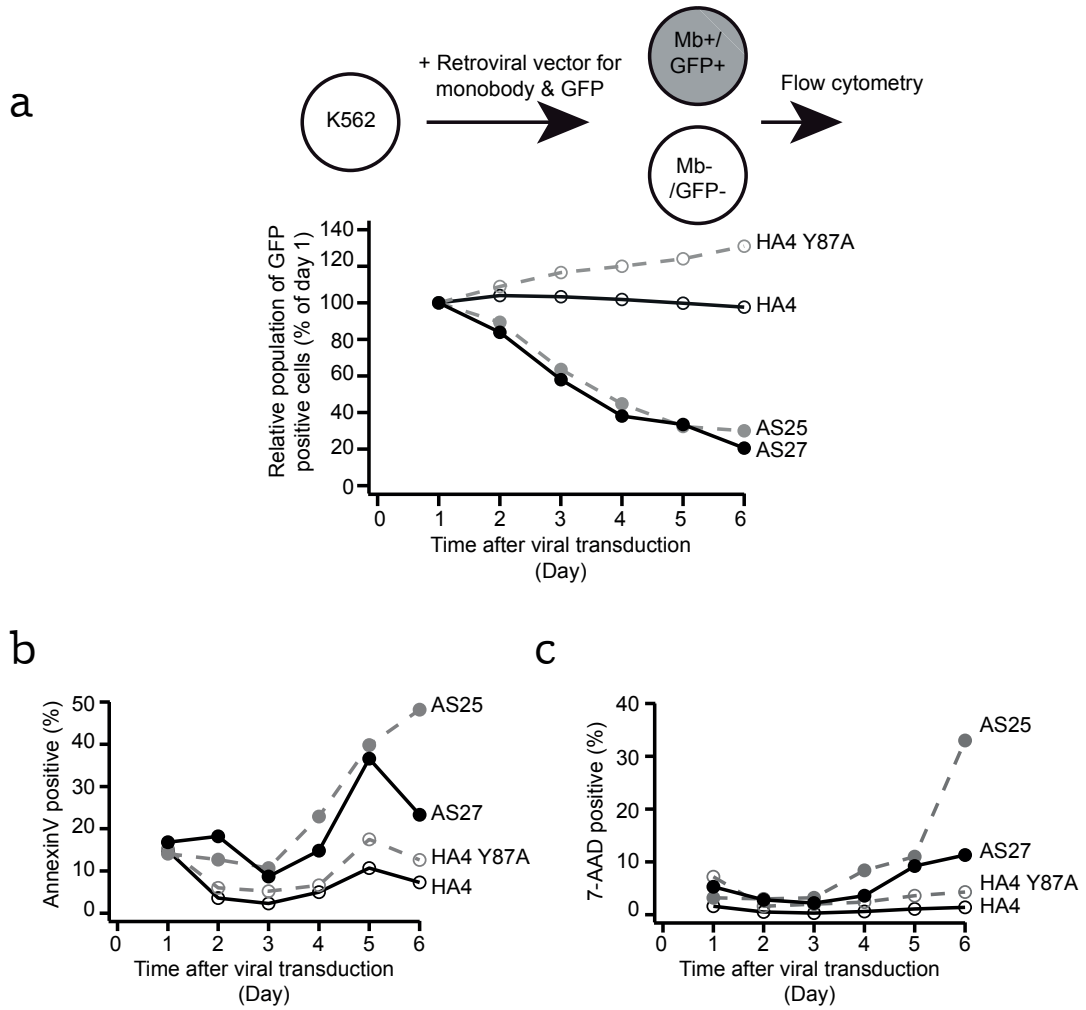


Figure 2.15 – Effects of AS25 and AS27 monobodies on transduced K562 cells (a) K562 cells were transduced with N-TAP fused monobodies (HA4, HA4 Y87A, AS25, AS27) and GFP positivity was followed overtime using flow cytometry. (b) GFP positive cells were stained for Annexin V and followed overtime. (c) GFP positive cells were stained for 7-AAD and followed overtime. This experiment was carried out by B. Gerig.

2.6 Development of screening assays for Abl SH2-KD interface disrupters

Based on the previous results, we showed that the SH2-KD interface can be targeted and that it inhibited Abl autophosphorylation and activity as well as affected K562 cells. As monobodies are difficult to deliver into cells, it was indispensable to develop a screening assay that could lead to the finding of small-molecules mimicking the effects of the AS25/27 monobodies or the I164E mutation.

2.6.1 Acrylodan-based fluorescent assay

We thought to find a way to detect interface disruption by harnessing Abl SH2 conformational changes that could happen upon SH2-KD interface disruption. This would allow us to potentially detect the disruption upon binding of small-molecules to either the Abl SH2 or tip of the kinase domain. Recently, a fluorescent molecule named acrylodan was successfully used to detect compound binding to the myristate pocket in Abl (Schneider et al., 2012). Acrylodan is a fluorescent dye that can be coupled to cysteine residues via formation of a covalent thioether bond at a neutral pH in aqueous solution. In solution, it has very low fluorescent levels but protein adducts of acrylodan become highly fluorescent (figure 2.16a). The fluorescent properties of these adducts are particularly sensitive to conformational changes and ligand binding (figure 2.16c).

We have selected three residues in the Abl SH2 domain at different sides and distances to the SH2-kinase interface based on the crystal structure. The three positions have been mutated to cysteines (L159C, T231C, E187C) while two exposed cysteines in the kinase domain have been mutated to non-cysteine residues (C324V, C349S) (figure 2.16b). The goal was to prepare recombinant Abl SH2-KD protein containing single engineered cysteine residues and being either WT or carrying the I164E mutation as well as using the AS25 monobody to disrupt the interface. Upon interface disruption, we were expecting a shift in acrylodan fluorescence compared to an intact SH2-KD interface (figure 2.16c). We would then select the positions of the acrylodan label in the SH2 domain that show the strongest differences in the emission spectrum between the WT (negative control) and the I164E or AS25-bound labelled SH2-KD (positive controls).

All purified cysteine mutants showed good purity and stability (data not shown). Importantly the C324V C349S double mutation in the kinase domain had no impact on Abl SH2-KD activity as well as the SH2 cysteine mutants (figure 2.17). As expected, the mutants showed decreased activity upon I164E mutation (figure 2.17). These results are in line with well-folded and stable cysteine mutants that can be further used for labeling.

2.6. Development of screening assays for Abl SH2-KD interface disrupters

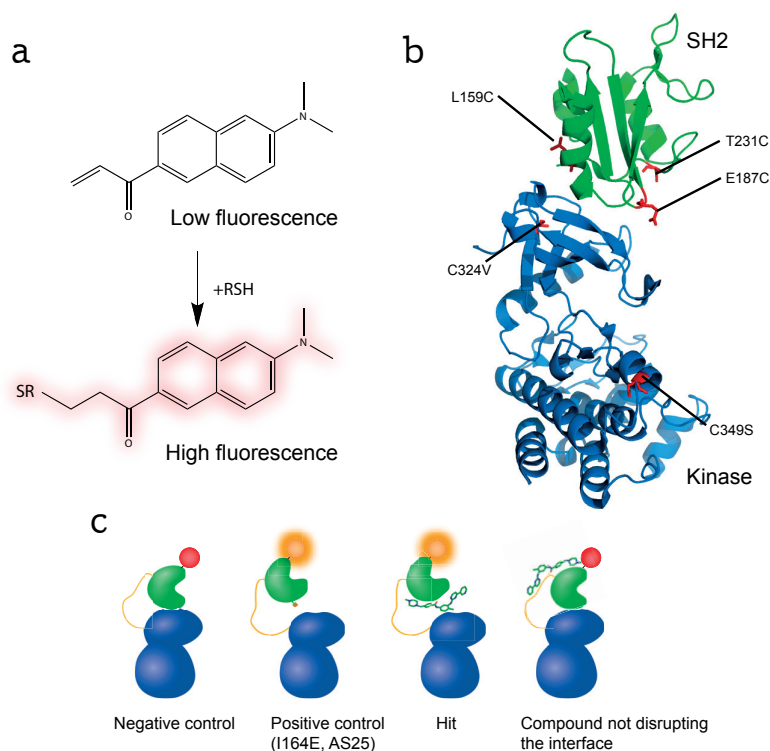


Figure 2.16 – Acrylodan-based screening principle. (a) Acrylodan has a low fluorescence that is increased upon thioether bond formation with a cysteine (RSH) (b) Positions of engineered cysteine mutations in the SH2 and the cysteine residues that were removed from the kinase domain. (c) Schematic representation of the proposed screening assay. Abl SH2 domain is depicted in green and kinase domain in blue. Once bound to the cysteine mutant in the SH2 domain, acrylodan will have high fluorescence (red). Any SH2-KD disruption via I164E mutation, monobodies or a hit compound will shift the fluorescence (yellow). Binding of a compound to a surface not disrupting the interface will not affect fluorescence.

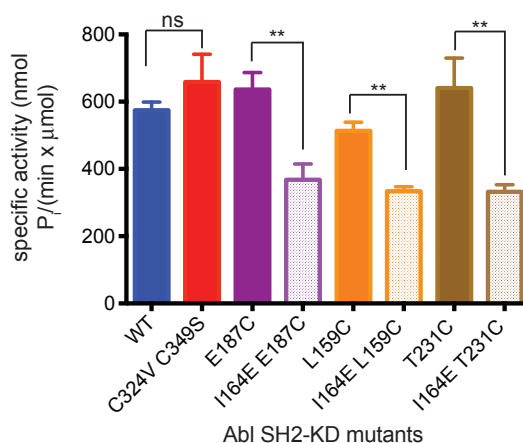


Figure 2.17 – Kinase activity of Abl SH2-KD cysteine mutants. Purified Abl cysteine mutants were assayed for kinase activity against an optimal Abl peptide and the kinetics fitted using the Michaelis-Menten equation. The maximum velocity is shown for each mutant.

Labeling of acrylodan SH2-KD mutants

To confirm correct labeling of the different cysteine mutants, we compared the labeling of the mutants with the Abl SH2-KD C324V C349S (SH2-KD*) that has no cysteines in the SH2 domain and for which two exposed cysteines have been mutated in the kinase domain to avoid kinase labeling. Acrylodan fluorescence has a main emission peak between 500-520 nm after excitation at 380 nm. Acrylodan alone in solution showed low fluorescence as expected (figure 2.18a). When any of the protein mutants was incubated with acrylodan in solution, a drastic increase in fluorescence was observed over the whole emission spectrum (figure 2.18b). This confirmed that acrylodan had reacted with cysteines in the proteins and thus became fluorescent. Out of the three cysteine mutants, Abl SH2-KD* E187C and L159C showed high fluorescence at their maximum (≈ 500 nm) compared to the control SH2-KD*. The last mutant, T231C, did not have an increase in fluorescence at the maximum of emission compare to Abl SH2-KD* (figure 2.18b).

Although not having any exposed cysteines, the Abl SH2-KD* also showed increased fluorescence. This increase could be due to a non-specific labeling of the Abl SH2-KD* kinase domain. Indeed mass spectrometry analysis of labeled Abl SH2-KD* showed that a minor proportion of the population was labeled with acrylodan (data not shown), which was enough to increase fluorescence of acrylodan in solution.

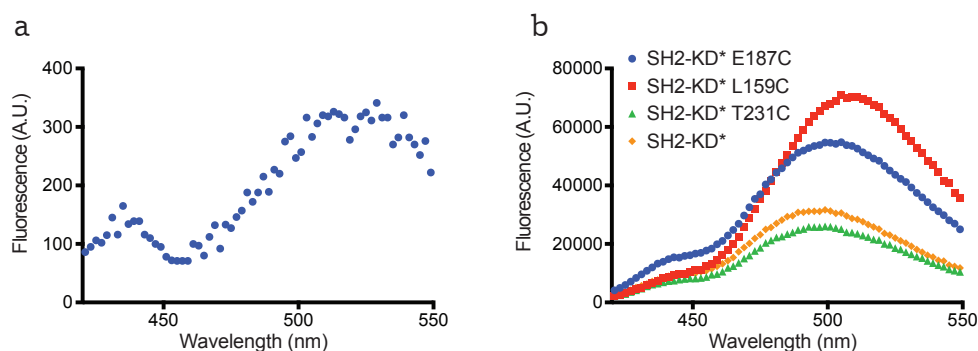


Figure 2.18 – Fluorescence spectrum of Abl SH2-KD cysteine mutants. (a) Fluorescence spectrum of acrylodan only in solution. (b) Abl SH2-KD cysteine mutants were labeled with acrylodan overnight and assayed for fluorescence by exciting acrylodan at 360 nm and detecting excitation between 400-550 nm. 10 μ M of proteins were used.

Analysis of acrylodan cysteine mutants upon interface disruption

To further continue analyzing the Abl SH2-KD cysteine mutants, we compared the fluorescence spectrum of the labeled mutants with or without the I164E mutation. Among the three mutants, only labeled Abl SH2-KD* E187C showed a decreased emission fluorescence at 500 nm upon interface disruption via I164E mutation, while no major shift of the maximum wavelength of emission was observed (figure 2.19b).

2.6. Development of screening assays for Abl SH2-KD interface disrupters

To mimic interface disruption in trans by possible small-molecules, we used the monobody AS25 as a positive control, which efficiently affected kinase activity in our biochemical assays. We co-incubated the SH2-KD* E187C mutant with several concentrations of the AS25 monobody. Increasing concentrations of AS25 monobody induced a decreasing maximum fluorescence of the labeled Abl SH2-KD* E187C from 35000 to less than 25000 A.U at monobody concentration of 25-40 μ M (figure 2.20a) and showing a sigmoidal response (figure 2.20c). No major shift of the peak maxima was observed. As a control, we used an unrelated monobody (Nsa5, Sha et al. (2013)) of a similar molecular weight than AS25. Incubation of Nsa5 concentration ranging from 17 to 40 μ M had no impact on maximum fluorescence (figure 2.20b). These results were in line with a specific decrease of maximum fluorescence upon Abl SH2-KD interface disruption. Despite robust fluorescence, the calculated Z' factor with the acrylodan-labeled Abl SH2-KD* E187C and using AS25 as a positive control only reached 0.4, which is considered as marginal (<0.5).

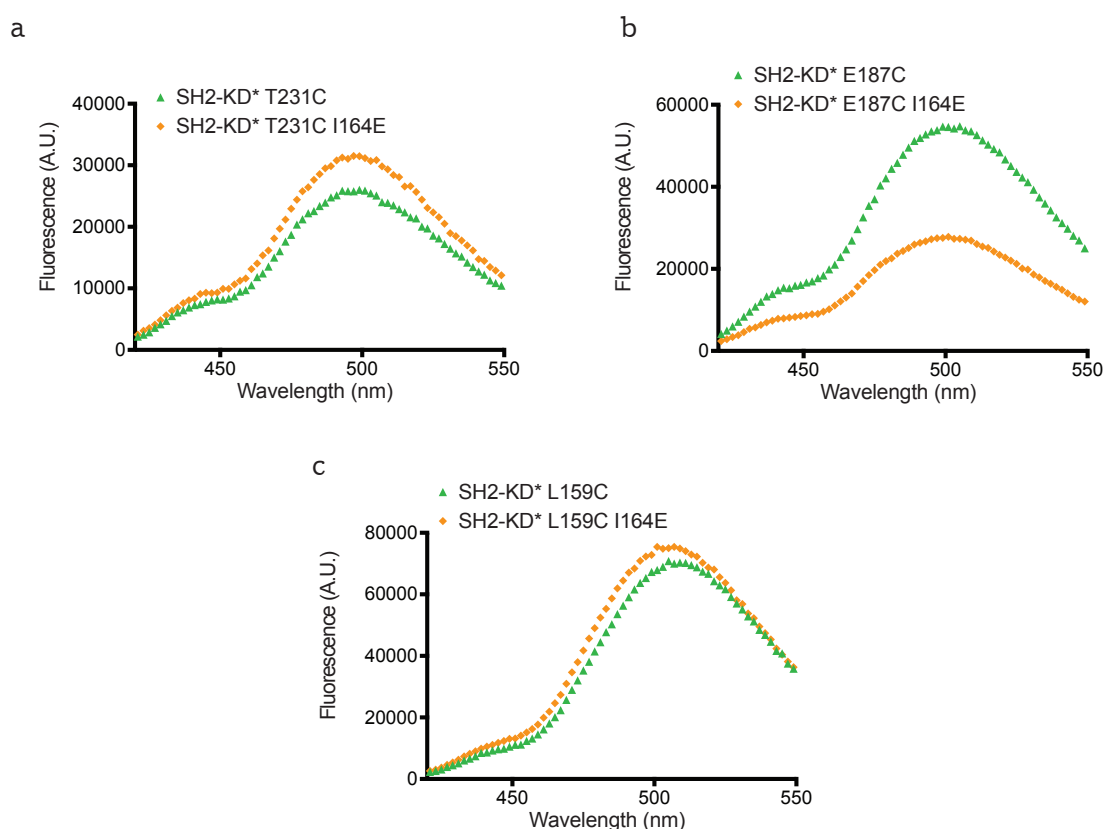


Figure 2.19 – Fluorescence spectrum of Abl SH2-KD cysteine mutants comparing intact SH2-KD interface and disrupted interface via I164E mutation. Each cysteine mutant, either WT or harbouring the I164E mutation was labeled with acrylodan and fluorescence spectrums compared. (a) Spectrum comparison of Abl SH2-KD* T231C and Abl SH2-KD* T231C I164E. (b) Spectrum comparison of Abl SH2-KD* E187C and Abl SH2-KD* E187C I164E. (c) Spectrum comparison of Abl SH2-KD* L159C and Abl SH2-KD* L159C I164E.

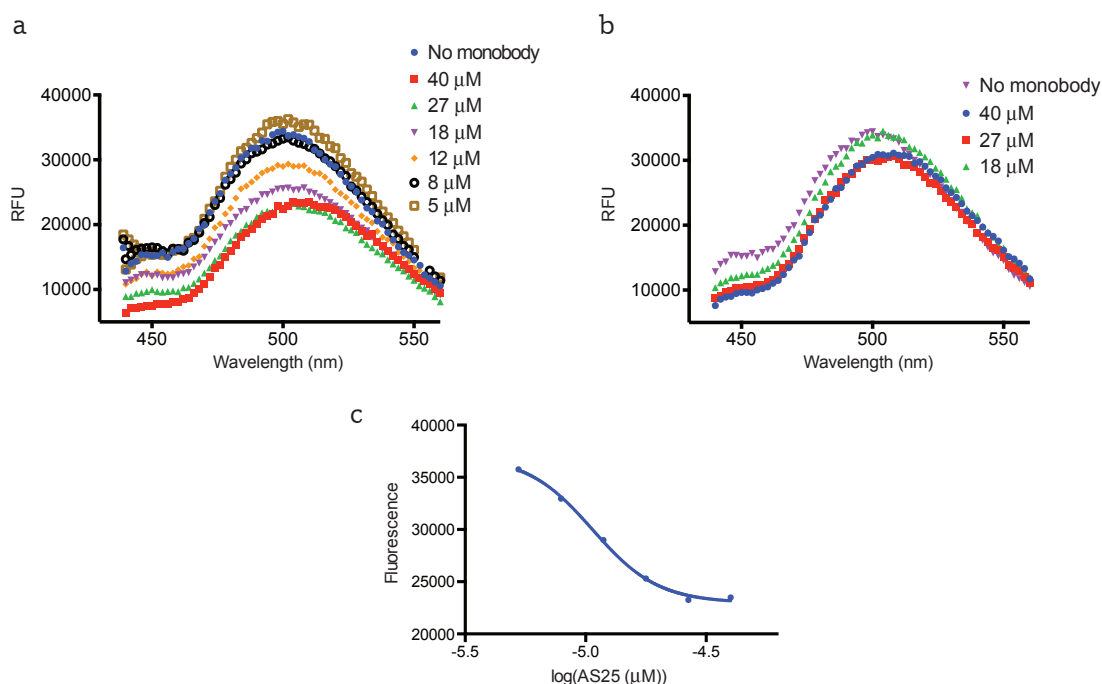


Figure 2.20 – Effect of AS25 on fluorescence spectrum of Abl SH2-KD* E187C. (a) Acrylodan-labeled SH2-KD* E187C was incubated with increasing concentrations of AS25 monobody and fluorescent spectrum measured. (b) Acrylodan-labeled SH2-KD* E187C was incubated with increasing concentrations of Nsa5 monobody and fluorescent spectrum measured. (c) Maximum fluorescence obtained from a was plotted over logarithmic concentrations of AS25.

2.6.2 HTRF-based screening assay

In order to develop a more robust assay we thought to develop a screening assay based on the binding of AS25 to the Abl SH2. This interaction is well-characterized, strong (nM affinity) and binding of AS25 indeed disrupted the SH2-KD interface as previously shown by the decreased Abl activation loop phosphorylation (see Section 2.5.3). A compound that could bind and disrupt the SH2-AS25 interaction would mimic the effect of AS25 and might disrupt the Abl SH2-KD interaction.

With the help of Cisbio (France) and their expertise in Homogenous Time-Resolved Fluorescence (HTRF), a screening assay development was started. HTRF couples the advantages of fluorescence resonance energy transfer (FRET) with time-resolved (TR) measurements. FRET is based on the transfer of energy between a donor (long-lived fluorescence) and acceptor (short-lived fluorescence) when the two are in close proximity. HTRF has the advantage to use long-lived acceptor fluorophores when engaged in a FRET process, increasing reliability and assay sensitivity. By introducing a time-delay (50-150 μ s) between the initial light excitation and fluorescence measurements, HTRF allows the elimination of short-lived background fluorescence such as compounds, medium or protein fluorescence. The assay will use tag-labeled AS25 and SH2 in which the tags are detected using anti-tag molecules labeled with donor

2.6. Development of screening assays for Abl SH2-KD interface disrupters

and acceptor fluorophores (figure 2.21a). Any compound binding to the AS25-SH2 interface and disrupting it will induce a decrease in the overall HTRF signal because of the donor and acceptor being far apart when the complex is not formed (figure 2.21b).

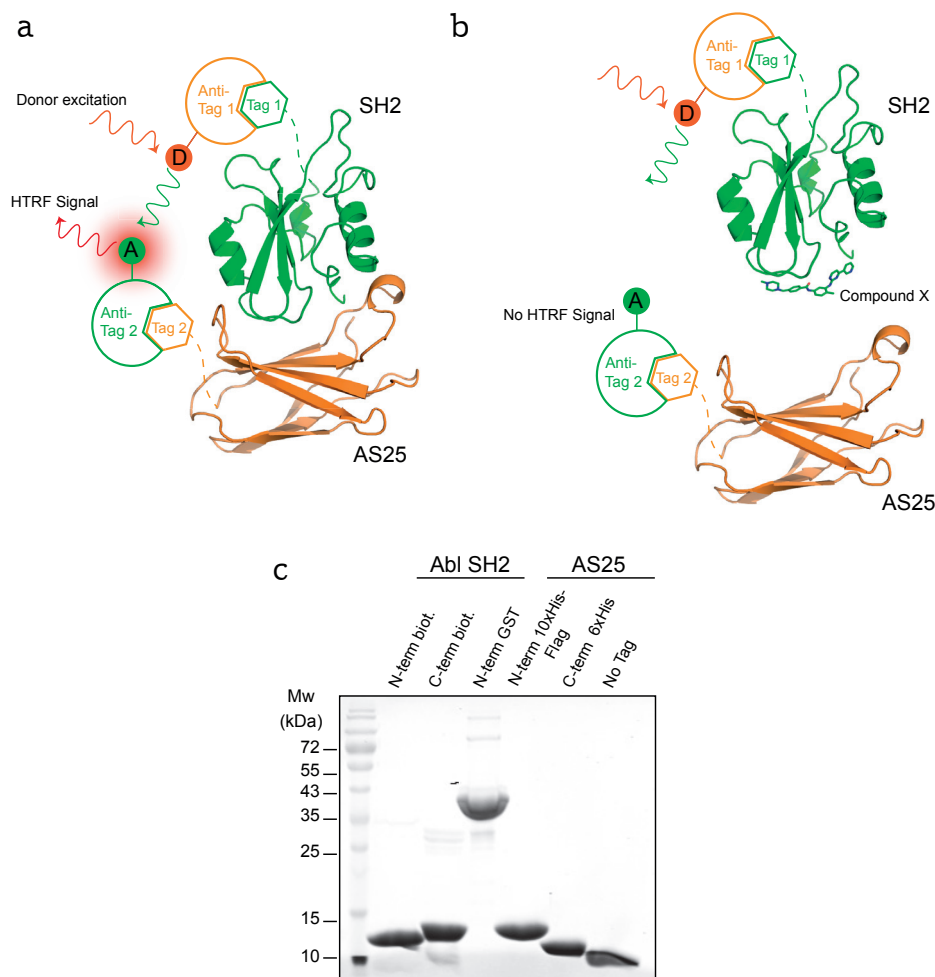


Figure 2.21 – Screening principle using indirect HTRF. The Abl SH2 is labeled with a chosen tag (tag 1) and AS25 with a second tag (tag 2). Tag 1 is detected with an anti-Tag 1 harbouring a donor fluorescent molecule (D), while the anti-Tag 2 harbours the acceptor molecule (A). (a) When both SH2 and AS25 are interacting the donor is in close proximity with the acceptor and an HTRF signal is generated through fluorescence resonance energy transfer once the donor is excited. (b) When the interaction is disrupted by a compound X binding to the Abl SH2, no HTRF is detected as the donor and acceptor are far apart in solution. (c) Coomassie staining of purified AS25 and SH2 versions used for the HTRF screening.

During the process development, we have decided to use AS25 and Abl SH2 with different tags and positions (either N- or C-terminal) to maximize the chance of finding the best possible pair and obtain a good signal/noise ratio. We have purified AS25 harbouring either N-terminal 10xHis-Flag tag or C-terminal 6xHis-Tag. The Abl SH2 was purified with a N-terminal GST

Chapter 2. Results

tag or harbouring a biotinylation at the N-or C-terminus (figure 2.21c). We chose to use as a donor Terbium (Tb)-Cryptate which is one of the brightest available at Cisbio. As acceptors, two molecules were used, either XL665 or d2. In total 28 combinations were tested by Cisbio (table 2.3).

Table 2.3 – Tested HTRF pair combinations. 28 HTRF pairs were tested using different antibodies (anti-), or Streptavidin (Strept) bound to one donor: Terbium (Tb) and two acceptors : d2 and XL665.

Combination	AS25		SH2	
	Tag	Anti-tag	Tag	Anti-tag
1	N-His	Tb-Anti-His	N-Biot	d2-Strept
2	N-His	Tb-Anti-His	N-Biot	XL665-Strept
3	N-His	Tb-Anti-His	C-Biot	d2-Strept
4	N-His	Tb-Anti-His	C-Biot	XL665-Strept
5	N-His	d2-Anti-His	N-Biot	Tb-Strept
6	N-His	d2-Anti-His	C-Biot	Tb-Strept
7	N-His	XL665-Anti-His	N-Biot	Tb-Strept
8	N-His	XL665-Anti-His	C-Biot	Tb-Strept
9	N-Flag	Tb-Anti-Flag	N-Biot	d2-Strept
10	N-Flag	Tb-Anti-Flag	N-Biot	XL665-Strept
11	N-Flag	Tb-Anti-Flag	C-Biot	d2-Strept
12	N-Flag	Tb-Anti-Flag	C-Biot	XL665-Strept
13	N-Flag	Tb-Anti-Flag	N-GST	d2-Anti-GST
14	N-Flag	Tb-Anti-Flag	N-GST	XL665-Anti-GST
15	N-Flag	d2-Anti-Flag	N-Biot	Tb-Strept
16	N-Flag	d2-Anti-Flag	C-Biot	Tb-Strept
17	N-Flag	d2-Anti-Flag	N-GST	Tb-Anti-GST
18	N-Flag	XL665-Anti-Flag	N-Biot	Tb-Strept
19	N-Flag	XL665-Anti-Flag	C-Biot	Tb-Strept
20	N-Flag	XL665-Anti-Flag	N-GST	Tb-Anti-GST
21	C-His	Tb-Anti-His	N-Biot	d2-Strept
22	C-His	Tb-Anti-His	N-Biot	XL665-Strept
23	C-His	Tb-Anti-His	C-Biot	d2-Strept
24	C-His	Tb-Anti-His	C-Biot	XL665-Strept
25	C-His	d2-Anti-His	N-Biot	Tb-Strept
26	C-His	d2-Anti-His	C-Biot	Tb-Strept
27	C-His	XL665-Anti-His	N-Biot	Tb-Strept
28	C-His	XL665-Anti-His	C-Biot	Tb-Strept

The first trial with all combinations was done in a 4 by 4 matrix testing 4 concentrations of each protein (0, 3, 30 and 300 nM). Sufficient signal-to-noise ratio was mostly obtained with both proteins co-incubated at 300 nM (data not shown). Among the 28 combinations, 8 combinations showed comfortable signals (figure 2.22, signal-to-noise ratio over 3).

2.6. Development of screening assays for Abl SH2-KD interface disrupters

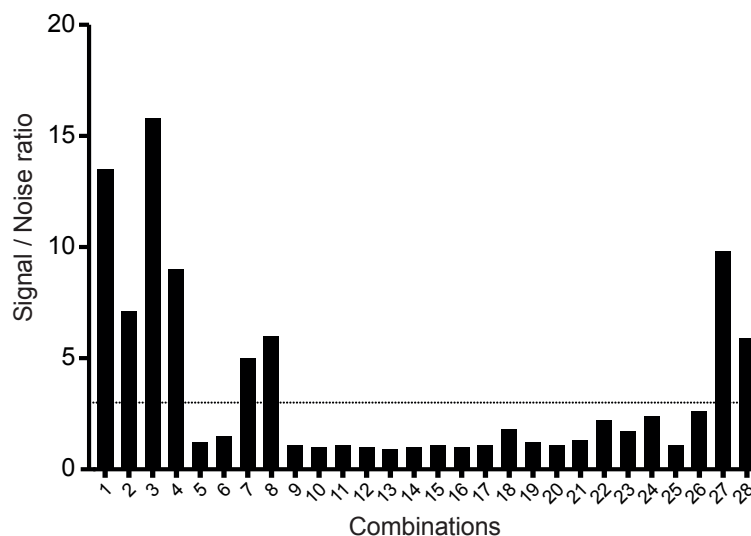


Figure 2.22 – Signal-to-noise ratio of 28 HTRF pair combinations. 28 HTRF pair combinations described in table 2.3 were tested with 300 nM of both AS25 and Abl SH2. Signal-to-noise ratios above 3 were considered as reliable (horizontal dash line). Data obtained by Cisbio France.

Most efficient combinations were observed with N-term 6xHis AS25 when detected by an anti-His bound to the Terbium donor and biotinylated SH2 detected by streptavidin bound to both d2 and XL665 (combination 1 to 4, 7 and 8), with slightly better signals obtained with C-term biotinylation (combinations 3 and 4). The combination 3 with Streptavidin-d2 gave a signal almost two times higher than with XL665. Combinations detecting N-term 6xHis AS25 with an anti-His bound to the acceptor instead of donor were efficient only if the donor was XL665 (combination 7 and 8) and again C-term biotinylated SH2 version was better (combination 7). Signal-to-noise above 3 were obtained with C-term 6xHis AS25 only when the anti-His antibody was bound to the XL665 acceptor but not d2 (combination 27 and 28) nor the Terbium donor (21 to 24), with this time N-term biotinylated SH2 showing improved signals (combination 27). All combinations using anti-Flag antibodies detecting the N-term Flag AS25 or anti-GST against GST-SH2 failed to give sufficient signals (9 to 20).

To further continue the analysis, the combinations 3, 8 and 27 were selected in order to have enough variation in the type of combination while keeping a good signal. Each combination was repeated two times with combination of 30 and 300 nM concentrations (figure 2.23). For the three combinations, as expected, the signal was high enough only when both AS25 and SH2 were co-incubated at 300 nM. Interestingly, the repeats 2 and 3 had very similar signal-to-noise ratio but were lower than the first trial, while still above 3, for all the three combinations (figure 2.23). Of note, samples were frozen and thawed between trials 1 and 2/3.

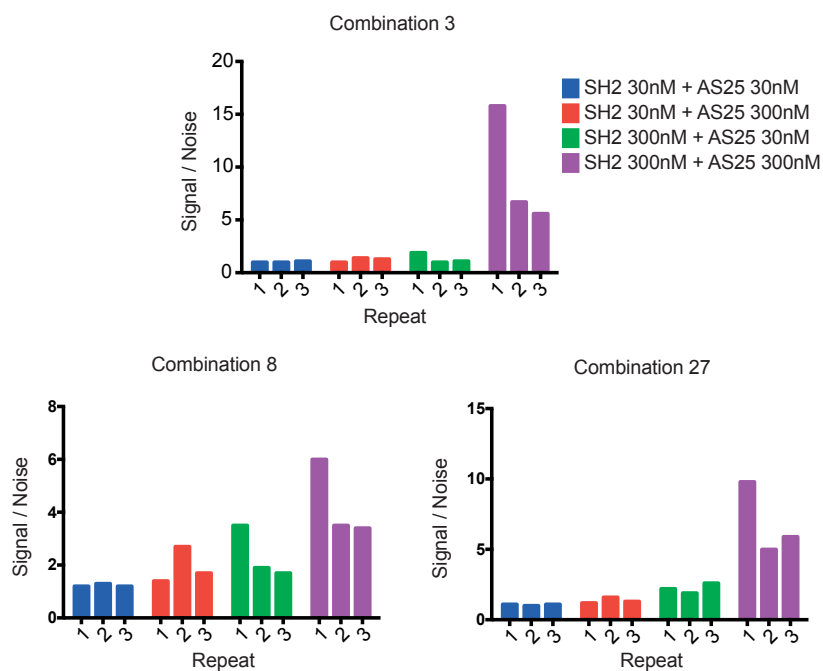


Figure 2.23 – Repeats of combinations 3, 8 and 27 at different protein concentrations. Combinations 3, 8 and 27 were repeated three times at several protein concentrations to confirm sufficient signal-to-noise ratio. Data obtained by Cisbio France.

Most of the combinations showed good signal overtime even after 18 hours incubation (figure 2.24). Combinations 8 and 27 showed excellent stability with the signal-to-noise ratio decreasing less than 10% after 18 hours. Combination 3 showed a decreasing signal overtime ($\approx 50\%$ after 18 hours).

The next important step was to show that the signal observed was specific. For that purpose, tagged AS25 and SH2 were incubated together with a cleaved, untagged, AS25. Overnight incubation with a 100-fold excess of cleaved AS25 returned the HTRF signal to the control (background) level for all 3,8 and 27 combinations, confirming that the observed signal was due to the AS25-SH2 interaction and can be competed with an excess of untagged AS25 (figure 2.25).

2.6. Development of screening assays for Abl SH2-KD interface disrupters

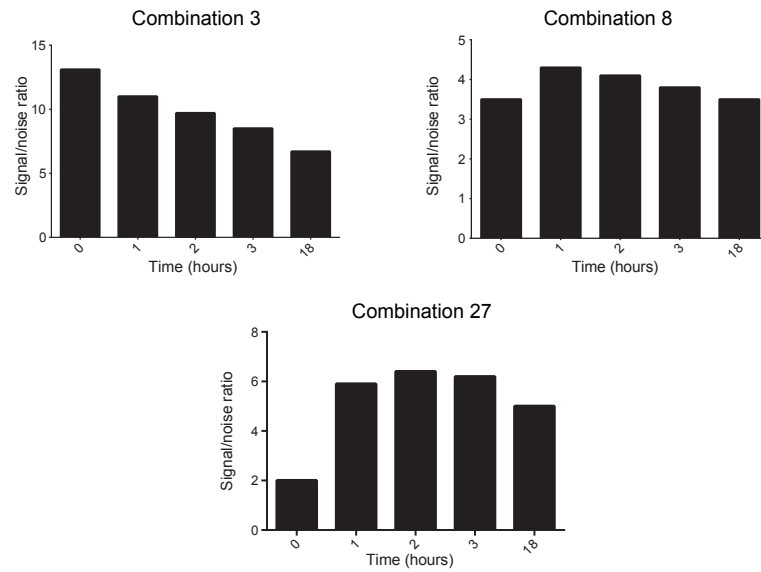


Figure 2.24 – Time-course signal-to-noise ratio of combinations 3,8 and 27. Signal-to-noise ratio of combinations 3,8 and 27 were measured at 5 different times points (hours) to assess for signal stability. Data obtained by Cisbio France.

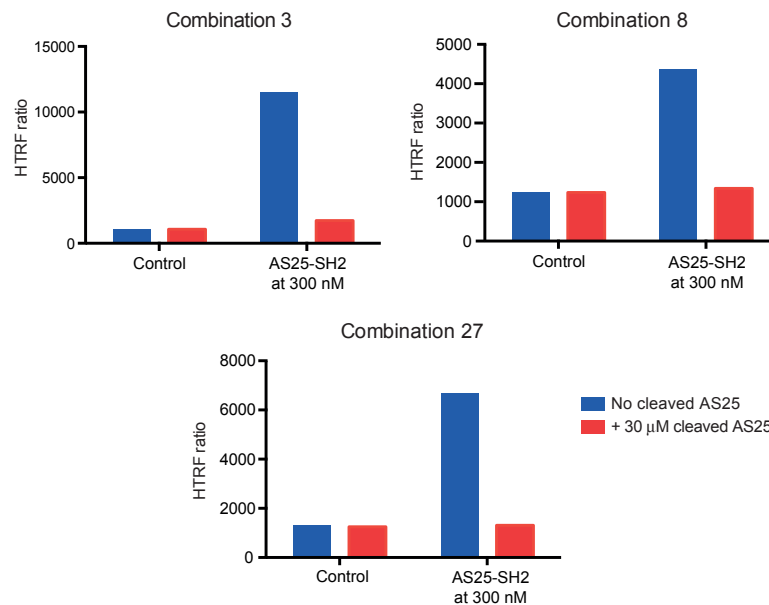


Figure 2.25 – Effect of cleaved AS25 on HTRF signal. Effect of competition by untagged AS25 was tested on combinations 3,8 and 27. HTRF signals of control experiments (no fluorophores) or AS25-SH2 complex at 300 nM were measured without (blue) and with (red) overnight co-incubation of untagged AS25. Data obtained by Cisbio France.

2.7 Roles of non-catalytic domains in cytoplasmic tyrosine kinases: focus on the Btk kinase

2.7.1 Targeted cytoplasmic tyrosine kinases and expression levels

We have selected 10 kinases (Btk, Csk, Hck, Lck, Src, Zap70, Syk, Ack, Fes and Brk) spanning 7 CTK families (Src, Csk, Brk, Tec, Fes, Syk, Ack) and tried to express several constructs in BL21 *E. coli* cells using the YopH co-expression strategy as well as transfected HEK293 cells. While most of the constructs showed detectable expression (Western Blot) in HEK293, recombinant expression in BL21 cells was more heterogenous. Some kinase domains were not expressed or mostly insoluble (Syk/Zap70, Lck/Hck) while others showed low-medium (Brk, Btk) to high yields (Csk, Fes, chicken-Src).

Table 2.4 – Selected cytoplasmic tyrosine kinases and expression in BL21 and HEK293 cells.

Kinase	Construct	Yield in <i>E. coli</i> (BL21)	Expressed in HEK293
Btk	KD	1 mg/L	Yes
	SH2-KD	<0.5 mg/L	Yes
	SH3-SH2-KD	<0.5 mg/L	Yes
	Full-length	1 mg/L	Yes
Csk	KD	2 mg/L	Yes
	SH2-KD	5 mg/L	Yes
	Full-length	>5 mg/L	Yes
Lck/Hck	KD	Not expressed	Yes
	SH2-KD	N.D	Yes
	Full-length	N.D	Yes
Src(chicken)	KD	>5 mg/L	N.D
	SH3-SH2-KD	>5 mg/L	N.D
Brk	KD	<1 mg/L	Yes
	SH2-KD	<1 mg/L	Yes
	Full-length	N.D	Yes
Zap70/Syk	KD	Insoluble	Yes
	SH2-KD	N.D	Yes
	Full-length	N.D	Yes
Fes	SH2-KD	>5 mg/mL	N.D
Ack	KD	Not expressed	Yes
	KD-SH3	N.D	Yes
	SAM-KD-SH3	N.D	Yes
	SAM-KD	N.D	Yes
	Full-length	N.D	No

2.7. Roles of non-catalytic domains in cytoplasmic tyrosine kinases: focus on the Btk kinase

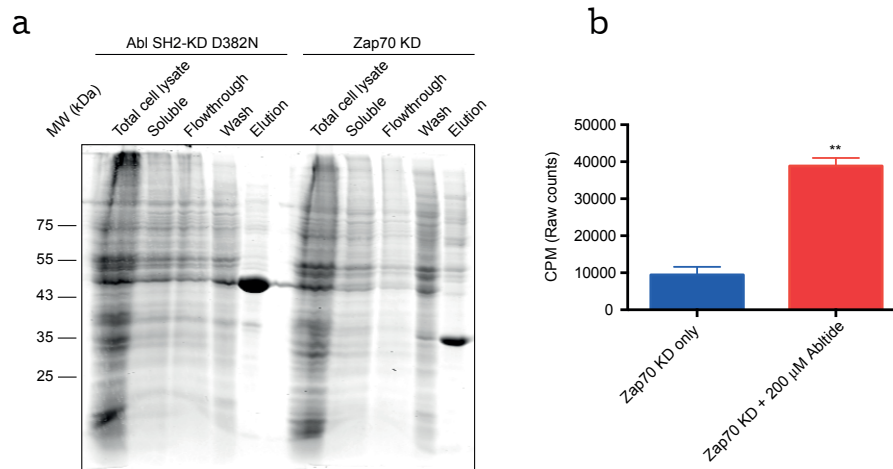


Figure 2.26 – Purification of Zap70 KD from transfected S2 cells. (a) Zap70 KD and Abl SH2-KD D382N (control) were expressed and purified from S2 cells after transfection. (b) Purified Zap70 KD in (a) was for tested kinase activity against an optimal Abl peptide (Abltide). Co-incubation of Zap70 KD with Abltide increased the raw count per minute by more than 4 times (CPM) (n = 2).

2.7.2 Expression trials in S2 insect cells

In order to be able to express fast and reliable amount of several CTKs constructs that were difficult targets in *E. coli*, we thought to develop in collaboration with David Hacker (EPFL) a transfection system using S2 drosophila cells. Trial assays with Zap70 KD, which was not expressed in BL21 cells, was compared to the expression of the Abl SH2-KD D382N (catalytically inactive) expected to be easily expressed, both containing a C-terminus 6xHis tag.

3 days after S2 cells transfection (300 mL), we have carried out cell lysis and protein purification. After a one step-purification using NiNTA beads, a band at the expected molecular weight was observed for both Zap70 KD and Abl SH2-KD D382N, as well as a relatively good purity (figure 2.26a). Estimated yields were 2 mg/L for Zap70 and more than 4 mg/L for Abl SH2-KD D382N. Importantly, the purified Zap70 KD showed activity against Abltide in an *in vitro* assay (figure 2.26b).

2.7.3 Role of non-catalytic domains in activation loop phosphorylation

We have selected kinases for which activation loop phosphorylation antibodies were available. Among the chosen kinases, we obtained antibodies detecting activation loop phosphorylation for Btk, Brk, Lck/Hck, and Zap70. No signal was obtained despite several trials for the Zap70 kinase (data not shown). After transfection in HEK293 cells, Btk and Brk showed a strong dependence on non-catalytic domains for activation loop phosphorylation whereas it was not the case for Hck (figure 2.27).

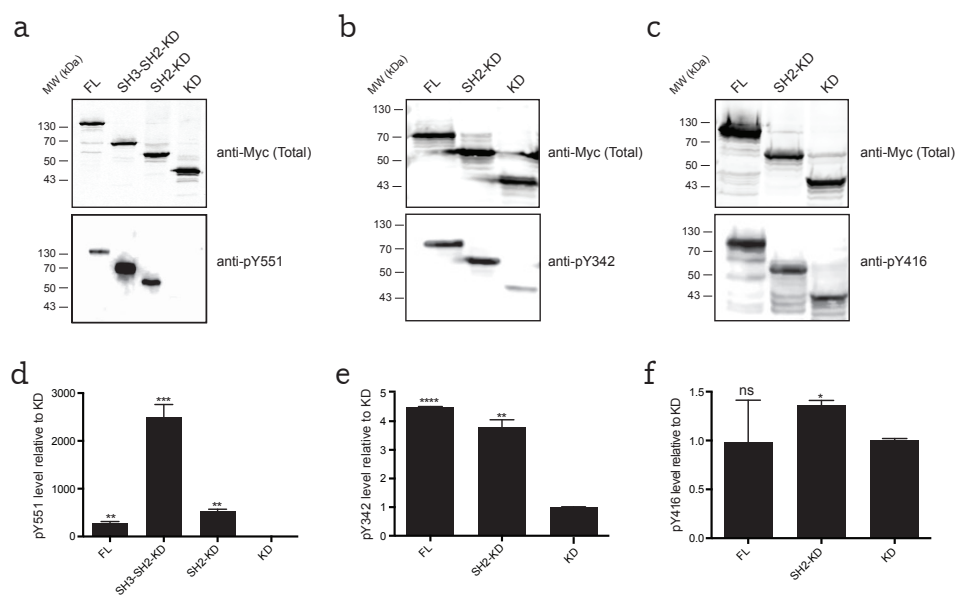


Figure 2.27 – Activation loop phosphorylation of several Btk, Brk and Hck kinase constructs in HEK293 cells. Several constructs were transfected in HEK293 for Btk (a), Brk (b) and Hck (c) kinases. Samples were blotted for anti-Myc (total protein expressed) and specific anti-phospho antibodies detecting activation loop phosphorylation for each kinase. Quantification of activation loop phosphorylation is shown relative to the level of the KD constructs for Btk (d), Brk (e) and Hck (f). FL: Full-length, KD: Kinase domain.

Almost no phospho-Y551 was detectable for Btk KD but adding the SH2 domain increased level drastically (>500-fold), and presence of both SH3 and SH2 gave an even stronger signal (>2500-fold increase), while the full-length construct showed a lower activation level (>250-fold). Brk kinase showed also a significant increase upon addition of the SH2 domain compare to the KD only (>4 fold), and a similar increase was also observed with the full-length protein.

Given the strong effects of both SH2 and SH3 domain on Btk kinase activation loop phosphorylation, we have further studied the activation loop phosphorylation of Btk kinase using mutants proteins. A preliminary study of several mutants that should affect SH2 (R307G, S309N) or SH3 (W251L) canonical binding as well as a kinase dead (D521N) and activation loop deficient mutant (Y551F) was carried out (figure 2.28). To confirm that the R307G and S309N mutants were indeed deficient in phosphotyrosine binding, we have used a fluorescent polarization assay that confirmed the R307G mutant as deficient in phosphotyrosine binding but not the S309N mutant which was only slightly affected (figure 2.28c-d). The R307G mutation did not affect the Abl SH2 folding *in vitro*. The SH3 W251L mutant was previously shown to prevent poly-proline motif binding and used in several studies (Yang et al. (1995), Yang and Desiderio (1997)). Interestingly, preventing phospho-tyrosine binding on the Btk SH2-KD construct did not affect pY551 level. On the contrary the Btk SH3-SH2-KD high phosphorylation level was drastically reduced upon disruption of phosphotyrosine binding, while preventing canonical binding of its SH3 only slightly decreased activation loop phosphorylation.

2.7. Roles of non-catalytic domains in cytoplasmic tyrosine kinases: focus on the Btk kinase

Finally, the kinase dead mutation completely prevented phosphorylation level of the SH3-SH2-KD construct, arguing for an autophosphorylation mechanism (figure 2.28a-b). No signal was observed upon mutation of the Y551 to phenylalanine (Y551F). Overall the results showed strong autophosphorylation ability of the Btk kinase in HEK293 cells, dependent on both the SH2 and SH3 domains, while the KD only was unable to undergo autophosphorylation in cells.

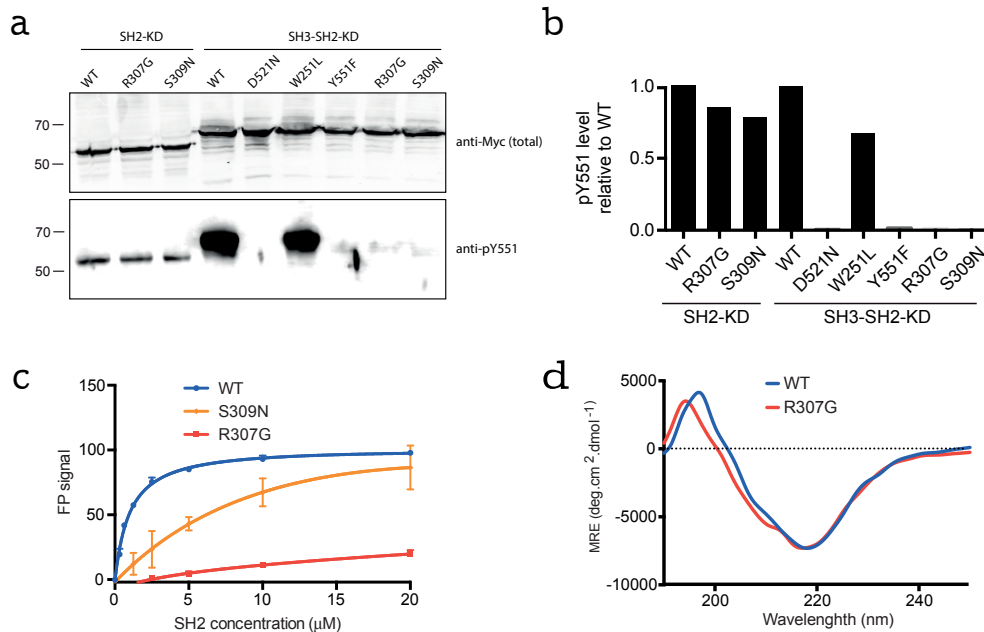


Figure 2.28 – Effect of several Btk mutants on activation loop phosphorylation. (a) Several mutant constructs of Btk SH2-KD and SH3-SH2-KD were transfected in HEK293 cells. (b) pY551 levels relative to WT construct were quantified. (c) Fluorescence polarization analysis of the Btk SH2 R307G and S309N mutants. (d) Far-UV spectrum of Btk SH2 WT and R307G.

2.7.4 Btk kinase autophosphorylation *in vitro*

Btk kinase autophosphorylation on its activation loop was analyzed *in vitro* using purified recombinant Btk kinase from *E. coli* as described in Wang et al. (2015). Purified Btk KD autophosphorylated very slowly while the presence of the Btk SH2 domain dramatically increased autophosphorylation rate (figure 2.29a-b). Despite a strong impairment of Btk KD autophosphorylation ability, no significant differences were observed in kinase activity between Btk KD and SH2-KD (figure 2.29c). This confirmed that both Btk KD and SH2-KD purified proteins were behaving well in solution and that the slow rate of Btk KD autophosphorylation was not due to unfolding of the protein or stability issues. The Btk SH3-SH2-KD construct was impaired in activation loop autophosphorylation with an autophosphorylation rate very close to the one of Btk KD.

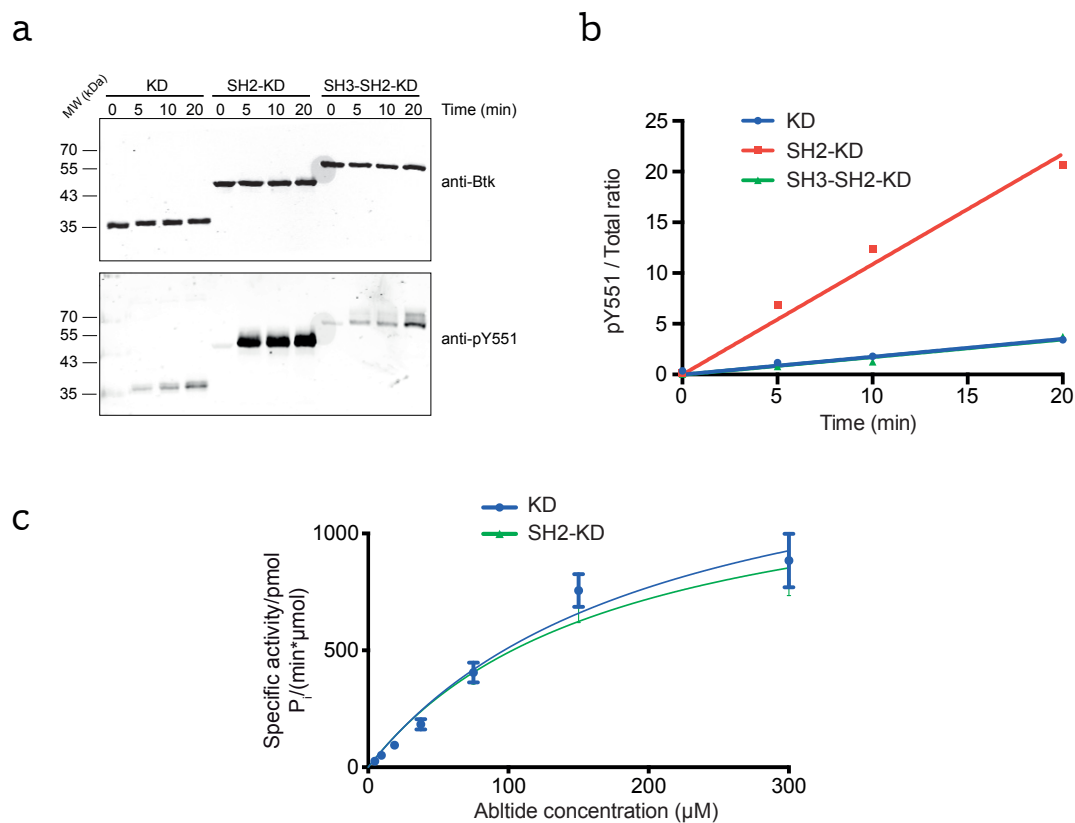


Figure 2.29 – Autophosphorylation ability of Btk kinase in solution. (a) Several Btk constructs (KD, SH2-KD and SH3-SH2-KD) were incubated with ATP and reaction stopped at different time points. Samples were immunoblotted with anti-Btk and anti-pY551 antibodies. (b) Activation loop phosphorylation levels were quantified using the Li-Cor system. (c) *In vitro* kinase activity of Btk SH2-KD and KD against Abltide. The kinetics were fitted using the Michaelis-Menten equation ($n = 3$).

3 Discussion

3.1 Role of the Abl SH2 domain in the kinase autophosphorylation

Despite expected differences in kinase activity when the Abl SH2-KD interface was disrupted via the I164E mutation (1.5 fold decrease) or increased via the T231R mutation (1.2 fold increase), the observed effects were mild and might not explain such a profound effect of interface disruption on transformation and leukemogenesis (Grebien et al., 2011). These effects are in line with a recent study using similar constructs (Lorenz et al., 2015). Regardless of robust kinase activity, the Abl KD was strongly deficient in autophosphorylation ability. Importantly, the I164E mutation did not affect the phospho-tyrosine binding of the SH2 (Grebien et al., 2011)

Most of the *in vitro* autophosphorylation sites strongly overlapped with cellular phosphorylation sites. This result does not exclude the possibility that Abl or Bcr-Abl can be phosphorylated by other tyrosine kinases in cells; however, this finding suggests that autophosphorylation likely plays a pivotal role in the Abl-activation process. Especially it has been shown that phosphorylation of Y412 in the activation loop was required for transformation of fibroblasts and hematopoietic progenitors (Pendergast et al., 1993).

We used type 1 and 2 Abl inhibitors to monitor activation loop conformation in the absence and presence of the SH2 domain using Y412 trans-phosphorylation assays. Dasatinib (type 1) converted the Abl KD from an inert to a good substrate for Y412 phosphorylation. This confirmed previous results obtained using NMR spectroscopy where dasatinib was shown to induce strong conformational shifts of Abl activation loop in solution (Vajpai et al., 2008). Interestingly, increased activation loop phosphorylation was also observed with JAK kinases type 1 inhibitors in a cellular set up (Andraos et al., 2012). This suggests that inhibitor-bound kinases gain some functional and conformational properties despite blockade of ATP binding and caution is needed when using the activation loop as a marker of kinases activation. On the contrary, Abl SH2-KD Y412 trans-phosphorylation was decreased when in complex with imatinib, confirming the closing of the activation loop by this type 2 inhibitor.

Chapter 3. Discussion

These trans-phosphorylation assays using inhibitor-bound Abl SH2-KD and KD constructs showed that the SH2 is an allosteric activator of activation loop opening, inducing Y412 phosphorylation. Based on the results we built a model where the activation loop is in an equilibrium between an open (active) and closed (inactive) conformation and for which the equilibrium is switched to the open conformation once the Abl SH2-KD interface is formed (figure 3.1). Disruption of the interface would favor the closed conformation as in the case of the KD only. The activation loop opening via SH2 binding to the kinase was also observed in molecular dynamics using *in silico* modelling in recent studies (Dölker et al. (2014), Tse and Verkhivker (2015)).

An abundant phosphorylation site in the SH2-KD linker was also detected: Y245 as previously observed (Brasher and Van Etten, 2000). The high levels of Y245 phosphorylation observed in our constructs suggests a strong phosphorylation consensus and excellent accessibility. While the structural role of Y245 in the inactive conformation is well understood, the consequences of its phosphorylation in the active conformation is unclear. Our autophosphorylation assays showed that phosphorylation of Y245 is also required for full activation loop phosphorylation, suggesting a temporal and functional coupling of Y412 and Y245. In addition, targeting the Abl SH2-KD interface had no impact on Y245 phosphorylation. Phosphotyrosine-binding by the SH2 was also required for efficient phosphorylation of Y412, but not of Y245. While a transient intermolecular interaction of SH2 binding to phospho-Y245 could be envisaged; however, no apparent dimerization of Abl SH2-KD upon autophosphorylation was observed. This type of mechanism is difficult to prove without a higher resolution crystal structure of phosphorylated Abl SH2-KD. Further functional studies have to be done to provide a reliable mechanistic explanation of these results.

Overall, we presented evidence that mechanisms of Abl activation can be deciphered using recombinant kinase produced in *E. coli*. This approach enabled us the understanding of a mechanism linking Abl SH2 allosteric regulation to two-phosphorylation events with an emphasis on activation loop phosphorylation.

3.2. Disruption of the Abl SH2-KD interface using monobodies

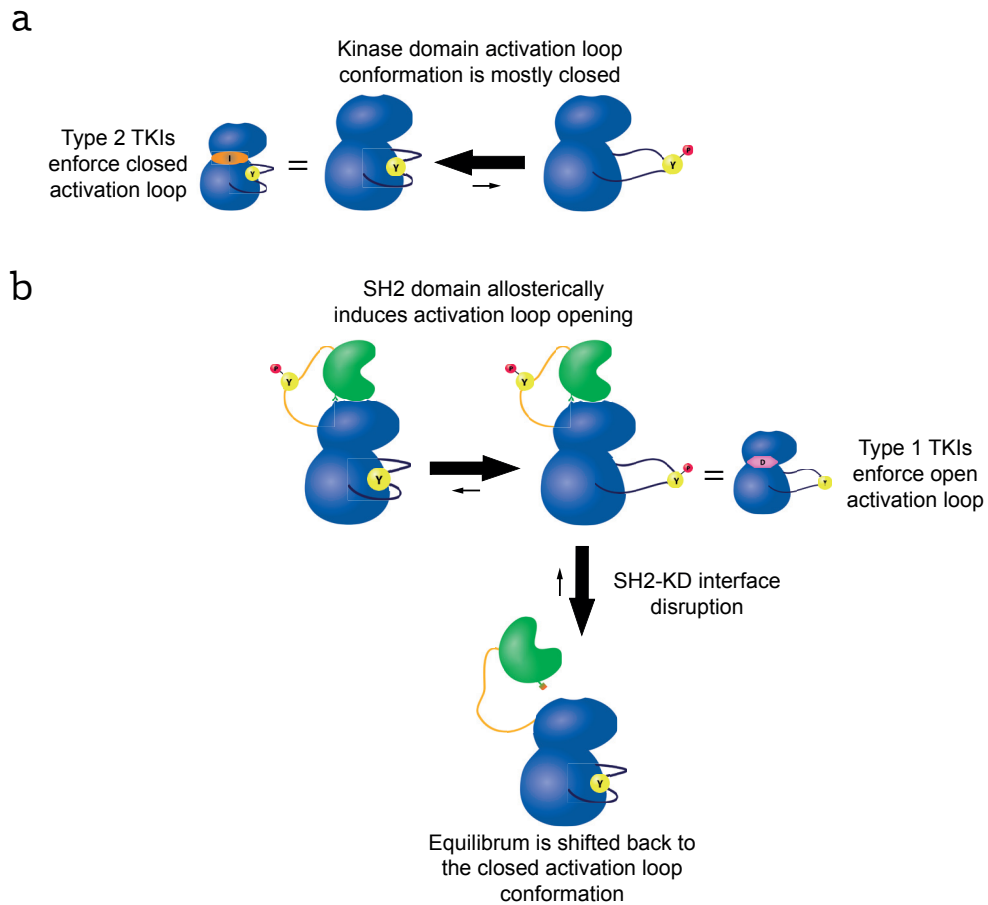


Figure 3.1 – Role of the Abl SH2-KD interface in activation loop opening summarized in a graphical model. (a) The Abl KD has a predominantly inactive activation loop conformation that is similar to the conformation once imatinib or other type-2 kinase inhibitor are bound. (b) Once the SH2-KD interface is formed, the equilibrium is shifted to a predominantly open activation loop similar to the conformation once dasatinib or type-1 inhibitors bind to the KD. TKI: tyrosine kinase inhibitor. Figure modified from Lamontanara et al. (2014).

3.2 Disruption of the Abl SH2-KD interface using monobodies

In order to establish the feasibility of targeting the Abl SH2-KD, we used two new monobodies termed AS25 and AS27 binding the SH2 domain that should compete with the KD binding. We first analyzed the effects of AS25 and AS27 on kinase activity using recombinant Abl SH2-KD and KD. The results were in line with the monobodies competing with kinase binding and disrupting the SH2-KD interface. Observed effects were obtained only at μM concentration ranges of monobodies. This was surprising as their binding affinities are in the nM concentration range. Possible unstability/precipitation of purified AS25 and AS27 was excluded as they eluted at the expected molecular weight during gel filtration and monobodies are very stable molecules. It is possible that the binding between Abl SH2-KD and Abl SH2 differs because of the presence of the KD.

Chapter 3. Discussion

Although there is often a good correlation between binding affinity of competitive inhibitor and their IC_{50} values in enzyme inhibition assays, for allosteric inhibition this is often not the case. Most notably, the allosteric Bcr-Abl inhibitor GNF-2/5 and its successor ABL001, that target the Bcr-Abl myristoyl binding site, showed no or only moderate inhibition in *in vitro* kinase assays, despite their low nanomolar binding affinities (Adrián et al., 2006). In general, and especially for allosteric inhibitors, affinity does not always directly translate to efficacy and biological effects.

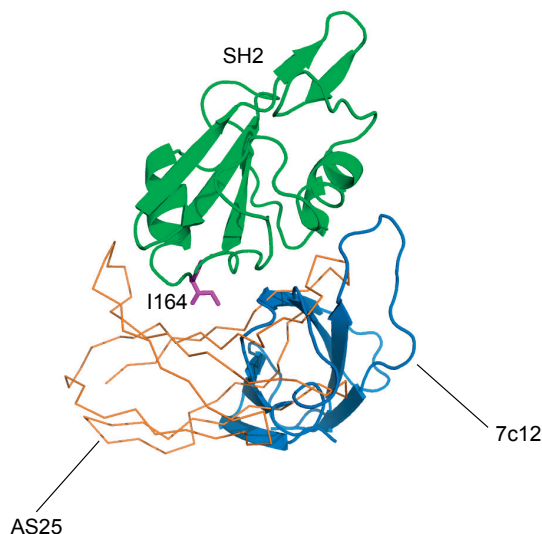


Figure 3.2 – Comparison of AS25 and 7c12 binding to Abl SH2. 7c12 (blue cartoon) binds to a different epitope when compared to AS25 (orange ribbon), further away from the I164 residue.

Both AS25 and AS27 binding to Abl PP or Bcr-Abl in cells were decreasing activation loop phosphorylation, in line with the effects observed *in vitro* when disrupting the SH2-KD interface via the I164E mutation (figure 2.14). The binding mode of 7c12 to the Abl SH2 is different from AS25 although partially overlapping (figure 3.2). Indeed, AS25 is binding in a very similar location as does the Abl KD, cradling the SH2 domain with I164 being a central residue. On the contrary, 7c12 is binding closer to the SH2 side, not being directly in contact with the I164E residue and further away from the KD binding site. It is not surprising therefore to observe stronger effects on Abl autophosphorylation and cell survival with Abl AS25/27. This is also a clear indication that potential therapeutics should bind closely to the I164 residue and that a potential molecule binding to the site as does 7c12 will likely have no effects.

We have also shown that AS25 and AS27 expressing K562 cells showed increased apoptosis overtime. This was a sign that monobody binding to Bcr-Abl SH2-KD interface affected cells dependent on the kinase. This experiment must now be completed by testing the monobodies in cells independent on Bcr-Abl. Indeed, specificity of AS25/AS27 in cells has to be evaluated and the monobodies should not affect cells that do not express Bcr-Abl, such as Ba/F3 cells. Because K562 cells were affected by the expression of AS25/27, it was impossible to do pull-

3.3. Screening assay development for Abl SH2-kinase interface disrupters

down analysis to check for AS25/27 specificity in cells via mass spectrometry, as usually done for monoclonal antibodies. Cell lines independent on Bcr-Abl should be used to check for possible off-target binding and confirm that the observed effects are specific for the Abl SH2-KD interface. Future experiments should also analyze the effects of monoclonal antibodies on phosphorylation of downstream Abl substrates such as STAT5, a clear indicator of Bcr-Abl activity in K562.

3.3 Screening assay development for Abl SH2-kinase interface disrupters

We first thought to develop a screening assay using a fluorophore which is able to detect changes in protein conformation (acrylodan). Based on a recent study (Schneider et al., 2012) where acrylodan was used to detect Abl myristate binders, we labeled several Abl SH2-KD cysteine mutants with acrylodan. Despite a clear fluorescence increase confirming labeling of the mutants, most showed no or little (E187C) change in fluorescence spectrum upon interface disruption with AS25. In general, once incubated with acrylodan, protein precipitation could be observed resulting in non-negligible protein loss. Even if binding of AS25 seemed to alter the maximum fluorescence of one of the mutant (E187C), only a decrease in fluorescence was observed, while acrylodan-based assays usually show also altered fluorescence spectrum with apparition or loss of secondary peaks in fluorescence. This was important as that type of assay is sensitive to the intrinsic fluorescence of tested compounds which can quench or increase the signal, leading to increasing false-positive or negative (Schneider et al., 2013). We doubted the robustness of this assay using the mutant we have chosen, and the calculated Z' (0.4) confirmed that the assay was marginal. Giving the tedious labeling of the Abl SH2-kinase and lack of robustness of the assay, we tried to find a way of using unlabeled protein that could be easily produced and at high yields.

Because the AS25 binding to Abl SH2 was well-characterized and we could show that it had biological effects, we postulated that some compounds binding to Abl SH2 and preventing the Abl SH2-AS25 complex formation might also later impair the Abl SH2-KD formation. In collaboration with Cisbio, we have developed an HTRF-based screening assay that will be able to detect small-molecules disrupting the formation of the Abl SH2-AS25 complex. The results showed high signal-to-noise ratios with several combinations and a complete abrogation of the signal when using an untagged AS25 as a competitor. A second optimization phase is currently ongoing with the combination 8 selected as the most reliable and stable pair. Further optimization will include testing other types of buffers, several concentrations of both proteins as well as reagents (antibodies or streptavidin bound to donor/acceptor) and the effects of freeze/thaw cycles. The screening method has been validated by the Biomolecular Screening facility (BSF) and the first screening trials are expected to be done early in 2016 (April-May). The BSF gives access to a library of more than 65.000 compounds and we are planning to start the screening using a dedicated protein-protein interaction inhibitors library (5441 compounds, Life Chemicals).

Only very few screening assays to find allosteric inhibitors are being currently developed or used. The real bottleneck is the lack of screening methods for such type of inhibitors as well as a limited knowledge of allosteric regulation among most of the targeted kinome. We hope that the use of monobodies could help in developing such assays in order to discover small-molecules binding to allosteric sites and important protein-protein interactions in cancer pathways.

3.4 Allosteric regulation in cytoplasmic tyrosine kinases

3.4.1 Recombinant protein expression strategy

In order to study allosteric regulation in several other CTKs, we needed to find expression systems that could give enough yield in order to carry out biochemical assays as well as conformational studies by SAXS. Although we were able to use *E. coli* expression for the Abl kinase study, some of the selected kinases were not well expressed in *E. coli*. This prompted us to develop another fast expression system using insect cells transfection. We showed that we could express the Zap70 kinase domain using this system. Thus, it might be possible to use S2 cells transfection as a fast replacement strategy for kinases that are difficult to purify from *E. coli*. New trials are ongoing to confirm the possible expression of other CTKs. This includes the use of constitutive as well as inducible expression vectors and co-expression with the YopH phosphatase. It is now clear that each kinase will require a specific expression system and the general strategy used for the Abl kinase is not applicable to most of the others CTKs.

3.4.2 Activation loop autophosphorylation: a focus on the Btk kinase

Preliminary studies of CTKs in transfected HEK293 cells led us to the observation that some kinases showed strong activation loop phosphorylation dependence on their protein-interacting domains (PIDs). Btk and Brk showed elevated activation loop phosphorylation only when one or more PIDs were present. Src family kinases such as Hck showed activation loop phosphorylation even in the absence of any PIDs in line with the rapid autophosphorylation of the Src KD already observed *in vitro* when using a generic phospho-tyrosine antibody (Seeliger et al., 2007). These results could be potentially indicating other type of positive allosteric interaction between the PIDs and kinase domains of other kinases than Abl. This study has to be completed by analyzing the effects of point mutations in the SH2 or SH3 disrupting their canonical functions to really confirm allosteric roles for the PIDs in activating kinase activity and autophosphorylation ability. This will also help mapping the possible kinase families that show dependence on their PIDs for kinase activation. We show here that the Btk and Brk could be potentially regulated allosterically while the Src family might be independent of such mechanisms.

Further evaluation of the Btk kinase has led to several interesting observations. Using mutants disrupting the SH2 phospho-tyr binding did not impair activation loop phosphorylation of

3.4. Allosteric regulation in cytoplasmic tyrosine kinases

Btk SH2-KD construct in transfected HEK293 cells. This is a strong indication that other mechanisms might be implied and that the SH2 could have non-canonical roles in activating Btk as observed for Abl. *In vitro* autophosphorylation of Btk KD, SH2-KD and SH3-SH2-KD confirmed a positive role of the SH2 but adding the SH3 reversed the activation loop autophosphorylation ability. This is in line with the recent structure of the Btk SH3-SH2-KD unit showing an autoinhibited conformation similar to the Src and Abl SH3-SH2-KD modules (Wang et al., 2015). The activating effect of the SH2 for Btk activation loop autophosphorylation was drastic while almost no differences were observed in catalytic activity comparing Btk KD and SH2-KD. This surprising result was in discrepancy with the recent study of Wang et al. (2015) where Btk KD showed very low activity and the SH2-KD activity was extensively higher. It is important to note that the peptide used in our assay, despite not being a natural substrate of the Btk kinase, harbours only one phosphorylatable tyrosine. In the case of Wang et al. (2015), the peptide was a natural sequence of PLC γ which has two tyrosines, making conclusions difficult as the observed increase in activity could be due to processive phosphorylation when the SH2 domain is present. Activation loop phosphorylation of Btk KD has been shown to drastically increase its catalytic activity (Lin et al., 2009). It is likely that the strong autophosphorylation of Btk SH2-KD in the activation loop might increase its catalytic activity to higher extents than the KD only and more experiments using deficient activation loop mutant and pre-phosphorylated proteins are ongoing.

We observed a discrepancy between the autophosphorylation rate of Btk SH3-SH2-KD in solution and in transfected HEK293. While the purified construct was unable to undergo fast autophosphorylation, we observed strong phosphorylation of the activation loop when transfected in HEK293 which was completely abrogated upon the R307G mutation in the SH2 phospho-tyrosine binding motif. One explanation could be an opening of the Btk SH3-SH2-KD closed conformation in cells by SH2 binders (tyrosine-phosphorylated partners) which have already been shown to open and activate Abl (Hantschel et al., 2003). This would be prevented by the R307G mutation in the SH2 which would keep the conformation closed and explain the low phosphorylation level of the SH3-SH2-KD R307G construct. Binding of other tyrosine kinases to the Btk SH3-SH2-KD construct could also induce trans-phosphorylation of the activation loop by those kinases, hence the increase phosphorylation levels. Indeed it is known that the activation loop of Btk is also trans-phosphorylated by other kinases such as Src kinase family members. Still, it is clear that the Btk kinase can autophosphorylate its activation loop and that trans-phosphorylation by its partners may not be the only responsible mechanisms for full Btk activation. Further studies are ongoing to understand the mechanism of Btk activation.

Loss of function mutations in Btk are the leading cause of X-linked agammaglobulinemia (XLA). The Btk SH2 domain is often mutated in XLA and more than 40 residues are found to be mutated among the 96 residues constituting the domain. Many of these mutations have been studied *in vitro* and it has been shown that even if some affect the canonical function of the SH2 domain (decreased binding affinity for phosphotyrosines) many have yet to be characterized. Surprisingly, no missense mutations have been observed in the SH3 (BtkBASE, last update in

november 2015), although this domain is known to harbour an autophosphorylation site (Y223) with a role that still remains elusive. In this study, we hope to find possible Btk SH2 mutations preventing autophosphorylation of the activation loop or decreasing overall kinase activity that would be implied in allosteric interactions with the kinase.

3.4.3 General strategies for studying positive allosteric mechanisms

With this study we would like to assess the strategies that one might use to understand allosteric regulation of CTKs both in solution but also in a cellular context. Thanks to the knowledge we gathered with the in-depth study of the Abl SH2-KD interface allosteric regulation as well as preliminary studies of the Btk kinase, we identified several critical points that one might address when studying CTKs regulation.

It is critical to correctly separate kinase activity and auto/trans-phosphorylation ability. Decreased autophosphorylation ability might not always be due to an impaired kinase activity, but could also be explained by more exquisite mechanisms such as sterical hindrance and conformational changes. The use of generic anti-phosphotyrosine antibodies such as 4G10 to compare kinase activity of constructs harbouring deletion of whole domains is not a viable solution. Indeed, deletion of such domains also means deletion of potential phosphorylated tyrosines, which in turns will lead to a decreased phospho-signal simply because critical tyrosines are absent. That is why we propose to use the activation loop phosphorylation status as a critical site to understand allosteric regulation. We observed that activation loop phosphorylation is for some CTKs highly dependent on the presence of PIDs. Whether this might indicate any allosteric activation effects need to be identified using mutational studies to prevent canonical functions of PIDs.

Analyzing activation loop phosphorylation status of CTKs constructs might provide a relatively quick method to detect potential CTKs that show allosteric activating effects of their PIDs. Overall, combining conformational SAXS studies, kinase activity assays, as well as harnessing the activation loop phosphorylation for each CTK might be a good way to start screening for potential PID-kinase interactions. As each CTK is only expressed in some types of cells, it is important that further studies will imply cell lines that are relevant for the disease-related CTKs such as using B-cell cell lines for Btk. The use of HEK293 cells provides a quick way to detect interesting mechanisms but would not be a good environment to understand how allosteric regulation can affect downstream effectors phosphorylation, as most effectors of Btk are for example absent in HEK293 cells. Using monobodies binding PIDs such as SH2 and SH3 and point mutations in PIDs will help to discover new hotspots in CTKs that can be later on targeted using small molecules (figure 3.3).

We are studying the conformation of several CTKs that we could express in *E. coli* including all possible constructs (KD to full-length) for Btk and Csk, the Fes SH2-KD and Src KD and SH3-SH2-KD. This first trial gave us a good base to know which conditions should be used for each construct and we should obtain SAXS reconstructions for some CTKs during this year.

3.4. Allosteric regulation in cytoplasmic tyrosine kinases

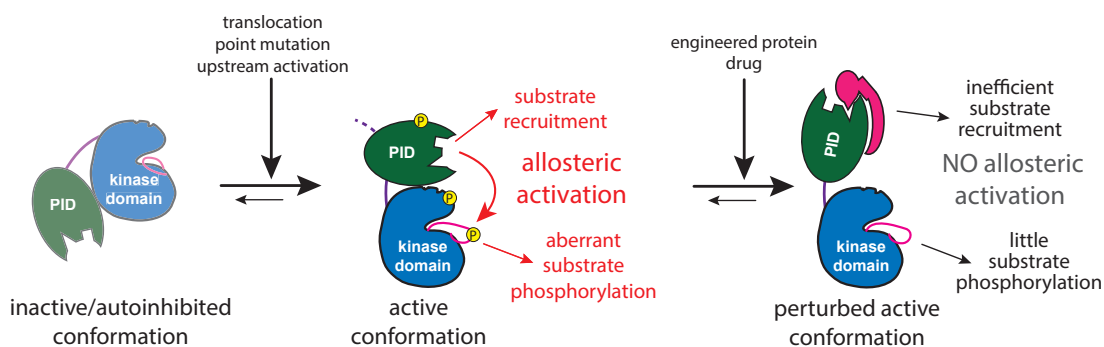


Figure 3.3 – Model of positive allosteric regulation via protein-interacting domains. Once activated, cytoplasmic tyrosine kinases active conformation is maintained through allosteric interactions between the kinase domain (blue) and PIDs (green). Preventing this interaction with a drug (purple) will induce a perturbed active conformation unable to correctly phosphorylate downstream targets. PID: Protein-interacting domain.

3.4.4 Targeting allosteric sites in kinases: combination therapies

Btk, essential component of the early BCR signaling pathway, is a validated cancer target in some type of hematological malignancies. Ibrutinib (PCI-32765) is a Btk inhibitor that binds covalently to cysteine 481 in Btk ATP-binding site (irreversible inhibition). It has shown remarkable clinical response in chronic lymphocytic leukemia and mantle cell lymphoma, and has been FDA-approved for the treatments of these diseases. However, more than 5% of the patients have progressed after a 1 year of follow-up (Woyach et al., 2014). Recently, studies have shown that most of these patients had the cysteine 481 mutated to a serine (Cheng et al., 2015), keeping the Btk kinase functional but rendering ibrutinib inhibition much less efficient. This is another example that a different strategy is needed for peculiar patients and targeting new sites in Btk kinase domain or any other domains might be efficient.

Most, if not all, classical ATP-competitions strategies are usually facing point mutations close to the inhibitor binding sites rendering the inhibitor inefficient. Similarly many suffer from undesired selectivity profiles. Allosteric inhibition of kinases is a recent field compared to classical inhibition but it has evolved rapidly in the past few years since the approval of the first allosteric inhibitor on the market: trametinib. Trametinib is targeting the MEK kinase family and showed good results and safety profiles, it was approved as a single agent therapy for patients with the BRAF V600E mutated metastatic melanoma. Within 6 to 8 months resistance appeared. Single-site mutations in the allosteric binding pocket and activation loop of MEK1 have been identified in melanoma that inhibit the binding of allosteric MEK inhibitors. Interestingly, a combination therapy with dabrafenib, an ATP-competitive inhibitor targeting the upstream kinase BRAF was shown to significantly improved survival of patients compared to single-therapy with trametinib (Flaherty et al., 2012). Still, most patients relapse after 9 to 11 months with this combination therapy mostly due to MAPK reactivation because of BRAF amplification or additional oncogenic mutation (Long et al., 2014). It is important to

note that trametinib, despite being considered as an allosteric inhibitor, binds very close to the ATP-binding site in a so-called "allosteric" pocket that needs specific orientation of the activation loop. This important feature prevents to actually target the same kinase, namely MEK, with both ATP-competitors and allosteric inhibitors.

Targeting of the same protein but at different sites has been recently achieved for the Abl kinase. A combination therapy using ABL001, targeting the myristate binding pocket, and Nilotinib, targeting the ATP-binding site, conducted by Novartis promoted a sustained tumor regression for over 150 days in CML mice model (Wylie et al., 2014). Importantly, and on the contrary to single agents dosing with both inhibitors, no resistance has been observed upon combination therapy. These results showed that therapeutically relevant inhibition of Bcr-Abl activity can be achieved by combining allosteric and ATP-competitive inhibitors and that this can overcome resistance to either agent alone. These exciting results might prove that combination therapy with allosteric agents might be a solution in certain type of cancers such as CML. It remains still elusive if such combinations will work with other type of kinases and we believe that using our strategies to understand CTKs allosteric regulation might help to answer this question.

3.5 Concluding remarks and future perspectives

We presented evidence that mechanisms of Abl activation can be mirrored using pure recombinant proteins produced in bacteria. This approach enabled the discovery of a novel mechanism that links the allosteric regulation of the SH2 domain to two critical phosphorylation events in the SH2-KD linker and in the activation loop and expanded our understanding of Abl kinase activation. Using monobodies disrupting the Abl SH2-KD interface we have been able to confirm the therapeutic potential of targeting allosteric intramolecular interactions in the Bcr-Abl oncogenic kinase. The monobodies could be further used to develop a screening assay for inhibitors that would mimic their effects. The monobody-based screening assay was robust and is further being improved.

Evidence of further allosteric activation is under investigation and interesting preliminary results showed that the Btk kinase might also be positively influenced by its PIDs domains. Although the ample availability of validated research tools, such as antibodies, kinase inhibitors and mutations, has accelerated the process, the proposed workflow and experimental approaches will facilitate future quantitative analyses of allosteric regulatory mechanisms in other tyrosine kinases.

Next generation technologies will be needed to identify complex regulatory interdomain communications at the full-length level of CTKs. It will also be interesting to analyze the dynamic binding of proteins/ligands that would alter the intramolecular interactions of certain CTKs such as SH2/SH3 binders. We hope that our structural and functional studies of multidomain constructs of CTKs will show the diversity of possible positive allosteric interactions as well as potential ways to target them.

4 Material and Methods

4.1 Abl protein expression, purification and biophysical analysis

4.1.1 Cloning of Abl constructs

Numbering of the isoform 1b of the human ABL1 gene is used in the manuscript. cDNAs encoding for human ABL1 (Abl kinase domain (KD): residues 248-534, Abl SH2-kinase domain (SH2-KD): 138-534) were cloned into the pET-21d vector using NheI and XhoI restriction sites. The 2xMyc-SBP tag was cloned into the XhoI and Sall site of pET-21d, adding the tag at the C-terminus of Abl SH2-KD cDNA. All point mutations were added using the Quickchange site-directed mutagenesis kit (Stratagene).

4.1.2 Abl co-expression with YopH phosphatase and purification

BL21(DE3) E.coli cells were transformed with both plasmids encoding for the desired Abl construct as well as a plasmid harbouring the YopH phosphatase. The transformed cells were grown in Terrific Broth medium until the culture reached an OD_{600nm} of 1.2. After adding 1 mM of IPTG, protein expression was carried out at 18°C. After 16 hours, cells were harvested and the pellet solubilized in resuspension buffer (500 mM NaCl, 50 mM Tris-HCl pH 7.5, 5% Glycerol, 25 mM imidazole and 1 mM DTT). Cells were lysed by homogenization using Avestin Emulsiflex C3 homogenizer with 3 cycles of lysis at 15.000 psi. Lysates were clarified by centrifugation at 20.000 rpm for 30 minutes. The soluble fraction was applied to a 5 mL HisTrapFF crude column and the protein eluted with a gradient (0-100%) of resuspension buffer + 500 mM imidazole. The eluted peak fractions were pooled and applied to a subsequent desalting column (HiPrep 26/60). Finally, the desalted sample was purified over a monoQ 5/50GL. Each purification step was followed by coomassie staining.

4.1.3 Multi-angle light scattering analysis of purified Abl constructs

Multi-angle light scattering was used to probe for protein quality and oligomerization states. All measurements were performed at RT using DAWN HELLIOS multi-angle light scattering detector (Wyatt Technology Corp, Santa Barbara CA) online with a size exclusion chromatography column (SEC). 80 μ L (0.5 mg/mL) of purified recombinant protein was injected onto a Superdex 75 HR10/30 column (GE Healthcare) in SEC buffer (25 mM Tris-HCl pH 7.5, 100 mM NaCl, 5% glycerol, 1 mM DTT) and eluted at a flow rate of 0.5 mL/min. Absolute molecular weights and homogeneity were determined using ASTRA version 5.3 from Wyatt Technologies.

4.1.4 Circular dichroism spectroscopy

The Far-UV spectrums (195-205 nm) of Abl SH2-KD WT and I164E were carried out in 25 mM phosphate buffer pH 7 at room temperature using a 0.1 cm quartz cell and Jasco J-815 CD Spectrometer equipped with a thermostated cell holder. Data was acquired at a step size of 0.5 nm and bandwidth of 1 nm. 3 scan records was used for each protein to generate the data reported in units of mean molar ellipticity per residue.

4.1.5 Small-Angle X-ray scattering

Synchrotron Small Angle X-ray Scattering (SAXS) data were collected at EMBL P12 beamline (DESY, Hamburg) and recorded at 10°C using PILATUS 1M pixel detector (DECTRIS) at a sample-detector distance of 2.7 m and a wavelength of 1.2 Å. This setup covers a range of momentum transfer of $0.0005 < s < 0.6 \text{ \AA}^{-1}$ ($s = 4\pi \sin(\theta)/\lambda$, where 2θ is the scattering angle). A robotic sample changer was used and the samples were measured in a concentration range from 4.5 to 0.6 mg/mL for WT and 1.3 to 0.4 mg/mL for the I164E mutant. Initial data processing and reduction were performed using an automatic pipeline and theoretical extrapolation to infinite dilution. For the calculation of the forward scattering $I(0)$ and the radius of gyration (R_g), the Guinier approximation implemented in PRIMUS was used, assuming that at very small angles ($s < 1.3/R_g$) the intensity is represented as $I(s) = I(0) * \exp(-(sR_g)^2/3)$. The pair-distance distribution function $P(r)$ was evaluated with GNOM and consecutively the maximum particle dimension (D_{max}) as well as R_g were estimated. The Porod volume was computed using the Porod invariant, and the molecular mass estimated. *Ab initio* models were computed with DAMMIF, using low resolution data in the range of $0.012 \text{ \AA}^{-1} < s < 0.200 \text{ \AA}^{-1}$. The algorithm constructs bead models yielding a scattering profile with the lowest possible discrepancy (χ) to the experimental data while keeping beads interconnected and the model compact. Twenty independent *ab initio* reconstructions were performed and then averaged using DAMAVER, which also provides a value of normalized spatial discrepancy (NSD), representing a measure of similarity among different models. Model superimposition was computed using the program SUPCOMB. Rigid Body Modelling were performed using the software BUNCH. Flexibility was assessed with the software Ensemble Optimization Method 2.0 which assumes coexistence of a range of conformations in solution for which an

average scattering intensity fits the experimental SAXS data. Using EOM 2.0, a pool of 10.000 independent models is initially generated. The theoretical scattering curve is automatically computed for each model in the pool by using CRY SOL. Afterwards, a genetic algorithm (GA) is employed to selected ensembles, randomly distributed in term of size from 5 to 20 cofomers, by calculating the average theoretical profiles and fitting them to the experimental SAXS data. The GA is hence repeated 100 times, and the ensemble with the lowest discrepancy is reported as the best solution out of 100 final ensembles.

4.2 Abl kinase assays and autophosphorylation

4.2.1 *In vitro* kinase assays

1 ng of recombinant protein, 75 μ M ATP, 7 μ Ci γ -³²P-ATP was incubated with an optimal Abl substrate sequence carrying an N-terminal biotin (biotin-GGEAIYAAPFKK) in kinase assay buffer (20 mM Tris-HCl pH 7.5, 5 mM MgCl₂, 1 mM DTT, 10 μ M BSA) for 12 minutes at room temperature in a final assay volume of 20 μ L. Peptide concentrations ranged from 3.125 μ M to 100 μ M. The terminated reaction (10 μ L 7.5 M guanidinihydrochlorid) was spotted onto a SAM2 Biotin Capture membrane (Promega) and further treated according to the instructions of the manufacturer. For monobodies co-incubation, recombinant kinase was first pre-incubated with selected monobodies at various concentrations for 10 minutes at room temperature before starting the reaction.

4.2.2 Mapping of Abl autophosphorylation sites

Recombinant Abl SH2-KD was incubated at 0.3 mg/mL in Tris 25 mM pH 7.5, 10 mM MgCl₂, 1 mM DTT, 300 μ M ATP for 2 hours at room temperature. Unphosphorylated Abl SH2-KD sample was also incubated in similar conditions with the omission of ATP, and used as a control during mass spectrometry analysis.

In gel digestion

Samples were separated by SDS-PAGE and Coomassie stained bands were In-Gel digested. Bands of interest were excised, reduced in 10 mM DTE, 50 mM AB and then alkylated in 55 mM Iodoacetamide, 50 mM AB. After a last washing step, gel extracts were digested with either MS Grade Trypsin, Endoproteinase GluC or Chymotrypsin over-night. Resulting peptides were finally extracted using a high organic containing solvent and dried by vacuum centrifugation prior to LC-MS2 measurements or Phosphopeptides enrichment.

Phosphopeptides enrichment

Around 90% of the extracted peptide amounts were used for Phosphopeptides enrichment step while the remaining 10% was used for sample identification. Titanium Dioxide affinity principle was used for the enrichment using home-made titania tips (based on Thingholm and Larsen 2009). After having equilibrated the tips with 0.75% TFA, 60% Acetonitrile, 300mg/ml Lactic acid (named solution A), dried samples were resuspended in this very same solution and loaded on tips. A first washing step in solution A was performed followed by a second one with 0.1% TFA, 80% Acetonitrile. A two-step elution was finally performed first with 0.5% Ammonium hydroxide and then with 5% Piperidine. Samples were acidified and dried down prior to LC-MS2 measurements.

Mass spectrometry measurements

Dried samples were resuspended in 0.1% TFA and separated by C18 Reverse Phase nano UPLC using a Dionex Ultimate 3000 RSLC system (Thermo Fischer Scientific) on line connected to an Orbitrap Elite Mass Spectrometer (Thermo Fischer Scientific). Samples were first trapped on a home-made capillary C18 pre-column and then separated on a C18 capillary column (Nikkyo Technos Co; Magic AQ C18; 3 μ m-100Å; 15cm x 75 μ m ID) at 250nl/min. over a 90min. biphasic gradient ranging from 99% A (2% ACN, 0.1% FA) to 90% B (90% ACN, 0.1% FA). Data-Dependent mode was used for MS acquisitions where the 20 most intense parent ions were selected for subsequent fragmentation by CID and then excluded for 40 seconds. A Potential Phosphopeptides m/z inclusion list was also generated and used to maximize detection chances.

4.2.3 Abl autophosphorylation assays

Abl autophosphorylation assays were carried out with 265 nM of recombinant Abl proteins in 20 mM Tris-HCl pH 7.5, 5 mM MgCl₂, 1 mM DTT, 300 μ M ATP in a total volume of 150 μ L. Reactions were stopped at desired time points by adding 50 μ L of 2X SDS-PAGE sample buffer, 400 ng (30% of the total reaction volume) of proteins were dot blotted on a nitrocellulose membrane using the BioDot Appartus (Bio-Rad) system following the manufacturer's recommendations. Total phosphotyrosine (4G10, Millipore), pY245 (2868S, Cell Signaling) or pY412 (2865S, Cell Signaling) levels were quantified using the Li-cor Odyssey imaging system and normalized for total Abl protein levels (Penta-His antibody, Qiagen, co-incubated with the phosphotyrosine antibody). Abl proteins incubated with no ATP were used as background and subtracted before normalizing values.

4.2.4 Abl transphosphorylation assays

Pairs of active and catalytically-deficient KD and SH2-KD protein were mixed in a 1:1 molar ratio at 265 nM final concentration in 50 μ L volume in 20 mM Tris-HCl pH 7.5, 5 mM MgCl₂, 1 mM

DTT, 300 μ M ATP. Reactions were stopped at desired time points by adding 50 μ L of 2X SDS-PAGE sample buffer. 100 ng of protein were resolved on a 12% SDS-PAGE gel, transferred onto a nitrocellulose membrane by semidry electroblotting and incubated with total phosphotyrosine (4G10, millipore), pY245 (2868S, Cell Signalling) or pY412 (2865S, Cell Signalling) antibodies mixed with a Penta-His antibody (Qiagen). Phosphorylation levels were quantified using the Li-Cor Odyssey imager system and normalized for total Abl protein levels, Abl proteins incubated with no ATP were used as background and subtracted before normalizing values. Abl KD/SH2-KD-drug complexes were obtained by incubating the protein with 3-fold molar excess of imatinib or dasatinib (Symansis) for 10 minutes at room temperature, followed by extensive dialysis against 150 mM NaCl, 20 mM Tris-HCl pH 7.5, 1 mM DTT, 5% glycerol to remove the free drug. The final dialyzed proteins were used as substrates for the assay.

4.3 HEK293 cell transfections

HEK293 cells were cultured in DMEM medium supplemented with 10% FCS and 1% penicillin/streptomycin. Cells were co-transfected with Abl PP (Barila and Superti-Furga, 1998) or Bcr-Abl and 6xMyc tagged monobodies expression vectors (pSGT vector for Abl and Bcr-Abl and pCS2-gateway vectors for monobodies) using the Polyfect transfection reagent according to the manufacturer's instructions. 48 hours after transfection, cells were harvested and lysed in IP buffer (50 mM Tris-HCl pH 7.5, 150 mM NaCl, 1% NP-40, 5 mM EDTA, 5 mM EGTA, 1 mM orthovanadate, 1 mM PMSE, 10 mg/mL TPCK and protease cocktail inhibitor from Roche) and cleared by centrifugation at 14,000 rpm, 4°C for 10 minutes. Total protein concentration was measured using Bradford assay (Bio-rad; 500-0006).

4.4 Western blotting, immunoprecipitation and antibodies

4.4.1 Western blotting analysis and antibodies

Immunoblotting analysis 100 μ g of cellular lysates were used. Samples were separated by SDS-PAGE and then transferred onto a nitrocellulose membrane (Whatmann, Protran BA85, GE healthcare) with a semi-dry blotting system (Hoefer Scientific Semi-phor TE70). Membrane and Whatman papers were pre-soaked in Western Blot buffer (25 mM Tris, 192 mM Glycine, 10% Glycine, 10% (v/v) methanol). After blotting for 1.5 hours at 0.075 mA/cm² the membrane was blocked with blocking solution according to the antibodies's manufacturer instructions. Primary antibodies were incubated overnight at 4°C. The next day, membrane was washed three times 5 minutes with TBS-T or PBS-T (0.1% Tween 20). Following the washing, the primary antibody was detected with IRDye680 and IRDye800-coupled antimouse or antirabbit antibody or HRP-conjugated IgG antibodies diluted in the washing buffer. Secondary antibodies were washed away (3 times, 5 minutes in washing buffer).

The following antibodies were used: total phosphotyrosine (4G10, millipore), anti-Abl (A5844, sigma), pY412 (2865S, Cell Signalling), anti-myc-IRDye800 (600-432-381, Rockland), IRDye680

Chapter 4. Material and Methods

and IRdye800-coupled anti mouse (Li-cor, 926-32210) and anti-rabbit (Rockland, 611-732-127), HRP conjugated anti-mouse (Jackson ImmunoResearch, 115-035-003), anti-rabbit (Jackson ImmunoResearch, 111-035-003). ECL prime detection reagent was used to detect HRP-conjugated antibodies (GE healthcare, RPN2232).

4.4.2 Abl immunoprecipitation

1 mg of total protein was used for immunoprecipitation from HEK293 cells lysates. The required volume of cell lysate was calculated and volume was added up to 1 mL with IP buffer. Home-made anti-Abl antibody was added to each IP sample and incubated for 3 hours on rotating wheel at 4°C. 50 μ L of Protein G sepharose (GE Healthcare, 17-0618-01) were added to each sample and incubated 1 hour on rotating wheel at 4°C. Subsequently, beads were washed 3 times with IP buffer. During the final wash, 20% of IP were spared to detected bait protein. Beads were finally boiled in laemmli buffer for 5 minutes at 95°C.

4.5 Expression and purification of recombinant monobodies

Monobodies were produced with an N-terminal 10xHis-FLAG tag using the pHFT2 vectors. Proteins were expressed in *E. coli* BL21(DE3). After bacterial transformation, P0.5G medium was inoculated and the preculture grown overnight at 37°C. 1 mL of the P0.5G preculture was used to inoculate 1 L of auto-induction medium (Formedium, LB-broth based with trace elements). The culture was grown at 37°C and after 4 hours the temperature decreased to 18°C for 18 hours. Bacteria were harvested and lysed similarly as in 4.1.2. Protein were purified to apparant homegeneity using Ni-affinity sepharose beads (GE healthcare). Final samples were purified using gel filtration Superdex 75 16/60 column and the corresponding peak fractions pooled and purity verified on coomassie staining.

4.6 Retroviral transduction and FACS analysis of K562 cells expressing monobodies

K562 cells were cultured in RPMI medium supplemented with 10% FCS and 1% penicillin/streptomycin. K562 cells stably-expressing N-TAP fused monobodies (AS25, AS27, HA4 and HA Y87A) were generated by retroviral gene transfer as described previously in (Wojcik et al., 2010). For six consecutive days starting 24 hours after the second retroviral infection of the target K562 cells and every 24 hours, aliquots of 10^6 cells were removed from the culture and were analyzed by flow cytometry (Accuri C6, BD Biosciences). Cells were analyzed for GFP expression (co-expressed with TAP-tagged monobodies) and in parallel stained with Annexin V Cy5 (BD PharmingenTM, 559933) and 7-AAD (BD PharmingenTM, 559925).

4.7 Cytoplasmic tyrosine kinase characterization

4.7.1 Recombinant purification from *E. coli*

Most of the CTKs were expressed in a similar way to Abl (see Section 4.1.2) except for the Btk kinase constructs that were co-expressed with YopH phosphatase as well as the GroEL/GroES co-chaperones system as described in (Wang et al., 2015).

4.7.2 Expression and purification trial from S2 insect cells

The human SH2-KD D382N of Abl1b isoform (S248 to V534) and KD of Zap70 (M327 to G606) harboring a C-terminus 6x-His-tag were cloned into the pEx-X plasmid. S2 cells were grown in suspension in SF900 II SFM medium (Thermo Scientific, 10902-096) at 28°C (180 rpm, 0% CO₂, 80 % humidity). On the day of transfection, the cells were centrifuged (300 rpm, 5 min) and re-suspended in culture media in 35% of the intended volume at a density of 5*10⁶ cells/mL. Plasmid DNA (600 µg for 200 mL culture) was mixed with 2 mg of PEI (1 mg/mL) and incubated at room temperature for 10 minutes. The mixture was added to the cells and the culture incubated at 28°C. After 45 minutes, culture medium was added to the cells in a final volume of 200 mL.

3 days after transfection, the cells were harvested at 500 rpm during 15 minutes and the pellet re-suspended in 20 mL of lysis buffer A (50 mM Tris pH 7.5, 500 mM NaCl, 5% glycerol, 5 mM β-mercaptoethanol, 1 mM PSMF (Roche, Basel, Switzerland) and Roche protease inhibitor (Roche)). Cells were lysed using 3 rounds of 5 minutes sonication at 30% amplitude with 10 sec on/off cycles on ice. Lysed cells were spun down at 18000 rpm for 30 min, and the supernatants were filtered at 0.45 µm. The supernatants were incubated with 2 mL of pre-equilibrated Ni-NTA beads (in lysis buffer) for 2 h at 4 °C. Beads were washed with 30 column volumes (60 mL) of washing buffer (Lysis buffer A + 25 mM imidazole). Proteins were eluted with 5 column volumes of elution buffer (Lysis buffer A + 500 mM imidazole), and extensively dialyzed against 50 mM Tris pH 7.5, 150 mM NaCl, 5% glycerol, 1 mM DTT buffer. Sample purity was verified by Coomassie Blue staining.

For measuring zap70 KD kinase activity, 50 ng of recombinant tyrosine kinase, 75 µM ATP, 7 µCi γ-32P-ATP was incubated with a peptide with 200 µM of an optimal Abl substrate in kinase assay buffer (20 mM Tris-HCl pH 7.5, 5 mM MgCl₂, 1 mM DTT) for 30 minutes at RT in a final assay volume of 20 µL. The terminated reaction (10 µL 7.5 M guanidiniumhydrochlorid) was spotted onto a SAM2 Biotin Capture membrane (Promega, Madison, WI) and further treated according to the instructions of the manufacturer.

4.7.3 HEK293 cells transfections

All kinase constructs presented in table 2.4) were cloned in pCS2-gateway plasmid containing an N-terminal Myc tag. For each kinase several plasmid amounts were tried in order to obtain

Chapter 4. Material and Methods

similar expression levels between the constructs. HEK293 cells were transfected as described in Section 4.3.

The following antibodies were used: anti-pY551 Btk (BD Biosciences, 558034), anti-pY416 Src family (Cell Signaling, 2101S), anti-pY342 Brk (Millipore, 09-144), anti-pY319 Zap70 (Cell signaling, 2701) and anti-myc-IRDye800 (600-432-381, Rockland).

4.7.4 Fluorescence polarization assay with Btk SH2 domain

Btk SH2 mutants were incubated at several concentrations with 250 nM of FITC-labeled pYEEI peptide in Tris 25 mM pH 7.4, 50 mM NaCl, 2 mM DTT. Fluorescence polarization was then measured using the SpectraMax M5 with excitation at 485 nm and emission at 530 nm (molecular devices) in a 96 well black-plate (Greiner, 784-900).

4.7.5 Btk autophosphorylation assay

Recombinant Btk kinase constructs were incubated in Tris 25 mM pH 7.5, 150 mM NaCl, 5% glycerol, 1 mM ATP, 20 mM MgCl₂, 1 mM DTT at 1 μ M concentration. Reactions were stopped at desired time points by adding 2X Laemmli buffer to each tube. Samples were immunoblotted on a nitrocellulose membrane. The following antibodies were used: anti-Btk kinase (Pierce, PA5-27392) and anti-pY551 Btk (BD Biosciences, 558034). Btk proteins incubated with no ATP were used as background and subtracted before normalizing values.

4.8 Screening assays

4.8.1 Acrylodan labeling and measurements

Abl acrylodan protein mutants were purified as in Section 4.1.2. In total 8 cysteines mutant were used. Abl SH2-KD C324V C349S was used as a control (no cysteine in SH2) and the following mutants were labeled: SH2-KD C324V C349S E187C, SH2-KD C324V C349S L159C, SH2-KD C324V C349S T231C as well as their corresponding I164E versions. Kinase mutants activity was measured as in Section 4.2.1 except using a fix Abl peptide concentration of 75 μ M.

Before labeling, DTT was removed from purified proteins using PD10-desalting columns (GE healthcare). Acrylodan was obtained from Thermo-Fisher (A-433) and resuspended in DMSO at 10 mM stock concentration. Labeling was carried out in HEPES 25 mM pH 7, 200 mM NaCl, 5% Glycerol, at 4°C overnight while shaking in a rotating wheel. Purified proteins were co-incubated in 1:3 to 1:10 molar ratio with acrylodan, with protein concentration ranging from 20 to 50 μ M. After labeling, reaction was quenched by adding 1 mM DTT and free acrylodan removed using PD-10 columns or extensive dialysis against labeling buffer.

Fluorescent measurements were carried out using TECAN SAFIRE 2 in 384 small-volume black

Greiner plates (low-binding, 784 900). 15 μL of labeled proteins were added to each well at various protein concentrations (5 to 20 μM). Acrylodan-conjugated proteins were then excited at 380 nm and emitted fluorescence measured in between 400 and 550 nm. For monobodies co-incubation assays the protein mutants were incubated with increasing concentrations of AS25 for 5 minutes at room temperature and then acrylodan fluorescence was measured. An unrelated monobody (Nsa5) was also used as a control.

4.8.2 HTRF measurements of AS25-SH2 complexes

All tagged proteins were purified in Tris buffer 25 mM pH 7.5, 100 mM NaCl, 1 mM DTT and 5% glycerol. 5 μL of tagged AS25, tagged Abl SH2, Anti-tag 1-donor (Terbium cryptate) and Anti-tag 2-acceptor (d2 or XL665) were mixed and added into a 384 low-volume white Greiner plate (784075). 4 background controls were measured: A cryptate blank (10 μL of buffer, 5 μL of detection buffer and 5 μL of Terbium-cryptate), a negative (10 μL of buffer, 5 μL of both donor and acceptor), a negative containing all reagents and only tagged Abl SH2, a negative containing all reagents and only tagged AS25. The following reagents were used (Cisbio): 61HI2TLA, 61HISDLA, 61HISXLA, 61GSTTLA, 61GSTDLA, 61GSTXLA, 61FG2TLA, 61FG2DLA, 61FG2XLA, 610SATLA, 610SADLA, 610SAXLA.

Samples were measured using the PHERAstar FS with an excitation wavelength set at 337 nm and emission measured simultaneously at 665 and 620 nm (delay time 60 μs , integration time 400 μs , 300 flashes). HTRF signal, Signal-to-noise ratio and assay window are defined as followed:

$$\text{HTRF signal} = \frac{665 \text{ nm}}{620 \text{ nm}} \times 10.000.$$

$$\text{Signal-to-noise ratio} = \frac{\text{HTRF signal}^{\text{assay}}}{\text{HTRF signal}^{\text{negative}}}$$

$$\text{Assay window} = \frac{\text{HTRF signal}^{\text{assay}}}{\text{HTRF signal}^{\text{untagged AS25}}}$$

Where 665 nm and 620 nm are the fluorescence emission intensities at the respective values (relative fluorescence unit), $\text{HTRF signal}^{\text{assay}}$ is the signal obtained when both tagged AS25 and Abl SH2 are added, $\text{HTRF signal}^{\text{negative}}$ is the highest HTRF value obtained from the 4 background controls measured, $\text{HTRF signal}^{\text{untagged AS25}}$ is the signal obtained after addition of cleaved (untagged) AS25 added to the assay sample at 100-fold excess over tagged AS25 (overnight).

Bibliography

- Adrián, F.J.; Ding, Q.; Sim, T.; Velentza, A.; Sloan, C.; Liu, Y.; Zhang, G.; Hur, W.; Ding, S.; Manley, P.; Mestan, J.; Fabbro, D., and Gray, N.S. Allosteric inhibitors of Bcr-Abl-dependent cell proliferation. *Nature chemical biology*, 2(2):95–102, 2006.
- Anastassiadis, T.; Deacon, S.W.; Devarajan, K.; Ma, H., and Peterson, J.R. Comprehensive assay of kinase catalytic activity reveals features of kinase inhibitor selectivity. *Nature biotechnology*, 29(11):1039–1045, 2011.
- Andraos, R.; Qian, Z.; Bonenfant, D.; Rubert, J.; Vangrevelinghe, E.; Scheufler, C.; Marque, F.; Regnier, C.H.; De Pover, A.; Ryckelynck, H.; Bhagwat, N.; Koppikar, P.; Goel, A.; Wyder, L.; Tavares, G.; Baffert, F.; Pissot-Soldermann, C.; Manley, P.W.; Gaul, C.; Voshol, H.; Levine, R.L.; Sellers, W.R.; Hofmann, F., and Radimerski, T. Modulation of Activation-Loop Phosphorylation by JAK Inhibitors Is Binding Mode Dependent. *Cancer Discovery*, 2(6):512–523, 2012.
- Bantscheff, M.; Eberhard, D.; Abraham, Y.; Bastuck, S.; Boesche, M.; Hobson, S.; Mathieson, T.; Perrin, J.; Raida, M.; Rau, C.; Reader, V.; Sweetman, G.; Bauer, A.; Bouwmeester, T.; Hopf, C.; Kruse, U.; Neubauer, G.; Ramsden, N.; Rick, J.; Kuster, B., and Drewes, G. Quantitative chemical proteomics reveals mechanisms of action of clinical ABL kinase inhibitors. *Nat Biotechnol.*, 25(23):1035–1044, 2007.
- Barila, D and Superti-Furga, G. An intramolecular SH3-domain interaction regulates c-Abl activity. *Nature Genetics*, 18, 1998.
- Beatty, P.G. Clinical and managed care issues in blood and marrow transplantation for hematologic diseases. report of a symposium, 14 march 1996, Washington, DC. *Exp Hematol.*, 25(11):1195–1208, 1997.
- Bennett, J.H. Case of hypertrophy of the spleen and liver in which death took place from suppuration of the blood. *Edinb Med Surg J*, 64, 1845.
- Bliska, J.B.; Guan, K.L.; Dixon, J.E., and Falkow, S. Tyrosine phosphate hydrolysis of host proteins by an essential Yersinia virulence determinant. *PNAS*, 88(4):1187–1191, 1991.
- Blume-Jensen, P. and Hunter, T. Oncogenic kinase signalling. *Nature*, 411(1):355–365, 2001.

Bibliography

- Brasher, B.B. and Van Etten, R.A. c-Abl has high intrinsic tyrosine kinase activity that is stimulated by mutation of the Src homology 3 domain and by autophosphorylation at two distinct regulatory tyrosines. *The Journal of Biological Chemistry*, 275(45):35631–35637, 2000.
- Buchdunger, E.; Zimmermann, J.; Mett, H.; Meyer, T.; Muller, M.; Druker, B.J. and Lydon, N.B. Inhibition of the Abl protein-tyrosine kinase in vitro and in vivo by a 2-phenylaminopyrimidine derivative. *Cancer Res.*, 56, 1996.
- Capdeville, R.; Buchdunger, E.; Zimmermann, J., and Matter, A. Glivec (STI571, imatinib), a rationally developed, targeted anticancer drug. *Nat. Rev. Drug. Discov.*, 1(7):493–502, 2002.
- Cheng, S.; Guo, A.; Lu, P.; Ma, J.; Coleman, M., and Wang, Y.L. Functional characterization of BTK C481S mutation that confers ibrutinib resistance: exploration of alternative kinase inhibitors. *Leukemia*, 29, 2015.
- Cortes, J.E.; Kim, D.-W.; Pinilla-Ibarz, J.; le Coutre, P.; Chuah, C.; Nicolini, F.; Paquette, R.; Apperley, J.F.; DiPersio, J.F.; Khoury, H.J.; Rea, D.; Talpaz, M.; Deangelo, D.J.; Abruzzese, E.; Baccarani, M.; Mueller, M.C.; Gambacorti-Passerini, C.; Wong, S.; Lustgarten, S.; Turner, C.D.; Rivera, V.M.; Clackson, T.; Haluska, F., and Kantarjian, H.M. A phase 2 trial of ponatinib in Philadelphia chromosome-positive leukemias. *N Engl J Med.*, 369(19):1783–1796, 2013.
- Cowan-Jacob, S.W.; Fendrich, G.; Manley, P.W.; Jahnke, W.; Fabbro, D.; Liebetanz, J., and Meyer, T. The crystal structure of a c-Src complex in an active conformation suggests possible steps in c-Src activation. *Structure*, 13(6):861–871, 2005.
- Cox, S.; Radzio-Andzelm, E., and Taylor, S.S. Domain movements in protein kinases. *Current Opinion in Structural Biology*, 4(6):893–901, 1994.
- Daley, G.Q.; Van Etten, R.A., and Baltimore, D. Induction of chronic myelogenous leukemia in mice by the P210 bcr/abl gene of the philadelphia chromosome. *Science*, 247(4944):824–830, 1990.
- Davis, M.I.; Hunt, J.P.; Herrgard, S.; Ciceri, P.; Wodicka, L.M.; Pallares, G.; Hocker, M.; Treiber, D.K., and Zarrinkar, P.P. Comprehensive analysis of kinase inhibitor selectivity. *Nature biotechnology*, 29(11):1046–1051, 2011.
- Dölker, N.; Górna, M.W.; Sutto, L.; Torralba, A.S.; Superti-Furga, G., and Gervasio, F.L. Activation by a Cyclin-Like Mechanism and Remodulation of the Hinge Motion. *PLoS Computational Biology*, 10(10), 2014.
- Doney, K.; Buckner, C.D.; Sale, G.E.; Ramberg, R.; Boyd, B., and E.D., Thomas. Treatment of chronic granulocytic leukemia by chemotherapy, total body irradiation and allogeneic bone marrow transplantation. *Exp Hematol.*, 6(9):738–747, 1978.
- Dorey, K.; Engen, J.R.; Kretschmar, J.; Wilm, M.; Neubauer, G.; Schindler, T., and Superti-Furga, G. Phosphorylation and structure-based functional studies reveal a positive and a negative role for the activation loop of the c-Abl tyrosine kinase. *Oncogene*, 20(56):8075–8084, 2001.

- Druker, B.J.; Tamura, S.; Buchdunger, E.; Ohno, S.; Segal, G.M.; Fanning, S.; Zimmermann, J., and Lydon, N.B. Effects of a selective inhibitor of the Abl tyrosine kinase on the growth of BCR-ABL positive cells. *Nat.Med.*, 2(5):561–566, 1996.
- Druker, B.J.; Talpaz, M.; Resta, D.J.; Peng, B.; Buchdunger, E.; Ford, M.; Lydon, N.B.; Kantarjian, M.; Capdeville, R.; Ohno-Jones, S., and Sawyers, C.L. Efficacy and safety of a specific inhibitor of the BCR-ABL tyrosine kinase in chronic myeloid leukemia. *N. Engl. J. Med.*, 344 (14):1037–1031, 2001.
- Fang, Z.; Grutter, C., and Rauh, D. Strategies for the Selective Regulation of Kinases with Allosteric Modulators: Exploiting Exclusive Structural Features. *ACS Chem. Biol.*, 8(1):58–70, 2012.
- Filippakopoulos, P.; Kofler, M.; Hantschel, O.; Gish, G.D.; Grebien, F.; Salah, E.; Neudecker, P.; Kay, L.E.; Turk, B.E.; Superti-Furga, G.; Pawson, T., and Knapp, S. Structural coupling of SH2-kinase domains links Fes and Abl substrate recognition and kinase activation. *Cell*, 134 (5):793–803, 2008.
- Flaherty, K.T.; Infante, J.R.; Daud, A.; Gonzalez, R.; Kefford, R.F.; Sosman, J.; Hamid, O.; Schuchter, L.; Cebon, J.; Ibrahim, N.; Kudchadkar, R.; Burris, H.A.; Falchook, G.; Algazi, A.; Lewis, K.; Long, G.V.; Puzanov, I.; Lebowitz, P.; Singh, A.; Little, S.; Sun, P.; Allred, A.; Ouellet, D.; Kim, K.B.; Patel, K., and Weber, J. Combined BRAF and MEK Inhibition in Melanoma with BRAF V600 Mutations. *New England Journal of Medicine*, 367(18):1694–1703, 2012.
- Gadzicki, D.; von Neuhoff, N.; Steinemann, D.; Just, M.; Büsche, G.; Kreipe, H.; Wilkens, L., and Schlegelberger, B. BCR-ABL gene amplification and overexpression in a patient with chronic myeloid leukemia treated with imatinib. *Cancer Genet Cytogenet.*, 159(2):164–167, 2005.
- Gazit, A.; Yaish, P.; Gilon, C., and Levitzki, A. Tyrphostins i: synthesis and biological activity of protein tyrosine kinase inhibitors. *J.Med. Chem.*, 32(10):2344–2352, 1989.
- Golas, J.M.; Arndt, K.; Etienne, C.; Lucas, J.; Nardin, D.; Gibbons, J.; Frost, P.; Ye, F.; Boschelli, D.H., and Boschelli, F. SKI-606, a 4-anilino-3-quinolinecarbonitrile dual inhibitor of Src and Abl kinases, is a potent antiproliferative agent against chronic myelogenous leukemia cells in culture and causes regression of K562 xenografts in nude mice. *Cancer Res.*, 63(2): 375–381, 2003.
- Gorre, M.E.; Mohammed, M.; Ellwood, K.; Hsu, N.; Paquette, R.; Rao, P.N., and Sawyers, C.L. Clinical resistance to STI-571 cancer therapy caused by BCR-ABL gene mutation or amplification. *Science*, 293(5531):876–880, 2001.
- Grebien, F.; Hantschel, O.; Wojcik, J.; Kaupe, I.; Kovacic, B.; Wyrzucki, A.M.; Gish, G.D.; Cerny-Reiterer, S.; Koide, A.; Beug, H.; Pawson, T.; Valent, P.; Koide, S., and Superti-Furga, G. Targeting the SH2-kinase interface in Bcr-Abl inhibits leukemogenesis. *Cell*, 147(2):306–319, 2011.

Bibliography

- Hantschel, O.; Nagar, B.; Guettler, S.; Kretzschmar, J.; Dorey, K.; Kuriyan, J., and Superti-Furga, G. A myristoyl/phosphotyrosine switch regulates c-Abl. *Cell*, 112(6):845–857, 2003.
- Hantschel, O.; Wiesner, S.; Güttler, T.; Mackereth, C.D.; Remsing Rix, L.L.; Mikes, Z.; Dehne, J.; Görlich, D.; Sattler, M., and Superti-Furga, G. Structural basis for the cytoskeletal association of bcr-abl/c-abl. *Molecular cell*, 19(4):461–473, 2005.
- Hantschel, O.; Rix, U., and Superti-Furga, G. Target spectrum of the BCR-ABL inhibitors imatinib, nilotinib and dasatinib. *Leukemia & Lymphoma*, 49(4):615–619, 2008.
- Hantschel, O.; Warsch, W.; Eckelhart, E.; Kaupe, I.; Grebien, F.; Wagner, K.U.; Superti-Furga, G., and Sexl, V. BCR-ABL uncouples canonical JAK2-STAT5 signaling in chronic myeloid leukemia. *Nature chemical biology*, 8(3):285–293, 2012.
- Hehlmann, R.; Lauseker, M.; Jung-Munkwitz, S; Leitner, A.; Muller, M.C.; Pletsch, N.; Proetel, U.; Haferlach, C.; Schlegelberger, B.; Balleisen, L.; Hanel, M.; Pfirrmann, M; Krause, S.W.; Nerl, C.; Pralle, H.; Gratwohl, A.; Hossfeld, D.K.; Hasford, J.; Hochhaus, A., and Saussele, S. Tolerability-adapted imatinib 800 mg/d versus 400 mg/d versus 400 mg/d plus interferon-alpha in newly diagnosed chronic myeloid leukemia. *J Clin Oncol.*, 29(12):1634–1642, 2011.
- Heinrich, M.C.; Corless, C.L.; Duensing, A.; McGreevey, L.; Chen, C.J.; Joseph, N.; Singer, S.; Griffith, D.J.; Haley, A.; Town, T.; Demetri, G.D.; Fletcher, C.D, and Fletcher, J.A. PDGFRA activating mutations in gastrointestinal stromal tumors. *Science*, 299(5607):708–710, 2003.
- Homewood, J.; Watson, M.; Richards, S.M.; Halsey, J., and Shepherd, P.C. Treatment of cml using IFN-alpha: impact on quality of life. *Hematol J*, 4(4):253–262, 1997.
- Hubbard, S.R. and Till, J.H. Protein tyrosine kinase structure and function. *Annual Review of Biochemistry*, 69(1):373–198, 2000.
- Huse, M. and Kuriyan, J. The conformational plasticity of protein kinases. *Cell*, 109(3):275 – 282, 2002.
- Illmer, T.; Schaich, M.; Platzbecker, U.; Freiberg-Richter, J.; Oelschlägel, U.; von Bonin, M.; Pursche, S.; Bergemann, T.; Ehninger, G., and Schleyer, E. P-glycoprotein-mediated drug efflux is a resistance mechanism of chronic myelogenous leukemia cells to treatment with imatinib mesylate. *Leukemia*, 18(1):401–408, 2004.
- Jabbour, E. and Kantarjian, H. CME information: Chronic myeloid leukemia: 2014 update on diagnosis, monitoring, and management. *Journal of American Hematology*, 89(5):547–556, 2014.
- Jemal, A.; Siegel, R; Xu, J., and Ward, E. Cancer statistics, 2010. *CA Cancer J Clin.*, 60(5):277–300, 2010.
- Kato-Stankiewicz, J.; Ueda, S.; Kataoka, T.; Kaziro, Y., and Satoh, T. Epidermal growth factor stimulation of the ack1/dbl pathway in a cdc42 and grb2-dependent manner. *Biochemical and Biophysical Research Communications*, 284(2):470–477, 2001.

- Khateb, M.; Ruimi, N.; Khamisie, H.; Najajreh, Y.; Mian, A.; Metodieva, A.; Ruthardt, M., and Mahajna, J. Overcoming Bcr-Abl T315I mutation by combination of GNF-2 and ATP competitors in an Abl-independent mechanism. *BMC Cancer*, 12(563), 2012.
- Koide, A.; C.W., Bailey; Huang, X., and Koide, S. The fibronectin type III domain as a scaffold for novel binding proteins. *J Mol Biol.*, 284(4):1141–1151, 1998.
- Lamontanara, A.J.*; Gencer, E.B.*; Kuzyk, O.*, and Hantschel, O. Mechanisms of resistance to BCR-ABL and other kinase inhibitors. *Biochimica et Biophysica acta*, 2012. *These authors contributed equally.
- Lamontanara, A.J.; Georgeon, S.; Tria, G.; Svergun, D.I., and Hantschel, O. The SH2 domain of Abl kinases regulates kinase autophosphorylation by controlling activation loop accessibility. *Nature Communications*, 5:5470, 2014.
- Levinson, A.D.; Oppermann, H.; Levintow, L.; Varmus, H.E, and Bishop, J.M. Evidence that the transforming gene of avian sarcoma virus encodes a protein kinase associated with a phosphoprotein. *Cell*, 15(2):561 – 572, 1978.
- Lin, L.; Czerwinski, R.; Kelleher, K.; Siegel, M.M; Wu, P; Kriz, R.; Aulabaugh, A., and Stahl, M. Activation Loop Phosphorylation Modulates Bruton's Tyrosine Kinase (Btk) Kinase Domain Activity. *Biochemistry*, 48(9):2021–2032, 2009.
- Long, G.V; Fung, C.; Menzies, A.M.; G.M.Pupo, Carlino-M.S.; Hyman, J.; Shahheydari, H.; Tembe, V; Thompson, J.F; Saw, R.P; Howle, J.; Hayward, N.K.; Johansson, P; Scolyer, R.A.; Kefford, R.F, and Rizos, H. Increased MAPK reactivation in early resistance to dabrafenib trametinib combination therapy of BRAF-mutant metastatic melanoma. *Nature Communication*, 5(5694), 2014.
- Lorenz, S.; Deng, P; Hantschel, O.; Superti-Furga, G., and Kuriyan, J. Crystal structure of an SH2-kinase construct of c-Abl and effect of the SH2 domain on kinase activity. *Biochemical Journal*, 468(2):283–291, 2015.
- Machida, K.; Thompson, C.M.; Dierck, K.; Jablonowski, K; Karkkainen, S.; Liu, B.; Zhang, H.; Nash, P.D.; Newman, D.K.; Nollau, P; Pawson, T.; Renkema, G.H.; Saksela, K.; Schiller, M.R.; Shin, D-G., and Mayer, B.J. High-throughput phosphotyrosine profiling using sh2 domains. *Molecular Cell*, 26(6):899–915, 2007.
- Mahon, F.X.; Deininger, M.W.; Schultheis, B.; Chabrol, J.; Reiffers, J.; Goldman, J.M., and Melo, J.V. Selection and characterization of BCR-ABL positive cell lines with differential sensitivity to the tyrosine kinase inhibitor STI571: diverse mechanisms of resistance. *Blood*, 96(3): 1070–1079, 2000.
- Manning, G.; Whyte, D. B.; Martinez, R.; Hunter, T., and Sudarsanam, S. The protein kinase complement of the human genome. *Science*, 298(5600):1912–1934, 2002.

Bibliography

- Mauno, V; Zvelebil, M.J.J.M; Zhu, Q.; Brooimans, R.A.; Ochs, H.D; Zegers, B.J.M.; Nilsson, L.; Waterfield, M.D., and Edvard Smith, C.I. Structural Basis for Pleckstrin Homology Domain Mutations in X-Linked Agammaglobulinemia. *Biochemistry*, 34(5):1475–1481, 1995.
- Mayer, B.J.; Hirai, H., and Sakai, R. Evidence that sh2 domains promote processive phosphorylation by protein-tyrosine kinases. *Current Biology*, 5(3):296–305, 1995.
- McGlave, P.B.; Miller, W.J.; Hurd, D.D.; Arthur, D.C., and Kim, T. Cytogenetic conversion following allogeneic bone marrow transplantation for advanced chronic myelogenous leukemia. *Blood*, 58(5):1050–1052, 1981.
- McWhirter, J.R. and Wang, J.Y. Activation of tyrosinase kinase and microfilament-binding functions of c-abl by bcr sequences in bcr/abl fusion proteins. *Mol Cell Biol.*, 11(3):1553–1565, 1991.
- McWhirter, J.R.; Galasso, D.L., and Wang, J.Y. A coiled-coil oligomerization domain of Bcr is essential for the transforming function of Bcr-Abl oncoproteins. *Mol Cell Biol.*, 13(12):7587–7595, 1993.
- Nagar, B.; Bornmann, W.G.; Pellicena, P.; Schindler, T.; Veach, D.R.; Miller, W.T.; Clarkson, B., and Kuriyan, J. Crystal structures of the kinase domain of c-Abl in complex with the small molecule inhibitors PD173955 and imatinib (STI-571). *Cancer Res.*, 62(15):4236–4243, 2002.
- Nagar, B.; Hantschel, O.; Young, M.A.; Scheffzek, Klaus; D. nd BornmannVeach, W.; Clarkson, B.; Superti-Furga, G., and Kuriyan, J. Structural basis for the autoinhibition of c-Abl tyrosine kinase. *Cell*, 112(6):859–871, 2003.
- Neet, K. and Hunter, T. Vertebrate non-receptor protein–tyrosine kinase families. *Genes to Cells*, 1(2):147–169, 1996.
- Nowell, P.C. and Hungerford, D.A. Minute chromosome in human chronic granulocytic leukemia. *Science*, 132(3438):1488–1501, 1960.
- O’Hare, T.; Walters, D.K.; Stoffregen, E.P.; Jia, T.; Manley, P.W.; Mestan, J.; Cowan-Jacob, S.W.; Lee, F.Y.; Heinrich, M.C.; Deininger, M.W., and Druker, B.J. In vitro activity of bcr-abl inhibitors AMN107 and BMS-354825 against clinically relevant imatinib-resistant Abl kinase domain mutants. *Cancer Res.*, 65(11):4500–4505, 2005.
- O’Hare, T.; Shakespeare, W.C.; Zhu, X.; Eide, C.A.; Rivera, V.M.; Wang, F; Adrian, L.T.; Zhou, T.; Huang, W.; Xu, Q.; Metcalf, C.A.; Tyner, J.W.; Loriaux, M.M.; Corbin, A.S.; Wardwell, S.; Ning, Y.; Keats, J.A.; Wang, Y.; Sundaramoorthi, R.; Thomas, M.; Zhou, D.; Snodgrass, J.; Commodore, L.; Sawyer, T.K.; Dalgarno, D.C.; Deininger, M.W.N.; Druker, B.J., and Clackson, T. AP24534, a pan-BCR-ABL inhibitor for chronic myeloid leukemia, potently inhibits the T315I mutant and overcomes mutation-based resistance. *Cancer cell*, 16(5):401–412, 2009.
- Pao, W.; Miller, V.A.; Politi, K.A.; Riely, G.J.; Somwar, R.; Zakowski, M.F; Kris, M.G., and Varmus, H. Acquired resistance of lung adenocarcinomas to gefitinib or erlotinib is associated with a second mutation in the EGFR kinase domain. *PLoS Med.*, 2(3):e73, 2005.

- Patwardhan, P. and Miller, W.T. Processive phosphorylation: mechanism and biological importance. *Cellular signalling*, 19(11):2218–2226, 2007.
- Pellicena, P. and Miller, W.T. Processive phosphorylation of p130Cas by Src is dependent on SH3-polyproline interactions. *J. Biol. Chem*, 276(30):28190–28196, 2001.
- Pendergast, A. M.; Gishizky, M. L.; Havlik, M. H., and Witte, O. N. SH1 domain autophosphorylation of P210 BCR/ABL is required for transformation but not growth factor independence. *Molecular and Cellular Biology*. *Molecular and Cellular Biology*, 13(3):1728–1736, 1993.
- Pluk, H.; Dorey, K., and Superti-Furga, G. Autoinhibition of c-Abl. *Cell*, 108(2):247–259, 2002.
- Puttini, M.; Coluccia, A.M.L.; Boschelli, F.; Cleris, L.; Marchesi, E.; Donella-Deana, A.; Ahmed, S.; Redaelli, S.; Piazza, R.; Magistroni, V.; Andreoni, F.; Scapozza, L.; Formelli, F., and Gambacorti-Passerini, C. In vitro and In vivo Activity of SKI-606, a Novel Src-Abl Inhibitor, against Imatinib-Resistant Bcr-Abl+ Neoplastic Cells. *Cancer Res.*, 66(23):11314–11322, 2006.
- Remsing Rix, L.L.; Rix, U.; Colinge, J.; Hantschel, O.; Bennett, K.L.; Stranzl, T.; Müller, A.; Baumgartner, C.; Valent, P.; Augustin, M.; Till, J.H., and Superti-Furga, G. Global target profile of the kinase inhibitor bosutinib in primary chronic myeloid leukemia cells. *Leukemia*, 23(3):477–485, 2009.
- Renshaw, M.W.; M.A., Capozza, and J.Y., Wang. Differential expression of type-specific c-abl mRNAs in mouse tissues and cell lines. *Molecular and Cellular Biology*, 8(10):4547–4551, 1988.
- Rix, U.; Hantschel, O.; Durnberger, G.; Remsing Rix, L. L; Planyavsky, M.; Fernbach, N.V.; Kaupe, I.; Bennett, K.L.; Valent, P; Colinge, J.; Kocher, T., and Superti-Furga, G. Chemical proteomic profiles of the BCR-ABL inhibitors imatinib, nilotinib, and dasatinib reveal novel kinase and nonkinase targets. *Blood*, 110(12):4055–4063, 2007.
- Robinson, D.R.; Wu, Y.M., and Lin, S.F. The protein tyrosine kinase family of the human genome. *Oncogene*, 19(49):5548 – 5557, 2002.
- Roumiantsev, S.; Shah, N. P; Gorre, M.E; Nicoll, J.; Brasher, B.B.; Sawyers, C.L., and Van Etten, R.A. Clinical resistance to the kinase inhibitor STI-571 in chronic myeloid leukemia by mutation of Tyr-253 in the Abl kinase domain P-loop. *PNAS*, 99(16):10700–10705, 2002.
- Rowley, J.D. Letter: A new consistent chromosomal abnormality in chronic myelogenous leukaemia identified by quinacrine fluorescence and giemsa staining. *Nature*, 243(5405): 290–293, 1973.
- Sanchez-Arevalo-Lobo, V.J.; Aceves Luquero, C.I.; Alvarez-Vallina, L.; Tipping, A.J.; Viniegra, J.G.; Hernandez Losa, J.; Parada Cobo, C.; Galan Moya, E.M.; Gayoso Cruz, J.; Melo, J.V.; Ramon y Cajal, S., and Sanchez-Prieto, R. Modulation of the p38 MAPK (mitogen-activated protein kinase) pathway through Bcr/Abl: implications in the cellular response to Ara-C. *Biochem J.*, 387(1):231–238, 2005.

Bibliography

- Schindler, T.; Bornmann, W.; Pellicena, P.; Miller, W.T.; Clarkson, B., and Kuriyan, J. Structural mechanism for STI-571 inhibition of abelson tyrosine kinase. *Science*, 289(5486):1938–1942, 2000.
- Schneider, R.; Gohla, A.; Simard, J.R.; Yadav, D.B.; Fang, Z.; van Otterlo, W.A., and Rauh, D. Overcoming compound fluorescence in the FLiK screening assay with red-shifted fluorophores. *Journal of the American Chemical Society*, 135(22):8400–8408, 2013.
- Schneider, Ralf; Becker, Christian; Simard, Jeffrey R; Getlik, Matthäus; Bohlke, Nina; Janning, Petra, and Rauh, Daniel. Direct Binding Assay for the Detection of Type IV Allosteric Inhibitors of Abl. *Journal of the American Chemical Society*, 134(22), 2012.
- Scott, M.P. and Miller, W.T. A peptide model system for processive phosphorylation by src family kinases. *Biochemistry*, 39(47):14531–14537, 2000.
- Seeliger, M.A.; Young, M.; Henderson, M.N.; Pellicena, P.; King, D.S.; Falick, A.M., and Kuriyan, J. High yield bacterial expression of active c-Abl and c-Src tyrosine kinases. *Protein science*, 14(12):3135–3139, 2005.
- Seeliger, M.A.; Nagar, B.; Frank, E.; Cao, X.; Henderson, M.N., and Kuriyan, J. c-Src Binds to the Cancer Drug Imatinib with an Inactive Abl/c-Kit Conformation and a Distributed Thermodynamic Penalty. *Structure*, 15(3):299 – 311, 2007.
- Sha, F.; Gencer, E.B.; Georgeon, S.; Koide, A.; Yasui, N.; Koide, S., and Hantschel, O. Dissection of the BCR-ABL signaling network using highly specific monobody inhibitors to the SHP2 SH2 domains. *PNAS*, 110(37):14924–14929, 2013.
- Sherbenou, D.W.; Hantschel, O.; Kaupe, I.; Willis, S.; Bumm, T.; Turaga, L.P.; Lange, T.; Dao, K.; Press, R.D.; Druker, B.J.; Superti-Furga, G., and Deininger, M.W. BCR-ABL SH3-SH2 domain mutations in chronic myeloid leukemia patients on imatinib. *Blood*, 116(17):3278–3285, 2010.
- Shuai, K.; Halpern, J.; ten Hoeve, J.; Rao, X., and Sawyers, C.L. Constitutive activation of STAT5 by the BCR-ABL oncogene in chronic myelogenous leukemia. *Oncogene*, 13(2):247–254, 1996.
- Silver, R.T.; Woolf, S.H.; Hehlmann, R.; Appelbaum, F.R.; Anderson, J.; Bennett, C.; Goldman, J.M.; Guilhot, F.; Kantarjian, H.M.; Lichtin, A.E.; Talpaz, M., and Tura, S. An evidence-based analysis of the effect of busulfan, hydroxyurea, interferon, and allogeneic bone marrow transplantation in treating the chronic phase of chronic myeloid leukemia: developed for the american society of hematology. *Blood*, 94(5):1571–1536, 1999.
- Skora, L.; Mestan, J.; Fabbro, D.; Jahnke, W., and Grzesiek, S. NMR reveals the allosteric opening and closing of Abelson tyrosine kinase by ATP-site and myristoyl pocket inhibitors. *PNAS*, 110(47):4437–4445, 2013.

- Skorski, T.; Bellacosa, A.; Nieborowska-Skorska, M.; Majewski, M.; Martinez, R.; Choi, J.K.; Trotta, R.; Wlodarski, P.; Perrotti, D.; Chan, T.O.; Wasik, M.A.; Tsichlis, P.N., and Calabretta, B. Transformation of hematopoietic cells by BCR/ABL requires activation of a PI-3k/Akt-dependent pathway. *EMBO J.*, 16(20):6151–6161, 1997.
- Smith, J.M.; Katz, S., and Bruce J. Mayer, B.J. Activation of the Abl tyrosine kinase in vivo by Src homology 3 domains from the Src homology 2/src homology 3 adaptor Nck. *The Journal of Biological Chemistry*, 274(1):27956–27962, 1999.
- Soverini, S.; Martinelli, G.; Rosti, G.; Iacobucci, I., and Baccarani, M. Advances in treatment of chronic myeloid leukemia with tyrosine kinase inhibitors: the evolving role of Bcr-Abl mutations and mutational analysis. *Pharmacogenomics*, 13(11):1271–1284, 2012.
- Taagepera, S.; McDonald, D.; Loeb, J.E.; Whitaker, L.L; McElroy, A.K.; Wang, J.Y.J, and Hope, T.J. Nuclear-cytoplasmic shuttling of C-ABL tyrosine kinase. *PNAS*, 95(13):7457–7462, 1998.
- Talpaz, M.; Kantarjian, H.M.; McCredie, K.; Trujillo, J.M.; Keating, M.J., and Gutterman, J.U. Hematologic remission and cytogenetic improvement induced by recombinant human interferon alpha A in chronic myelogenous leukemia. *N Engl J Med.*, 314(17):1065–1069, 1986.
- Tokarski, J.S; Newitt, J.A.; Chang, C.Y.; Cheng, J.D.; Wittekind, M.; Kiefer, S.E.; Kish, K.; Lee, F.Y.F; Borzilleri, R.; Lombardo, L.J.; Xie, D.; Zhang, Y., and Klei, H.E. The structure of dasatinib (BMS-354825) bound to activated ABL kinase domain elucidates its inhibitory activity against imatinib-resistant ABL mutants. *Cancer Res.*, 66(11):5790–5797, 2006.
- Tse, A. and Verkhivker, G.M. Molecular Dynamics Simulations and Structural Network Analysis of c-Abl and c-Src Kinase Core Proteins: Capturing Allosteric Mechanisms and Communication Pathways from Residue Centrality. *Journal of Chemical Information and Modeling*, 55(8):1645–1662, 2015.
- Vajpai, N; Strauss, A.; Fendrich, G.; Cowan-Jacob, S.W.; P.W., Manley; Grzesiek, S., and Jahnke, W. Solution conformations and dynamics of ABL kinase-inhibitor complexes determined by NMR substantiate the different binding modes of imatinib/nilotinib and dasatinib. *J. Biol. Chem*, 283(26):18292–18302, 2008.
- Valent, P; Hadzijusufovic, E.; Schernthaner, G-H.; Wolf, D.; Rea, D., and le Coutre, P. Vascular safety issues in CML patients treated with BCR/ABL1 kinase inhibitors. *Blood*, 125(6): 901–906, 2014.
- Van Etten, R.A. Cycling, stressed-out and nervous: cellular functions of c-Abl. *Trends in Cell Biology*, 9(5):179–186, 1999.
- Wang, Q.; Vogan, E.M.; Nocka, L.M.; Rosen, C.E.; Zorn, J.A.; Harrison, S.C., and Kuriyan, J. Autoinhibition of Bruton's tyrosine kinase (Btk) and activation by soluble inositol hexakisphosphate. *eLife*, 18, 2015.

Bibliography

- Weisberg, E.; Manley, P.W.; Cowan-Jacob, S.W.; Hochhaus, A., and Griffin, J.D. Second generation inhibitors of BCR-ABL for the treatment of imatinib-resistant chronic myeloid leukaemia. *Nature Reviews Cancer*, 7(5):345–356, 2007.
- Wetzler, M.; Talpaz, M.; Van Etten, R.A.; Hirsh-Ginsberg, C.; Beran, M., and Kurzrock, R. Subcellular localization of Bcr, Abl, and Bcr-Abl proteins in normal and leukemic cells and correlation of expression with myeloid differentiation. *Journal of Clinical Investigation*, 92(4):1925–1939, 1993.
- Wojcik, J.; Hantschel, O.; Grebien, F.; Kaupe, I.; Bennett, K.L.; Barkinge, J.; Jones, R.B.; Koide, A.; Superti-Furga, G., and Koide, S. A potent and highly specific FN3 monobody inhibitor of the Abl SH2 domain. *Nature structural & molecular biology*, 17(4):519–527, 2010.
- Woyach, J.A.; Furman, R.R.; Liu, T-M.; Ozer, H.G.; Zapatka, M.; Ruppert, A.S.; Xue, L.; Li, Daniel H-H.; Steggerda, S.M.; Versele, M.; Dave, S.S.; Zhang, J.; Yilmaz, A.S.; Jaglowski, S.M.; Blum, K.A.; Lozanski, A.; Lozanski, G.; James, D.F.; Barrientos, J.C.; Lichter, P.; Stilgenbauer, S.; Buggy, J.J.; Chang, B.Y.; Johnson, A.J., and Byrd, J.C. Resistance mechanisms for the bruton tyrosine kinase inhibitor ibrutinib. *New England Journal of Medicine*, 370(24), 2014.
- Wu, P.; Nielsen, T.E., and Clausen, M.H. FDA-approved small-molecules kinase inhibitors. *Trends in Pharmacological science*, 36(7):422–439, 2015.
- Wylie, A.; Schoepfer, J.; Berellini, G.; Cai, H.; Caravatti, G.; Cotesta, S.; Dodd, S.; Donovan, J.; Erb, B.; Furet, P.; Gangal, G.; Grotzfeld, R.; Hassan, Q.; Hood, T.; Iyer, V.; Jacob, S.; Jahnke, W.; Lombardo, F.; Loo, A.; Manley, P.W.; Marzinzik, A.; Palmer, M.; Pelle, X.; Salem, B.; Sharma, S.; Thohan, S.; Zhu, S.; Keen, N.; Petruzzelli, L.; Vanasse, K.G., and Sellers, W.R. ABL001, a Potent Allosteric Inhibitor of BCR-ABL, Prevents Emergence of Resistant Disease When Administered in Combination with Nilotinib in an in Vivo Murine Model of Chronic Myeloid Leukemia. *Blood*, 124(21):398–398, 2014.
- Yaish, P.; Gazit, A., and C. LevitzkiGilon, A. Blocking of EGF-dependent cell proliferation by EGF receptor kinase inhibitors. *Science*, 242(4880):933–935, 1988.
- Yang, W. and Desiderio, S. BAP-135, a target for Bruton's tyrosine kinase in response to B cell receptor engagement. *Proceedings of the National Academy of Sciences*, 94(2):604–609, 1997.
- Yang, W.; Malek, S.N., and Desiderio, S. An SH3-binding Site Conserved in Bruton's Tyrosine Kinase and Related Tyrosine Kinases Mediates Specific Protein Interactions in Vitro and in Vivo. *Journal of Biological Chemistry*, 270(35):20832–20840, 1995.
- Ye, D.; Wolff, N.; Li, L.; Zhang, S., and Illaria, R.L. Jr. STAT5 signaling is required for the efficient induction and maintenance of CML in mice. *Blood*, 107(12):4917–4925, 2006.
- Young, M.A.; Shah, N.P.; Chao, L.H.; Seeliger, M.; Milanov, Z.V.; Biggs, W.H.; Treiber, D.K.; Patel, H.K.; Zarrinkar, P.P.; Lockhart, D.J.; Sawyers, C.L., and Kuriyan, J. Structure of the kinase domain of an imatinib-resistant Abl mutant in complex with the aurora kinase inhibitor VX-680. *Cancer Res.*, 66(2):1007–1014, 2006.

Zhang, J.; Adrián, F.J.; Jahnke, W; Cowan-Jacob, S.W.; Li, A.G; Iacob, R.E.; Sim, T.; Powers, J.; Dierks, C.; Sun, F; Guo, G-R.; Ding, Q.; Okram, B.; Choi, Y.; Wojciechowski, A.; Deng, X.; Liu, G.; Fendrich, G.; Strauss, A.; Vajpai, N.; Grzesiek, S.; Tuntland, T.; Liu, Y.; Bursulaya, B.; Azam, M.; Manley, P.W; Engen, J.R.; Daley, G.Q; Warmuth, M, and Gray, N.S. Targeting Bcr-Abl by combining allosteric with ATP-binding-site inhibitors. *Nature*, 463, 2010.

Zhang, S. and Yu, D. Targeting src family kinases in anti-cancer therapies: turning promise into triumph. *Trends Pharmacol Sci.*, 33(3):122–128, 2012.

Allan Lamontanara

4B, Avenue de Sévelin
1007, Lausanne, Switzerland
+ 41.76.66.52.680
allan.lamontanara@gmail.com
28 years old, French



Engineer - PhD in Biotechnology

Responsible, dynamic, curious
Strong background in protein biochemistry and cancer signaling

EDUCATION

- 2012-2016 PhD degree at EPFL** *Lausanne, Switzerland*
Doctoral Program in Biotechnology and Bioengineering (EDBB)
- Project: Allosteric targeting of Abl tyrosine kinase in chronic myeloid leukemia
Advisor: Prof. Oliver Hantschel
- 2008-2011 Engineer's Degree in Biotechnology** *Marseille, France*
Polytech' Marseille
- Master of engineering majoring in life sciences: General microbiology, cell biology, immunology, process engineering, molecular biology, healthcare industries.
- 2006-2008 Technical degree in Biochemical and Biological Analyses** *Lyon, France*
Institut Universitaire de Technologie A (I.U.T. A)

WORK EXPERIENCE

- 2012-2016 PhD student in Cancer Biology, EPFL** *Lausanne, Switzerland*
- Allosteric regulation of cytoplasmic tyrosine kinases in cancer:**
- Recombinant protein expression/purification
 - Biophysical/Biochemical characterization of proteins in solution
 - Kinase activity/inhibition assays
 - Small-molecule screening development
- 2011-2012 Research associate, Expertise Platform Kinase at Novartis:** *Basel, Switzerland*
- Development of cell-based assays for studying c-Abelson kinase phosphostatus:**
- Proliferation assays, ELISA, Reverse Protein Array (Zeptosens technology)
 - Evaluation of drug potencies using Western Blot and ELISA
 - Maintenance of a wide range of mammalian cell lines

2010 Internship, AFMB

Marseille,
France

Production, purification and analysis of the oligomeric states of the *Pseudomonas aeruginosa* RetS sensor:

- Regular use of molecular biology: classical cloning, Gateway® cloning
- Protein production and purification, analysis of proteins conservation in solution
- Analyses of protein oligomerization in solution

SKILLS

- Biology:**
- Strong expertise in **recombinant protein expression and purification**
 - Strong expertise in **molecular biology (Western blotting, cloning)**
 - Advanced user of **Akta purification systems**
 - Strong background in **cancer signaling with emphasis in kinase regulation**
 - Good expertise in **protein biophysical characterization** (ITC, SAXS, CD, Light scattering)
 - Cell biology: **mammalian and insect cells transfections**
- Languages:**
- English: Fluent
 - French: mother tongue
 - Italian: basic knowledge
- Others:**
- Excellent communication and organization skills (association activities)
 - Good knowledge in website design and development (Dreamweaver)
 - Advanced user of Microsoft office suite
 - Regular user of GraphPad Prism
 - Regular user of Adobe Illustrator

EXTRA-CURRICULAR ACTIVITES

President of Bioscience Network Lausanne (BSNL, www.bsnl.ch), a non-profit EPFL based association:

- Set-up industry presentations and workshops in the Lausanne area
- Organizer of the Life Science career day in Lausanne (>400 attendants)
- Regular meeting with members and industrial partners

Co-organizer of a joint EPFL - ETHZ summer school in Translational Biology 2015:

- Selection of speakers, communication with speakers from universities and industry
- Advertising event in Switzerland and Europe
- Responsible for logistic during the event and chair of 2 sessions

Sport and music: Regular practice of running and gym. Self-taught piano.

PUBLICATIONS

A.J. Lamontanara, S. Georgeon, G. Tria, D.I. Svergun and O. Hantschel. *The SH2 domain of Abl kinases regulates kinase autophosphorylation by controlling activation loop accessibility*, in Nature communications, vol. 5, num. 5470, 2014.

A.J. Lamontanara, E.B. Gencer, O. Kuzyk and O. Hantschel. *Mechanisms of resistance to BCR-ABL and other kinase inhibitors*, in Biochimica Et Biophysica Acta-Proteins And Proteomics, vol. 1834, num. 7, 2013.

A.L. Mahul-Mellier, B. Fauvet, A. Gysbers, I. Dikiy, A. Oueslati, S. Georgeon, **A.J. Lamontanara**, A. Bisquertt, D. Eliezer, E. Masliah, G. Halliday, O. Hantschel, H.A. Lashuel. *c-Abl phosphorylates α -synuclein and regulates its degradation: implication for α -synuclein clearance and contribution to the pathogenesis of Parkinson's disease*, in Human molecular genetics, vol. 23, num. 11, 2014